

**PARAMETRIC STUDY OF PROCESS-INDUCED WARPAGE IN
COMPOSITE LAMINATES**

By

MADHAVA PRASAD KOTESHWARA

A thesis

submitted to the Faculty of Graduate Studies

in partial fulfillment of the

requirements for the degree of

Master of Science

DEPARTMENT OF MECHANICAL & INDUSTRIAL ENGINEERING

UNIVERSITY OF MANITOBA

WINNIPEG, MANITOBA

©AUGUST 2001



National Library
of Canada

Acquisitions and
Bibliographic Services

395 Wellington Street
Ottawa ON K1A 0N4
Canada

Bibliothèque nationale
du Canada

Acquisitions et
services bibliographiques

395, rue Wellington
Ottawa ON K1A 0N4
Canada

Your file *Votre référence*

Our file *Notre référence*

The author has granted a non-exclusive licence allowing the National Library of Canada to reproduce, loan, distribute or sell copies of this thesis in microform, paper or electronic formats.

The author retains ownership of the copyright in this thesis. Neither the thesis nor substantial extracts from it may be printed or otherwise reproduced without the author's permission.

L'auteur a accordé une licence non exclusive permettant à la Bibliothèque nationale du Canada de reproduire, prêter, distribuer ou vendre des copies de cette thèse sous la forme de microfiche/film, de reproduction sur papier ou sur format électronique.

L'auteur conserve la propriété du droit d'auteur qui protège cette thèse. Ni la thèse ni des extraits substantiels de celle-ci ne doivent être imprimés ou autrement reproduits sans son autorisation.

0-612-76984-4

THE UNIVERSITY OF MANITOBA
FACULTY OF GRADUATE STUDIES

COPYRIGHT PERMISSION PAGE

Parametric Study of Process-Induced Warpage in Composite Laminates

BY

Madhava Prasad Koteshwara

**A Thesis/Practicum submitted to the Faculty of Graduate Studies of The University
of Manitoba in partial fulfillment of the requirements of the degree**

of

MASTER OF SCIENCE

MADHAVA PRASAD KOTESHWARA ©2001

Permission has been granted to the Library of The University of Manitoba to lend or sell copies of this thesis/practicum, to the National Library of Canada to microfilm this thesis and to lend or sell copies of the film, and to University Microfilm Inc. to publish an abstract of this thesis/practicum.

The author reserves other publication rights, and neither this thesis/practicum nor extensive extracts from it may be printed or otherwise reproduced without the author's written permission.

ACKNOWLEDGEMENT

I would like to express my gratitude to my advisor Dr. Raghavan Jayaraman for his valuable guidance and financial support throughout my program.

I would like to gratefully acknowledge the significant interaction and support from Loren Hendrickson and Dwayne Smith at Boeing Technology Ltd, Winnipeg. I would like to acknowledge the summer students Jeff Gibbings and Ian Smallwood for manufacturing the angle laminates and measuring the warpage.

I would like to thank technicians Van Dorp.J and Penner.I for their help. I would also like to thank all my co-graduate students for their technical and moral support throughout my program. Specially, I would like to thank Michael Edward Hudek for providing the accurate thermal boundary conditions for the current work.

ABSTRACT

The high strength to weight ratio and good fatigue resistance of advanced composite materials make them very useful for high performance aerospace applications. Currently, autoclave processing is the most widely used processing route for manufacturing of composite structures by the aerospace industries. A high quality autoclave cured composite part should have maximum cure, uniform thickness, minimum voids and minimum residual stress and warpage. However, process-induced stress and warpage is one of the major current concerns during autoclave processing of composite structures. Minimization of process-induced warpage through optimal cure cycle requires a good understanding of various mechanisms that contribute to process-induced warpage and of the influence of various process and material parameters. For this purpose a systematic experimental and simulation parametric study, using ANSYS-based process model developed at the UM was pursued. The influence of material parameters (such as tool material and composite material properties), process parameters (such as compaction pressure and dwell temperature), and geometry parameters (such as autoclave heat transfer and laminate thickness) was studied. The angle laminates and flat laminates manufactured using Cytec Fiberite HMF 5-322/34C carbon fiber plane weave fabric composite were used as case studies. Contribution to measured spring-back from the mechanism of anisotropy in coefficient of thermal expansion (CTE) and cure shrinkage, and the mechanism of tool-part interaction was delineated, and the later was found to be smaller than the former. In addition, the tool-part interaction was found to cause warping of the arms of the angle laminate. Based on this study process-induced spring back was found to be cure cycle path dependent. It was found to decrease with increase in rate of

heating of the composite part and decrease in rate of cure. Hence, by choosing a tool with CTE similar to the composite part and low thermal mass along with autoclave cycle parameters that result in higher rate of heating of the composite part, composite structures with minimum warpage can be manufactured.

TABLE OF CONTENTS

| | |
|--|------|
| ACKNOWLEDGEMENT | i |
| ABSTRACT | ii |
| TABLE OF CONTENTS | iv |
| LIST OF FIGURES | ix |
| LIST OF TABLES | xiii |
| LIST OF ACRONYMS | xiv |
| | |
| 1. INTRODUCTION | 1 |
| 1.1 AUTOCLAVE PROCESSING | 1 |
| 1.2 PROCESS-INDUCED RESIDUAL STRESS & WARPAGE | 6 |
| 1.3 SCOPE OF THIS THESIS | 6 |
| 1.4 ORGANIZATION OF THESIS | 8 |
| | |
| 2. LITERATURE REVIEW | 11 |
| 2.1 MECHANISMS OF PROCESS-INDUCED STRESS & WARPAGE | 11 |
| 2.1.1 Anisotropy in CTE & Cure Shrinkage | 13 |
| 2.1.2 Tool-Part Interaction | 15 |
| 2.1.3 Other Reasons | 17 |
| 2.2 PARAMETRIC STUDY OF PROCESS-INDUCED WARPAGE & RESIDUAL STRESS..... | 18 |
| 2.3 PROCESS MODELS | 29 |
| 2.4 SUMMARY OF LITERATURE REVIEW & OBJECTIVES OF THIS THESIS | 32 |
| | |
| 3. PROCESS MODEL DETAILS | 34 |
| 3.1 INPUT MODULE..... | 35 |

| | | |
|-----------|--|-----------|
| 3.2 | THERMOCHEMICAL MODULE | 38 |
| 3.3 | MATERIAL MODULE | 43 |
| 3.4 | STRESS MODULE..... | 45 |
| 3.5 | TOOL REMOVAL MODULE | 50 |
| 3.6 | MODEL VALIDATION | 51 |
| 3.6.1 | Validation of Thermochemical Module | 51 |
| 3.6.2 | Validation of Stress Module..... | 52 |
| 3.7 | SUMMARY | 53 |
| 4. | EXPERIMENTAL & SIMULATION DETAILS..... | 58 |
| 4.1 | MATERIAL CHARACTERIZATION..... | 58 |
| 4.1.1 | PHYSICAL PROPERTIES..... | 59 |
| 4.1.2 | CURE KINETICS PARAMETERS..... | 62 |
| 4.1.3 | THERMOPHYSICAL PROPERTIES | 64 |
| 4.1.3.1 | Specific Heat Capacity | 64 |
| 4.1.3.2 | Thermal Conductivity | 66 |
| 4.1.3.3 | Coefficient of Thermal Expansion (CTE) | 68 |
| 4.1.3.4 | Cure Shrinkage Coefficient | 70 |
| 4.1.4 | RHEOLOGICAL PROPERTIES..... | 71 |
| 4.1.4.1 | Gel Point | 71 |
| 4.1.4.2 | Viscosity of Resin | 72 |
| 4.1.4.3 | Glass Transition Temperature (T_g) | 75 |
| 4.1.5 | MECHANICAL PROPERTIES..... | 75 |
| 4.1.5.1 | Longitudinal & Transverse Moduli | 75 |
| 4.1.5.2 | Shear Modulus | 77 |
| 4.2 | EXPERIMENTAL PARAMETRIC STUDY..... | 78 |
| 4.2.1 | Reasons For Experimental Parametric Study | 78 |
| 4.2.2 | Parameters Used in Experimental Parametric Study | 78 |

| | |
|---|-----|
| 4.2.3 Manufacturing of Angle Laminates and Flat Laminates | 80 |
| 4.2.4 Warpage Measurement | 83 |
| 4.3 SIMULATION PARAMETRIC STUDY | 84 |
| 4.3.1 Material | 86 |
| 4.3.2 Thermal Boundary Condition | 86 |
| 4.3.3 Stress Boundary Conditions | 86 |
| 4.3.4 Simulation Study Parameters | 87 |
| 4.3.4.1 Material Parameters | 87 |
| 4.3.4.2 Geometric Parameters | 87 |
| 4.3.4.3 Cure Cycle Parameters | 88 |
| 4.3.4.4 Thermophysical Properties | 93 |
| 4.3.4.5 Cure Kinetics Parameters | 93 |
| 4.3.4.6 Mechanical Properties | 94 |
| 4.4 SUMMARY | 94 |
| | |
| 5. RESULTS | 98 |
| 5.1 MATERIAL CHARACTERIZATION..... | 98 |
| 5.1.1 Cure Kinetics..... | 98 |
| 5.1.2 Thermophysical Properties..... | 102 |
| 5.1.2.1 Specific Heat Capacity | 102 |
| 5.1.2.2 Thermal Conductivity | 104 |
| 5.1.2.3 Coefficient of Thermal Expansion (CTE) | 104 |
| 5.1.2.4 Cure Shrinkage | 106 |
| 5.1.3 Rheological Properties | 109 |
| 5.1.3.1 Gel Point | 109 |
| 5.1.3.2 Viscosity of Resin | 109 |
| 5.1.3.3 Glass Transition Temperature (T_g) | 111 |

| | |
|---|-----|
| 5.1.4 Mechanical Properties | 111 |
| 5.1.4.1 Longitudinal & Transverse Moduli | 111 |
| 5.1.4.2 Shear Modulus | 113 |
| 5.1.5 Summary of Material Characterization | 113 |
| 5.2 RESULTS FROM EXPERIMENTAL PARAMETRIC STUDY | 118 |
| 5.2.1 Introduction | 118 |
| 5.2.2 Measured Air Temperature & Part Temperature | 118 |
| 5.2.3 Measured Warpage in Angle Laminates | 119 |
| 5.2.3.1 Effect of Process Cycle Parameters | 119 |
| 5.2.3.2 Effect of Tool Material CTE & Thermal Mass | 120 |
| 5.2.4 Error in The Measured Spring Back Angle Due To Warpage in The Arm | 120 |
| 5.2.4.1 Process Parameters | 121 |
| 5.2.4.2 Tool Material CTE & Thermal mass | 122 |
| 5.2.4.3 Measurement error of ROMER Instrument | 122 |
| 5.2.5 Measured Warpage in Flat Laminates | 126 |
| 5.2.5.1 Process Parameters | 126 |
| 5.2.5.2 Tool Material CTE & Thermal mass | 127 |
| 5.2.6 Summary of Experimental Parametric Study | 127 |
| 5.3 RESULTS OF SIMULATION PARAMETRIC STUDY | 128 |
| 5.3.1 Predicted Part Temperature & Degree of Cure | 130 |
| 5.3.2 Process-Induced Warpage Due To Anistropy in CTE & Cure Shrinkage | 131 |
| 5.3.2.1 Effect of Process Cycle Parameters | 136 |
| 5.3.2.2 Effect of Tool Thermal Mass | 136 |
| 5.3.2.3 Effect of Part Thickness | 137 |
| 5.3.2.4 Effect of Autoclave Heat Transfer Coefficient | 137 |
| 5.3.2.5 Effect of Cure-Kinetics Parameters | 140 |
| 5.3.2.6 Effect of Thermo physical Parameters | 140 |
| 5.3.2.7 Effect of Mechanical Properties | 143 |

| | |
|---|------------|
| 5.3.2.8 Combination runs | 143 |
| 5.3.3 Summary of Simulation Parametric Study | 143 |
| | |
| 6. DISCUSSION | 147 |
| 6.1 PREDICTION USING ANALYTICAL SOLUTION | 147 |
| 6.2 CURE KINETICS PARAMETERS | 148 |
| 6.3 LAMINATE THICKNESS | 152 |
| 6.4 TOOL THERMAL MASS..... | 153 |
| 6.5 PROCESS CYCLE PARAMETERS..... | 159 |
| 6.6 DELINEATED WARPAGE DUE TO TOOL-PART INTERACTION | 162 |
| | |
| 7. CONCLUSIONS & RECOMMENDATIONS..... | 164 |
| 7.1 SUMMARY OF THE CURRENT WORK | 164 |
| 7.1.1 Process Model..... | 164 |
| 7.1.2 Experimental Parametric Study..... | 165 |
| 7.1.3 Simulation Parametric Study..... | 165 |
| 7.2 CONCLUSIONS BASED ON CURRENT WORK..... | 166 |
| 7.3 RECOMMENDATIONS..... | 167 |
| | |
| REFERENCES | 169 |
| | |
| APPENDIX | 175 |

LIST OF FIGURES

| | |
|---|----|
| Figure 1.1. Schematic of composite and tool assembly in an autoclave..... | 3 |
| Figure 1.2. Typical autoclave used in the manufacturing of composite..... | 4 |
| Figure 1.3. A typical temperature/pressure (cure) cycle | 5 |
| Figure 1.4 Reduction in included angle of angle laminate due to process-induced warpage..... | 9 |
| Figure 1.5 Methods for minimizing the process-induced residual stress and warpage..... | 10 |
| Figure 2.1 Mechanisms causing process-induced residual stress and warpage in composite laminates..... | 12 |
| Figure 2.2 Mechanism of anisotropy in CTE & cure shrinkage..... | 14 |
| Figure 2.3. Mechanism of tool-part interaction..... | 19 |
| Figure 2.4 Process-induced warpage due to uneven resin flow..... | 20 |
| Figure 3.1 ANSYS based process model..... | 36 |
| Figure 3.2 Schematic & details of elements used in the ANSYS based process model..... | 37 |
| Figure 3.3 Functional structure of thermochemical module..... | 40 |
| Figure 3.4 Functional structure of the material module..... | 47 |
| Figure 3.5 Schematics of determination of materials constants..... | 48 |
| Figure 3.6 Schematic of functional structure of stress module..... | 49 |
| Figure 3.7 Schematic of Prediction of residual stress and warpage in the part..... | 54 |
| Figure 3.8 Tool removal simulation..... | 55 |
| Figure 3.9 Validation of thermochemical module..... | 56 |
| Figure 3.10 Boundary conditions used for Finite Element Analysis..... | 57 |
| Figure 4.1. Manufacturer recommended cure cycle for Cytec Fiberite HMF 5-322/34C Carbon Fiber Composite and 934 neat resin..... | 60 |
| Figure 4.2. Required material properties..... | 61 |
| Figure 4.3. Raw data for a DSC dynamic scan..... | 65 |
| Figure 4.4. Isothermal DSC data for 934-resin..... | 65 |

| | |
|--|-----|
| Figure 4.5 Schematic diagram of set-up for thermal conductivity measurement..... | 69 |
| Figure 4.6 Raw TMA data obtained during the measurement of through-the-thickness CTE..... | 69 |
| Figure 4.7 Cure shrinkage raw data from TMA..... | 73 |
| Figure 4.8 Through the thickness cure shrinkage as a function of degree of cure..... | 73 |
| Figure 4.9 Gel point of 934-neat resin..... | 74 |
| Figure 4.10 Viscosity of 934-resin at three different heating rates..... | 74 |
| Figure 4.11 T_g of 88% cured composite measured from DSC..... | 76 |
| Figure 4.12 Longitudinal modulus measured from DMA..... | 79 |
| Figure 4.13 Shear modulus of the composite measured from Rheometer..... | 79 |
| Figure 4.14 Cure cycles used in the manufacturing of angle and flat laminates..... | 82 |
| Figure 4.15 Location of the tools in the autoclave during processing..... | 82 |
| Figure 4.16 Data collected using ROMER for an angle laminate..... | 85 |
| Figure 4.17 Measured warpage in flat laminate..... | 85 |
| Figure 4.18 Thermal BC's used in simulation study..... | 89 |
| Figure 4.19 Boundary conditions used for Finite Element Analysis..... | 91 |
| Figure 4.20 Cure cycles used in the simulation study..... | 92 |
| Figure 4.21 Cycles used in the simulation study of gel time and cure path..... | 96 |
| Figure 5.1 Reaction order "n" as a function of Temperature..... | 101 |
| Figure 5.2 Heat capacity of uncured composite showing effect of T_g | 103 |
| Figure 5.3 Heat capacity change as a function of degree of cure of the composite..... | 103 |
| Figure 5.4 Thermal conductivity of the composite..... | 105 |
| Figure 5.5 TMA result for composites cured to different degree of cure..... | 105 |
| Figure 5.6 Cure shrinkage in thickness direction as a function of degree of cure at 177°C..... | 108 |
| Figure 5.7 Illustration of temperature dependence of cure shrinkage profile..... | 108 |
| Figure 5.8 Gel Point for 934-resin..... | 110 |
| Figure 5.9 T_g of 88% cured composite measured from DSC..... | 114 |

| | |
|---|-----|
| Figure 5.10 Glass transition temperatures as a function of degree of cure..... | 114 |
| Figure 5.11 Longitudinal modulus of the Cytac Fiberite composite during cure..... | 115 |
| Figure 5.12 Transverse modulus of the composite as a function of degree of cure..... | 115 |
| Figure 5.13 Shear modulus of composite as a function of degree of cure..... | 116 |
| Figure 5.14 Measured autoclave temperature and part temperature..... | 123 |
| Figure 5.15 Measured spring back in angle laminates (based on slope of the fitted line)..... | 123 |
| Figure 5.16 Warpage in the arm of the angle laminate and corrected spring back angle..... | 124 |
| Figure 5.17 Warpage in the arm of the angle laminates for three tools and four process cycles..... | 125 |
| Figure 5.18 Calculated spring back angles (based on the slope of the line joining end points of the arm of the angle laminates)..... | 125 |
| Figure 5.19 Measured warpage in flat laminates for four cycles and three tool materials..... | 129 |
| Figure 5.20 Predicted part temperature & degree of cure for cycle 1, ALH tool..... | 132 |
| Figure 5.21 Predicted part temperature & degree of cure for cycle 4, ALH tool..... | 133 |
| Figure 5.22 Comparison of predicted temperature & degree of cure for three tools and Cycle1..... | 134 |
| Figure 5.23 Predicted part temperature at the middle of the cure cycle for cycle 1 and ALH tool..... | 135 |
| Figure 5.24 Predicted part temperature based on scatter in thermal boundary condition..... | 139 |
| Figure 5.25 Variation in reaction order model as a function of model constants..... | 142 |
| Figure 6.1 Sensitivity of reaction order model constants on degree of cure prediction and predicted thermal strain in through-the-thickness direction..... | 150 |
| Figure 6.2 Predicted part temperatures for variation in reaction order model constants..... | 151 |
| Figure 6.3 Effect of laminate thickness on predicted part temperature and degree of cure for three different laminate thicknesses..... | 154 |
| Figure 6.4 Comparison of degree of cure and thermal strain for three tools and cycle 1..... | 156 |
| Figure 6.5 Comparison of predicted part temperature and thermal strain for three tools and | |

| | |
|---|-----|
| cycle 1..... | 157 |
| Figure 6.6 Predicted effective CTE for a 0-direction ply..... | 158 |
| Figure 6.7 Predicted part temperature for five cycles and ALH tool..... | 160 |
| Figure 6.8 Predicted part temperature and degree of cure for different dwell temperature..... | 161 |
| Figure 6.9 Warpage due to tool-part interaction delineated from the measured warpage..... | 163 |
| Figure 6.10 Variation in the autoclave air temperature during manufacturing of angle laminates and flat laminates..... | 163 |

LIST OF TABLES

| | |
|---|-----|
| Table 2.1 Summary of results of the previous parametric analysis | |
| (a)..... | 23 |
| (b)..... | 27 |
| (c)..... | 28 |
| Table 3.1 Properties of the cured composite used in ANSYS and analytical solution..... | 57 |
| Table 4.1 Effective C values used in autoclave heat transfer for three tools..... | 90 |
| Table 4.2 Material, Geometric and Process parameters used in simulation study..... | 95 |
| Table 4.3 Cure kinetics parameters used in the simulation parametric study..... | 97 |
| Table 4.4 Mechanical properties used in the simulation study..... | 97 |
| Table 5.1 Cure Kinetics parameters for Cytec Fiberite 934 Resin and composite..... | 100 |
| Table 5.2 Cure kinetics reaction order as a function of temperature..... | 100 |
| Table 5.3 The summary of the results of material characterization..... | 117 |
| Table 5.4 Predicted spring back angle for three tools, four autoclave air temperature cycles and a manufacturer recommended cycle..... | 138 |
| Table 5.5 Effect of dwell temperature on spring back angle..... | 138 |
| Table 5.6 Variation in the predicted spring back angle as a function of laminate thickness and autoclave heat transfer..... | 139 |
| Table 5.7 Influence of 10 % scatter in cure kinetics parameters on predicted spring back angle... | 141 |
| Table 5.8 Effect of 10 % scatter in the thermo physical properties on predicted spring back..... | 141 |
| Table 5.9 Effect of modulus of the composite on spring back..... | 144 |
| Table 5.10 Combined effect of cure kinetics, thermo physical and mechanical properties on predicted spring back..... | 144 |
| Table 6.1 Predicted warpage for five cycles for ALH tool..... | 160 |

LIST OF ACRONYMS

ALH – Aluminum high mass tool
ALL – Aluminum low mass tool
APDL – ANSYS parametric design language
Auto_Temp (Clave_Temp) - Measured autoclave air temperature
CSC – Coefficient of cure shrinkage
CTE – Coefficient of thermal expansion
DMA – Dynamic mechanical analyzer
DSC – Differential scanning calorimeter
GUI – Graphic user interface
INV – Invar tool
MDSC – Modulated differential scanning calorimeter
Pred_DOC - Predicted degree of cure
Pred_Temp: Predicted part temperature
TC1&TC2 – Thermocouple reading for Invar
TC3&TC4 – Thermocouple reading for ALL
TC5&TC6 – Thermocouple reading for ALH
TMA – Thermo mechanical analyzer

CHAPTER 1

INTRODUCTION

A composite is a combination of two or more distinct materials and is stronger, tougher, and more durable than its constituents. A reinforcement material such as fiber or particle and a matrix or binder material such as polymer, ceramic or metal are the constituents of a composite material. High strength to weight ratio, high modulus to weight ratio, and good fatigue resistance properties of advanced thermoset composite materials make them attractive for high performance aerospace applications such as space structures, antenna, struts, wing boxes, frames, turbine blades and transmission cases. In addition, composites are also used in automotive applications (such as engine blocks, piston rods, battery plates and frames), electrical accessories (such as motor brushes and cables), medical applications (such as prostheses and wheel chairs) and sports equipment (such as tennis racquets, bicycle frames and skis). Autoclave processing, filament winding, pultrusion, resin transfer molding and electron beam curing are some of the methods used for manufacturing composite structures. Currently autoclave processing is the most widely used processing route in aerospace industries for manufacturing of large and complex shaped composite structures.

1.1 AUTOCLAVE PROCESSING

In this method of manufacturing of the composite structures, composite prepreg plies consisting of a single layer of high modulus fibers impregnated with resin are cut and stacked on a tool to form the desired shape and size of the structure. This process is called the lay-up process. A non-stick agent such as frekote is applied on the tool before the

lay-up process. The plies are oriented in a pre-determined direction to obtain the desired mechanical properties. The inserts and honeycomb cores can be placed in the laminate to acquire the desired structural requirements. Figure 1.1 shows the schematic diagram of a composite structure and tool for autoclave curing. The laminate is covered with bleeder and breather cloths and sealed in a vacuum tight bag. The bleeder can be placed around the laminate if excess resin has to be absorbed from the laminate. A breather cloth covers the assembly and provides the path for airflow. The composite-tool assembly is then placed inside an autoclave. Figure 1.2 shows a typical autoclave used for the processing of composites. The external vacuum supply is connected to the vacuum plug in the composite-tool assembly. The composite and tool assembly in the autoclave is subjected to a temperature/pressure (cure) cycle. Figure 1.3 shows a typical cure cycle used for the manufacturing of composites. The application of high temperature initiates the resin polymerization reaction. The application of high pressure consolidates the laminate and results in the flow of polymer matrix of the composite. The bag pressure is maintained such that it will remove any entrapped air or volatile gases during the cure. After the complete cure cycle the autoclave pressure is released and parts are debagged. The debagged part is then sent for the finishing process. A high quality autoclave cured composite part is expected to have a maximum degree of cure, uniform thickness, minimum voids, minimum residual stress, and minimum warpage. However, process-induced residual stress and warpage are two major current concerns during autoclave processing of large complex composite laminates. The selection of cure cycle parameters and design of a tool to produce a fully cured, void free, unwarped composite structure is a challenging task today in the autoclave processing of composite structures.

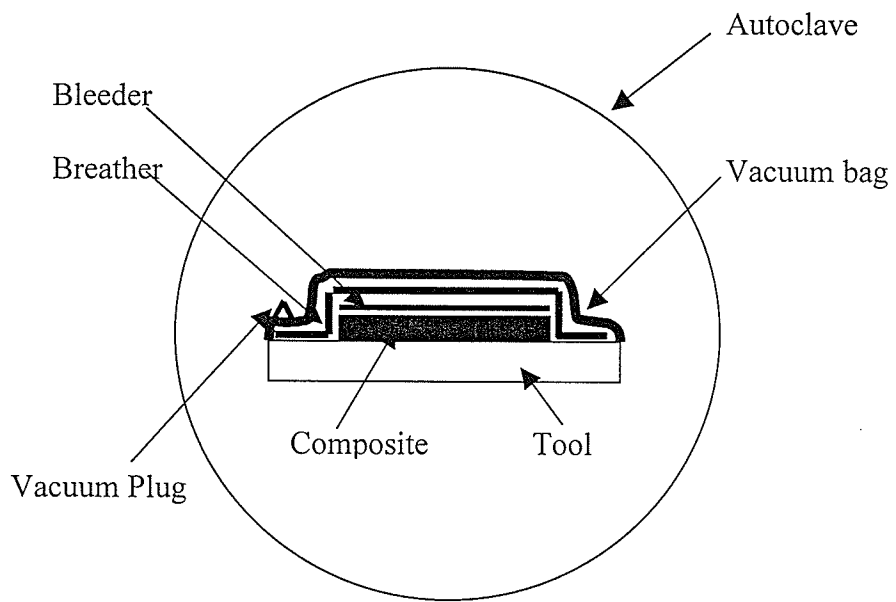


Figure 1.1. Schematic of composite and tool assembly in an autoclave

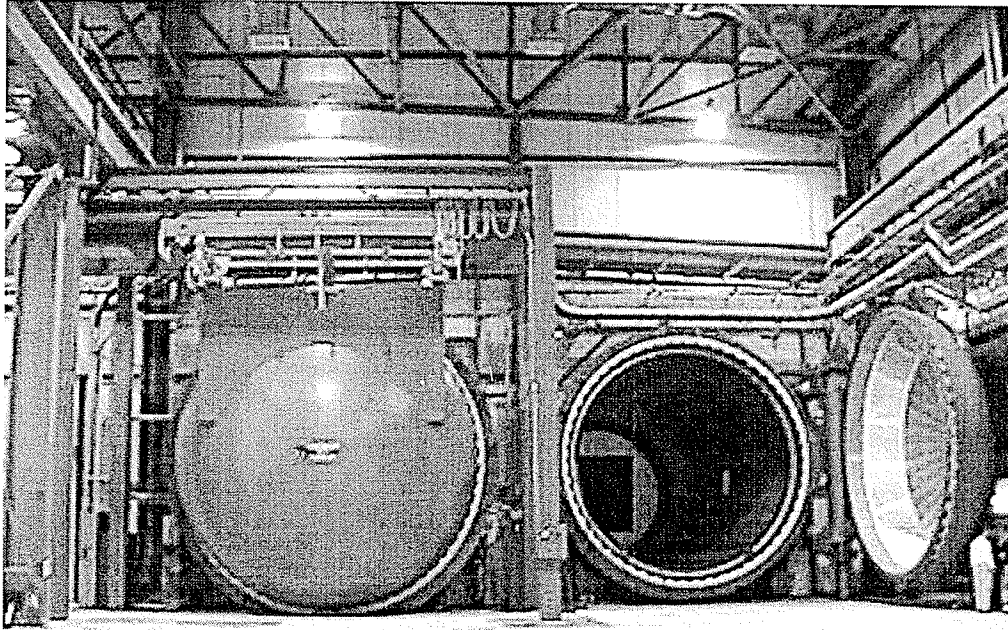


Figure 1.2. Typical autoclave used in the manufacturing of composite (Courtesy: -
Thermal Equipments Ltd.)

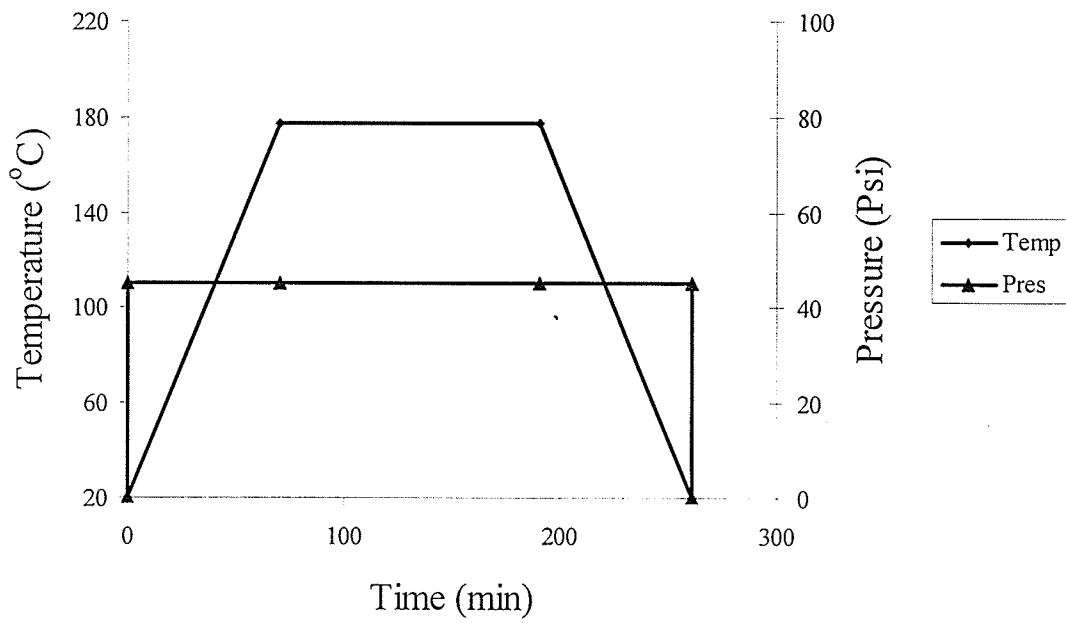


Figure 1.3. A typical temperature/pressure (cure) cycle (Courtesy: -Cyttec Fiberite
Manufacturer Data Sheet)

1.2 PROCESS-INDUCED RESIDUAL STRESS & WARPAGE

Process-induced warpage and residual stresses influence significantly the dimensional accuracy and strength of the composite structures respectively and hence are highly undesirable. For example, as shown in Figure 1.4 an angle laminate can exhibit a spring-in (warpage) and change in the dimension of the structure. The angle laminate is supposed to have a right angle. However, due to the process-induced warpage we can observe a reduction in the included angle. Process-induced warpage is an important issue in an application that requires an accurate tolerance requirement. Such warped structures are currently accepted if they could be force-fitted with an acceptable force per unit length. However, there are potential problems for large stiff structures where the required force per length to force-fit the structure is practically prohibitive. Current practice to minimize this warpage is to design a tool with appropriate allowances. However this is a trial and error, and costly method. In addition, composite structures are expensive to repair and it is necessary to manufacture them to the required shape and dimension the first time, without the need for additional repair. Moreover, residual stresses, if tensile, can significantly reduce the mechanical and fatigue properties of the composite structures. In addition, the residual stress may lead to defects such as micro cracking, delamination and fiber waviness. However no attention is paid currently, during design of cure cycle or processing, to minimize the residual stress and warpage.

1.3 SCOPE OF THIS THESIS

It is evident from the previous section that it is necessary to minimize or eliminate the process-induced residual stress and warpage for cost-effective and reliable manufacturing

of high quality composite structures. As shown in Figure 1.5, there are two ways a manufacturer can reduce or eliminate the process-induced residual stress and warpage in composite laminates. The manufacturer can minimize the process-induced warpage by providing suitable allowances in the tool, based on his/her experience or by trial and error modification of the process cycle. This method requires a number of tool design and manufacturing trials to achieve the desired dimension and shape of the part. The above process would be expensive and time consuming. On the other hand, using a process model would be cost effective and efficient. Using the process model the process-induced warpage and residual stress can be predicted for any complex geometry structure and the composite material system. A parametric analysis could be performed for various process cycles as well as tool geometry to determine the most efficient and shortest cure cycle that results in complete cure with minimum warpage of the part. This would dominate costly tool redesign and manufacturing trails.

The process model approach was taken in this thesis. An existing ANSYS based process model developed at University of Manitoba was refined, improved, and used in this thesis. Minimization of process-induced warpage through optimal cure cycle requires a good understanding of various mechanisms that contribute to process-induced warpage and of the influence of various process and material parameters. This is the focus of this thesis. Using warpage data from experimental and simulation study on an angle laminate, the contributions from two important mechanisms, anisotropy in CTE and cure shrinkage and tool-part interaction are delineated. Subsequently, systematic experimental and simulation parametric study involving material parameters (such as tool material and

composite material properties), process parameters (such as compaction pressure and dwell temperature), and geometry parameters (such as autoclave heat transfer and laminate thickness) was carried out. Results were analyzed to understand the relationship among various process and material parameters and warpage.

1.4 ORGANIZATION OF THESIS

Chapter 2 is a literature review, where published research on process-induced warpage, residual stress, and process models is reviewed. Details on the ANSYS-based process model, used in this thesis, are given in chapter 3. Details on material characterization, experimental and simulation parametric studies are given in chapter 4. Experimental and simulation results are presented in chapter 5. The results are discussed in chapter 6. Finally, conclusions and recommendations are presented in chapter 7.

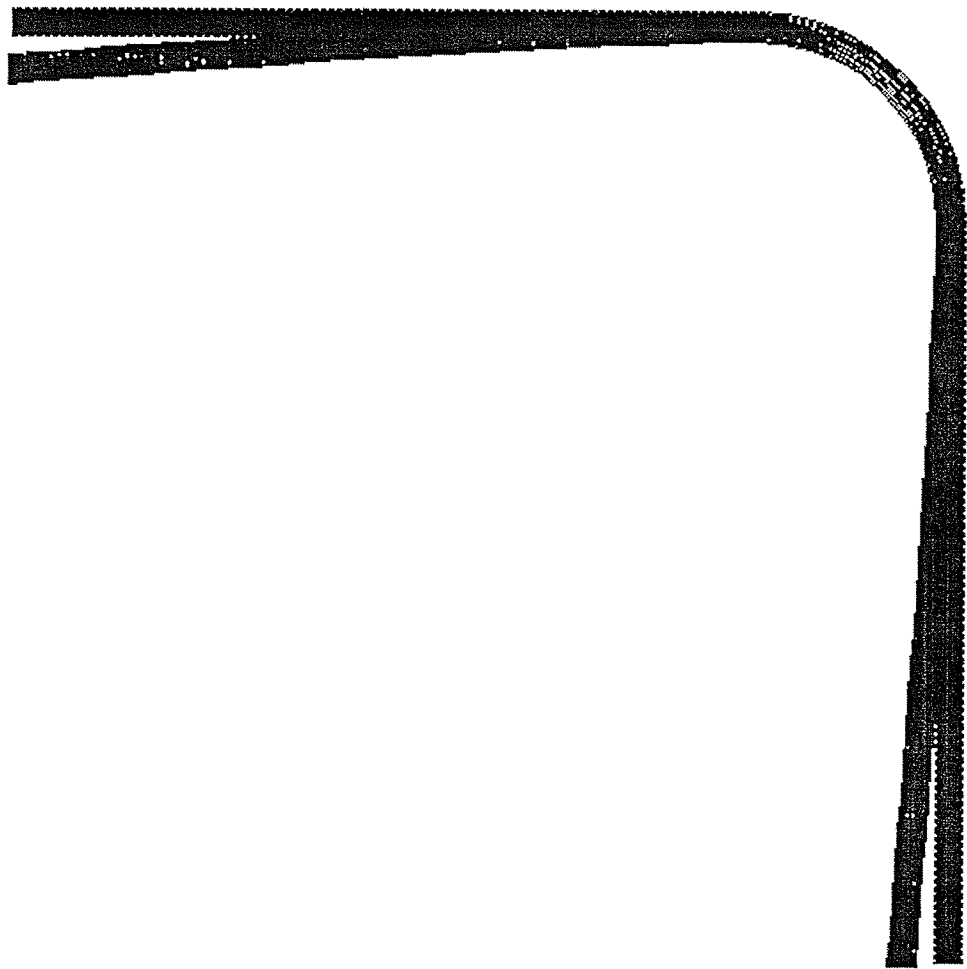


Figure 1.4 Reduction in included angle of angle laminate due to process-induced warpage

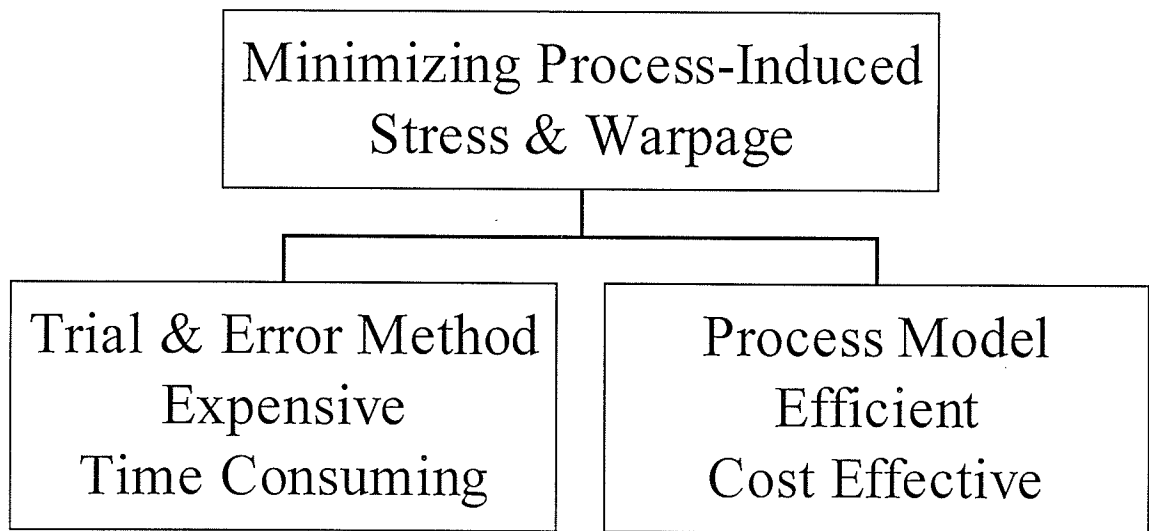


Figure 1.5 Methods for minimizing the process-induced residual stress and warpage

CHAPTER 2

LITERATURE REVIEW

At the outset, the current status of knowledge on various mechanisms causing process-induced residual stress and warpage in composite structures is presented. Following this, published literature on experimental and simulation studies on the influence of process and material parameters on process-induced warpage and residual stress is reviewed. Finally, the various process models used in the simulation parametric study are critically reviewed.

2.1 MECHANISMS OF PROCESS-INDUCED STRESS & WARPAGE

A previous research study (1) assumed that the residual stress and warpage developed in the composite structures during processing was due to a mismatch among Coefficient of Thermal Expansion (CTE) of various plies in the laminate and between the composite and the tool. However subsequent studies by Loos and Springer (2), Bogetti and Gillespie (3) and White and Hahn (4,5) have shown that the residual stress and warpage in autoclave-cured composites is a coupled effect of multi-physical phenomena such as heat transfer, chemical cure kinetics, resin flow through a porous medium, void generation, and thermal stress development. Based on the findings of these studies major sources of process-induced stress and warpage in autoclave cured composite structures can be classified as shown in Figure 2.1. The following section describes each of these mechanisms in detail.

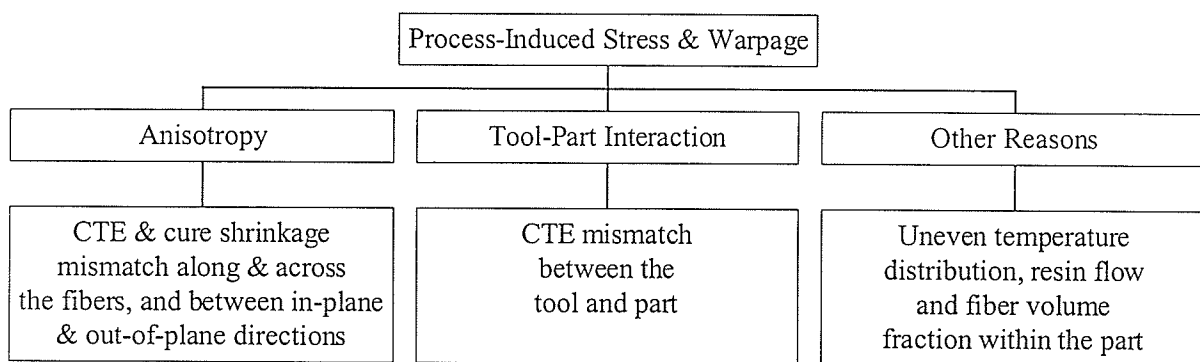


Figure 2.1 Mechanisms causing process-induced residual stress and warpage in composite laminates

2.1.1 Anisotropy in CTE & Cure Shrinkage:

One of the major sources of process-induced warpage in composite structures with curvilinear shape is the anisotropy in CTE and cure shrinkage. This mechanism can be understood using Figure 2.2. During the processing of cylindrical composite structures, there will be a reduction in the enclosed angle of cylindrical segments of composite due to a large mismatch in the in-plane (x-y plane) and out-of-plane (z-direction) CTE and cure shrinkage. Due to the low CTE of the fibers, fibers prevent expansion or contraction of the resin. Hence, thermal expansion or contraction of the resin as well as contraction of the resin due to cure shrinkage will be less in a direction parallel to the fiber axis and more in a direction transverse to the fiber axis. Therefore, large cure shrinkage during curing and any residual thermal contraction after the cool-down part of the process cycle in through-the-thickness direction forces the curved segments of composite to approach each other. However due to a very small contraction in the in-plane direction there will be a reduction in the included angle of the cylindrical segment of the composite part to maintain straight edges (14&15). This phenomenon of reduction in included angle ($\beta < \alpha$) is illustrated in Figure 2.2. This reduction in the included angle is called spring-in or spring-back or spring-forward in the literature. In addition to this, in-plane and out-of-plane CTE and cure shrinkage mismatch will also introduce residual stress in the matrix. There will be also residual stress induced in the plies in symmetric laminates due to the constraint placed by one layer on another.

Composite with cylindrical segment

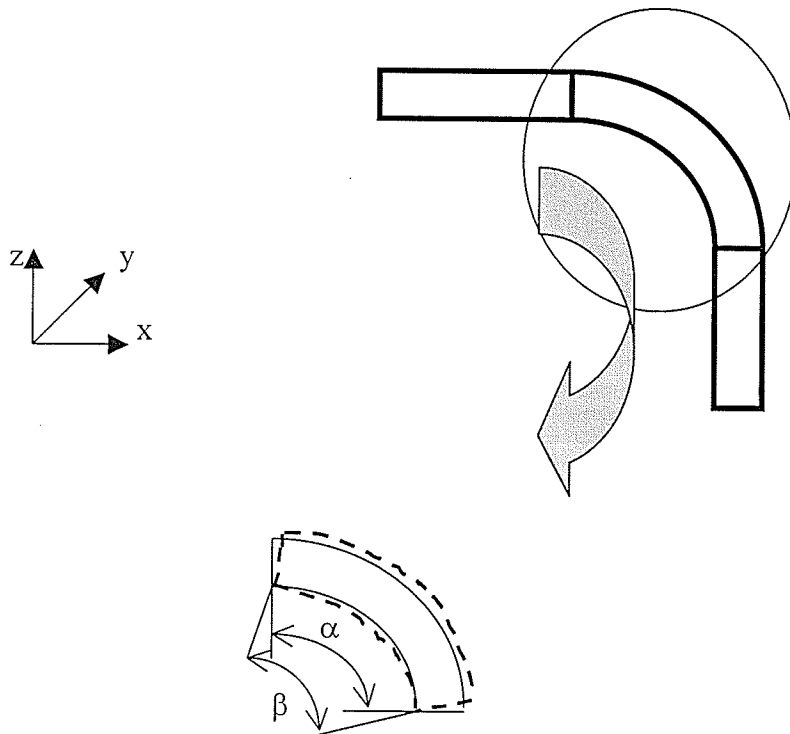


Figure 2.2 Mechanism of anisotropy in CTE & cure shrinkage

2.1.2 Tool-Part Interaction:

The tool-part interaction during the autoclave curing process is one of the most important and least studied sources of process-induced deformation and residual stress in composite structures. This mechanism can be understood using Figure 2.3. The CTE mismatch between the tool and part will cause the restriction of expansion or contraction of the part by the tool and vice versa. Ideally, any stress caused by this restriction during the ramp-up part of the process cycle will be relieved during the ramp-down part of the cycle. However since the composite cures before the ramp-down part of the process cycle a part of the induced stress will be frozen. Therefore, when the tool is removed, part of this frozen stress will be relieved resulting in warpage. If the entire part of the frozen stress is not relieved, it will result in residual stress. The above scenario is possible only if there is good bonding between the tool and the part. Since the tool is normally coated with Teflon – based release film, it is likely that frictional contact as well as Van-der-walls bonding between the tool and the part might be influencing the level of tool-part interaction and resulting warpage and residual stress. However there is no published work on the nature of tool-part interaction and its effect on experimentally observed warpage.

Research studies in this area have started to emerge. Johnston (6) assumed a thin imaginary shear layer between the tool and the part to represent tool-part interaction. He calibrated the shear modulus of this shear layer to match the measured value with the predicted value. Jose & Radford (7) studied the phenomenon of tool-part interaction experimentally through flat laminates as well as using a model. They studied the influence of various mould release agents and different tool material on process-induced

warpage. In their model they used one coefficient (C_1) for tool-part interaction in the calculation of non-thermoelastic component of the induced strain of the sub layer closest to the tool, which is given by,

$$\varepsilon^{s(t)} = C_1(\varepsilon_t^T - \varepsilon_f^T) \quad (2.1)$$

Where,

$\varepsilon^{s(t)}$ is the non-thermoelastic component of the induced longitudinal strain in the sub-layer

C_1 is the coefficient of part/tool interaction

ε_t^T is the thermal strain in the tool

ε_f^T is the thermal strain of the fiber of the layer closest to the tool

The other coefficient (C_2) for ply-to-ply interaction is used in the calculation of the non-thermoelastic component of the induced strain due to fiber-to-fiber interaction, which is given by,

$$\varepsilon_1^{sk} = C_2 \varepsilon_1^{sk+1} \quad (2.2)$$

Where,

ε_1^{sk} is the non-thermoelastic component of the induced longitudinal strain in the sub-layer sk

C_2 is coefficient of interaction between sub-layers

ε_1^{sk+1} is the non-thermoelastic component of the longitudinal induced strain of the sub-layer sk+1

They assumed C_1 to be a function of the mould release agent, tool material and applied pressure. C_2 was assumed to be the function of applied pressure only. Similar to reference (6) values of C_1 and C_2 were obtained by fitting the experimental data with their model. They concluded that it is necessary to develop an experimental procedure to generate these coefficient values related to various process conditions if distortion predictions are to be applied in commercial composite design. However predictive capability of the approach used by Johnston, and Jose and Radford are not satisfactory. Cahn & Adams (8) studied process-induced warpage in flat laminates due to tool-part interaction. They concluded that tool-part interaction is an important factor in producing the process-induced warpage and must be accounted for in the predictive model. However they did not attempt to develop a predictive model based on their study.

2.1.3 Other Reasons:

In the case of complex composite structures uneven temperature distribution, uneven resin flow, gradient in the fiber volume fraction and CTE within the part, could be other sources of process-induced warpage and residual stress. Figure 2.4 shows the warpage in the composite structure due to the uneven resin flow. In autoclave curing of composite laminates, a bleeder may be used on the top surface and near the edges to bleed out excess resin from the laminate. During this process, more resin may bleed out from the top plies of the composite than from the plies close to the tool surface. This would result in uneven resin flow causing variation in CTE and fiber volume fraction variation within the composite part. The top plies with a lesser amount of resin will experience less cure shrinkage than the plies close to the tool with higher resin content. This gradient within

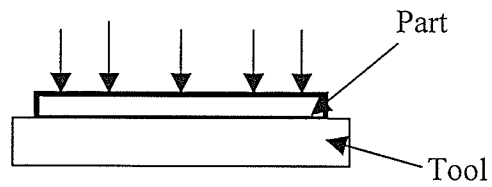
the part would result in residual stress and warping of the part as mentioned in the reference (9).

Mike et al. (10) have observed that heat transfer within the autoclave varied along the length of the autoclave as well as with the orientation of the composite parts with the free-stream within the autoclave. Such an uneven temperature distribution within the autoclave and variation in the heat transfer within the autoclave might result in uneven temperature distribution and hence an uneven degree of cure within the part. In thick composite laminates, large temperature gradient have been observed due to high amounts of exothermic heat as mentioned in the simulation study performed by previous researchers (11,12). Such a temperature gradient as well as resulting cure gradients are other sources of process-induced residual stress and warpage.

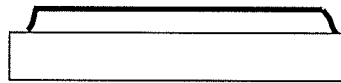
2.2 PARAMETRIC STUDY OF PROCESS-INDUCED WARPAGE & RESIDUAL STRESS

In the past, several researchers have used experimental and simulation parametric study to identify the important parameters influencing the process-induced warpage and sensitivity of the process model. However none of these studies have focused on the contribution of various mechanisms discussed in section 2.1 nor have they delineated the influence of various parameters on the level of contribution to overall warpage and residual stress. However a good knowledge on all these issues is very essential in minimizing warpage and residual stress.

Applied Pressure



Initial shape of the part



Induced strain in the part due to expansion of the tool



Final shape of the part

Figure 2.3. Mechanism of tool-part interaction

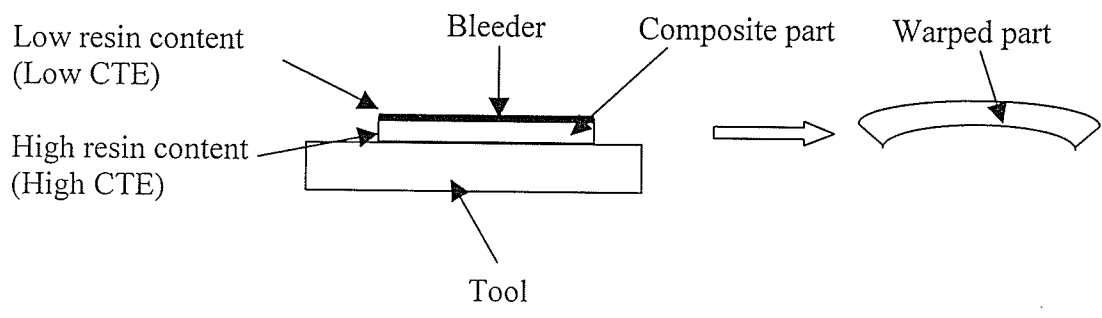


Figure 2.4 Process-induced warpage due to uneven resin flow

Some of the parameters considered by the past researchers in the parametric analysis are:

- a) Process Parameters: Cure temperature and pressure cycle
- b) Geometric Parameters: Laminate thickness, tool radius, tool angle and radius to thickness ratio
- c) Material Parameters: Thermo physical properties of the tool and composite, and mechanical properties of the composite

Results of these parametric studies are reviewed below.

Loos & Springer (2) were the first to develop a process model and to perform a parametric study. In this study they performed a parametric study of cure cycle parameters, compaction pressure, gel time and laminate thickness on predicted part temperature and laminate compaction. However they did not study the influence of these parameters on process-induced warpage and residual stress. In addition, the model was restricted for 1-D analysis and was not capable of predicting process-induced warpage and residual stress in complex composite structures.

Johnston (13) performed a sensitivity analysis of the COMPRO process model, and process-induced warpage in angle laminates and J-stiffened structures. The summary of the parametric study is given in Table 2.1(a). He studied the effect of thermophysical properties, mechanical properties and initial and boundary conditions on process-induced warpage. He perturbed each parameter individually by about 10 % and studied its influence on predicted warpage. Based on this study he concluded that,

- The predicted warpage is insensitive to the thermophysical properties of the composite
- The cure kinetics parameters and initial degree of cure plays an important role in the prediction of warpage
- The predicted warpage is very sensitive to the modulus of the composite and the modulus of the shear layer used to represent the tool-part interaction

In this study, the parametric analysis was performed using the process model with a calibrated shear layer representing tool-part interaction, which could result in a poor prediction. Hence, in order to understand clearly the influence of various parameters on process-induced residual stress and warpage it is necessary to develop a better model for the mechanism of tool-part interaction. In addition, the reasons for higher impact of one parameter over another on process-induced warpage were not explained in that study. The gel time and dwell temperature play an important role in the prediction of evolution of composite modulus properties and cure path. The effect of these parameters on process-induced warpage and residual stress were not studied. Besides, the combined effect of various process and material parameters on process-induced warpage and residual stress was not studied.

Cann & Adams (8) performed a parametric study of process-induced warpage in flat laminates due to tool-part interaction. They studied the effect of tool material, tool surface roughness, ply orientation and ply thickness on the process-induced warpage.

Table 2.1(a) Summary of simulation parametric study (13)

| Parameter | Variation from nominal value | Effect on warpage (Angle/Deflection) | Case study & Nature of study |
|---|------------------------------|--------------------------------------|--|
| Analysis Parameter | | | Angle laminate & J-stiffened structure Simulation |
| Maximum Overall time step (s) and degree of cure step | ±30 % ±50 % | Negligible | |
| Thermophysical Properties | | | |
| C _p , k and V _f | ±10 % | Insignificant | |
| Cure Kinetics Model | | | |
| Heat of reaction Cure kinetics | ±10 % | Insignificant Significant | |
| Mechanical Properties | | | |
| Resin modulus development Cure shrinkage and Composite CTE | ±10 % | Significant Negligible | |
| Initial & Boundary Conditions | | | |
| Initial degree of cure Heat transfer coefficient | ±10 % | Significant | |
| Process Cycle | | | |
| Process cycle | | Insignificant | |

They concluded that,

- The tool material CTE has a strong influence on process-induced warpage
- The ply sequence was found to have a significant impact on process-induced warpage. Specimens with 0° plies adjacent to the tool showed a significant curvature where as the specimen with 90° plies adjacent to the tool showed near zero curvature
- Process-induced warpage was found to decrease with the increase in laminate thickness
- The effect of tool surface roughness on warpage was found to be insignificant

Similar to most of the previous studies, this study focused on process-induced warpage due to the tool-part interaction only. The results were not used in any predictive model or in comparison with the other mechanisms of process-induced warpage.

Jain & Mai (14,15) performed both an experimental and analytical parametric study of process-induced warpage in composite laminates. They studied the effect of tool material, tool geometry, lay-up sequence and ply orientation on the process-induced warpage. The summary of this parametric study is given in Table 2.1(b). Since they didn't consider tool-part interaction, and gradient in temperature, cure and fiber volume fraction, their results could be considered to be indicative of the contribution of anisotropy in CTE and cure shrinkage to warpage. Based on this result they concluded that,

- The effect of tool material on process-induced warpage was insignificant in contrast to the results in references (6,7,8)
- The effect of male or female tool on the warpage was found to be insignificant

- In the case of curved composite structures, the spring back decreased with increase in tool angle
- The effect of tool radius to part thickness ratio in the case of angle laminates was not significant
- The warpage was independent of laminate sequence, for a given laminate in the case of symmetric laminates
- In the case of fabric laminates, the process-induced warpage was independent of the orientation angles

The analytical prediction was found to match very well with the measured process-induced warpage even without considering the tool-part interaction. In addition, in the prediction of process-induced warpage they used the cured composite mechanical properties. The continuous evolution of composite mechanical properties were not studied and not used in the prediction of process-induced residual stress and warpage. However for an accurate prediction of process-induced warpage and residual stress it is necessary to measure the continuous evolution of composite mechanical properties and use them in the prediction of process-induced residual stress and warpage.

Sarrazin et.al. (17) performed an experimental parametric study of the process-induced deformation in flat laminates. He studied the effect of process and lay-up parameters on the process-induced warpage. The results of his study are summarized in Table 2.1(c). He observed that,

- The process-induced warpage increased with increase in cure temperature
- The warpage increased with degree of cure

- A two-step cure cycle reduced the warpage, in contrast to the conclusions in references (7) and (8)
- The process-induced deformation decreased with decrease in cooling rate
- The effect of cure pressure on process-induced warpage was negligible
- The influence of arrangement of porous or non-porous Teflon on process-induced deformation was insignificant, and
- The warpage was found to decrease with increase in laminate thickness.

In this study the above experimental observations were made using a case study of flat laminates. However the reasons for the above trend in process-induced warpage were not studied and explained. In addition, the above conclusions on process-induced warpage and residual stress were derived based on the case study of flat laminates without considering the contribution of various mechanisms on process-induced warpage and residual stress.

Fernlund & Anoush (18) performed the experimental and simulation parametric study of the process-induced warpage in C-channel composite structure. They studied the influence of cure cycle and tool surface finish on process-induced warpage. From their study a trend in the process-induced warpage was not observed for the case of cure cycles with and without dwell. In addition, a trend was not observed for a different tool surface finish. Besides, the predicted warpage using COMPRO process model was about 20 % higher than the measured process-induced warpage. This could be due to the use of a calibrated shear layer for tool-part interaction and the lack of knowledge of the contribution of tool-part interaction on process-induced warpage.

Table 2.1(b) Summary of experimental and simulation parametric study (14,15)

| Parameter | Variation from nominal value | Effect on warpage (Angle) | Case study & Nature of study |
|-------------------------------------|------------------------------|---------------------------|---|
| Ply sequence for symmetric laminate | [90/0/90/0]s | 1.23 | Angle laminate Experimental & Analytical |
| | [0/90/0/90]s | 1.2 | |
| Tool material | Aluminum | 1.39 | |
| | Steel | 1.34 | |
| | Composite | 1.45 | |
| Tool angle | 45 | 2.09 | |
| | 70 | 2.05 | |
| | 90 | 1.39 | |
| | 135 | 0.78 | |
| Radius/Thickness (R/h) | 0 – 20 | 1.4 | |

Table 2.1(c) Summary of experimental parametric study (17)

| Parameter | Variation from nominal value | Effect on warpage ($\Delta L/L$) | Case study & Nature of study |
|---|---|------------------------------------|-----------------------------------|
| Cure T | Nominal | 0.16 | Flat laminate Experimental |
| | -15 % | 0.1 | |
| | +15% | 0.24 | |
| Cure cycle Pressure | Applied Removed after 70% cure | Negligible | |
| Cooling rate | 7.5 F/min | 0.25 | |
| | 1.0 F/min | 0.2 | |
| Tool | Aluminum | 0.15 | |
| | Ceramic | 0.15 | |
| Teflon | Porous | 0.23 | |
| | Non-porous | 0.22 | |
| Part thickness [0 _n /90 _n], n | 1 | 0.74 | |
| | 2 | 0.24 | |
| | 4 | 0.05 | |
| | 8 | 0.0 | |
| Stacking sequence | [0/90] ₄ | 0.0 | |
| | [0 ₂ /90 ₂] ₂ | 0.005 | |
| | [0 ₄ /90 ₄] _t | 0.04 | |

Kim & Brian et.al (19) studied the influence of the process cycle on process-induced residual stress development. They measured the residual strain induced in composite laminate by inserting strain gauges in the laminate in 0 and 90 directions during the curing process. It was observed that the residual strain decreased with the application of dwell and decreasing the ramp rate in the process cycle.

Most of the previous studies focused on warpage and the number of studies on the measurement or prediction of process-induced residual stress are limited.

2.3 PROCESS MODELS

Early research studies (1) assumed that the residual stress developed during the cool-down stage of processing. However, subsequent studies have shown that the residual stress and warpage in autoclave-processed composites is a coupled effect of multi-physical phenomena such as heat-transfer, resin cure-kinetics, resin flow, void generation, and thermal stress development and have developed models of differing complexity to predict process-induced stress and warpage. Notable among these studies is that of Loos and Springer (2), Bogetti and Gillespie (3), and White and Hahn (4,5). These studies were either 1-D or 2-D analysis of simple composite parts using either finite-difference or finite-element methods and they have not been applied to examine realistic structures encountered in aircraft industries. A comprehensive model, marketed commercially as COMPRO, was developed by the researchers at the University of British Columbia (6,9), has been applied to examine residual stress and warpage in intermediate-size 2-D composite structural parts. A comparable ANSYS-based model referred as UM

model in this thesis, has been developed by the advanced composites group at the University of Manitoba.

A process model includes thermo chemical module, resin flow module, stress module and tool removal module. The thermochemical module uses the Fourier heat conduction equation and a cure-kinetics model to predict the temperature and cure distribution within the part at any given time of the process cycle. The flow module, based on a Darcian flow theory through a porous medium, predicts the resin flow, consolidation and fiber volume fraction at any given time of the process cycle. The stress module predicts the deformation and stress using a plane strain condition. The entire part is divided suitably using either a 2-D finite-difference grid or 2-D finite-element mesh. The entire cure cycle is divided into time increments and the nodal variables (DOF) are determined for each time step assuming that the various physical phenomena are de-coupled during each time-increment. Most of the studies have developed their own computer codes for either meshing or accepting a mesh generated by another program and for numerical solution of equations. While Rayleigh-Ritz method has been used in the stress module, Galerkin weighted residual method has been used in the other modules. While most of the models assumed the autoclave set-temperature to be the part boundary condition, COMPRO incorporated an autoclave simulation module to predict the part temperature using the air-temperature inside the autoclave (related to the autoclave set-temperature using a virtual lead-lag controller), and the convective heat transfer coefficient related to autoclave pressure and air temperature using an empirical relation. UM model uses a relatively sophisticated model (SIMCLAVE) to predict part's thermal boundary conditions. While

the above-mentioned studies have significantly improved our understanding of autoclave processing, there are limitations that need to be overcome to improve their accuracy and their applicability to practical composite structures. Important limitations of these models, that are relevant to the proposed study, are discussed below.

Loos and Springner (2) were the first to develop a 1-D computational model called CURE, taking into account major phenomena such as heat transfer, resin flow and stress development. However CURE model could be used only for analysis of 1-D simple structures. And therefore the model cannot be used for commercial applications. White & Hahn (4,5) developed a viscoelastic model called LAMCURE to predict the cure kinetics and process-induced warpage. White & Hahn were the first to study the continuous evolution of composite modulus properties and use them in their model for the prediction of process-induced residual stress and warpage. However they used simplified mechanical boundary conditions and the model is restricted to thin laminates due to the assumption of uniform through the thickness temperature distribution for cure kinetics calculation. A most recent and developed model COMPRO could be used to perform 2-D analysis of intermediate size composite parts. But the contribution due to the mechanism of tool-part interaction was modeled using a shear layer that requires calibration for different geometry and tool-composite material systems. Therefore, the accuracy and reliability of the model prediction is not satisfactory for critical applications such as space structures. In addition, for accurate prediction of the process-induced residual stress and warpage it is necessary to perform a 3-D analysis and hence 2-D analysis is inadequate.

2.4 SUMMARY OF LITERATURE REVIEW & OBJECTIVES OF THIS THESIS

Development of process models has come a long way and relatively comprehensive process models are available today. However their capability to predict warpage and residual stress is relatively poor due to lack of knowledge on tool-part interaction. In addition, these models cannot be applied to complex 3-D structures. In this study only 2-D structures were considered. Composites research group at the University of Manitoba are currently developing a 3-D finite element based process model. As a preliminary work, Zeng and Raghavan (38) have developed a 2-D finite element (ANSYS-based) process model. Refinement of this model using accurate sub-models for composite property evolution during cure, before usage for this thesis, is one objective of this thesis. This UM model also cannot predict warpage due to tool-part interaction. The nature of tool – part interaction was not focused in this thesis though this is currently studied by the composites group at the University of Manitoba.

Previous research studies focused mainly on the development of an analytical solution and process models to predict the process-induced warpage and residual stress. However they did not try to understand and delineate the contribution of various mechanisms discussed in 2.1. Hence, in this study an effort was made to delineate the contribution to warpage from anisotropy in CTE and cure shrinkage, and tool-part interaction. The latter's contribution was delineated by subtracting the contribution of the former from the total warpage. In addition, the previous parametric studies focused on the relative importance of individual parameters on the process-induced stress and warpage. They perturbed values of a single parameter at a time and studied the effect of that on process-

induced residual stress and warpage. The reasons for a relatively higher impact of one over the other have not been enunciated by these studies. Hence, this thesis was focused on understanding how and why various parameters influence process-induced warpage.

Based upon the existing knowledge, this research chose important process and material parameters for the parametric study. Influence of process cycle parameters, tool material and thermal mass on process-induced stress and warpage were studied both experimentally and through simulation. The effects of other parameters such as cure kinetics parameters, composite thermo-physical and mechanical properties, which cannot be studied experimentally were studied through simulation. During simulation parametric studies, the influence of these parameters was studied individually as well as a group. In addition, the effects of dwell temperature and cure path on process-induced warpage were studied through simulation. All the results were comprehended to develop an understanding of the influence of various parameters on process-induced warpage.

The objectives of the current study can be summarized as:

- To improve the existing finite element (ANSYS) based process model to predict accurately the process-induced stress and warpage in composite laminates.
- To delineate the contribution of various mechanisms such as anisotropy in CTE and cure shrinkage and tool-part interaction to process-induced warpage.
- To develop a comprehensive understanding of the influence of various parameters on process-induced warpage.

CHAPTER 3

PROCESS MODEL DETAILS

A finite element (ANSYS) based process model has been developed at the University of Manitoba for the prediction of process-induced residual stress and warpage of 2-D composite parts. Similar to models available in the literature UM model also has sub-module structure as shown in Figure 3.1 The model includes different modules for,

- Input Module: Input tool-part geometry and mesh, tool material and composite material properties, cure cycle details, lay-up sequence, and boundary conditions
- Thermochemical Module: Prediction of part temperature and resin degree of cure during the entire cure cycle
- Material Module: Evolution of composite properties during the entire cure cycle
- Stress Module: Thermal stress development during the entire cure cycle, and
- Tool Removal Module: Simulation of composite part removal from processing tool and prediction of final shape of the part.

These modules are discussed in subsequent sections. With the exception of part-tool geometry, mesh, and mechanical boundary conditions which could be input through GUI of ANSYS, all other input parameters to thermochemical module, stress module and tool removal module requires special functions that are not available in ANSYS. Therefore these modules have been programmed using APDL (ANSYS Parametric Design Language) and interfaced with Frontal solver of ANSYS program. APDL is a scripting language that can be used to build model in terms of parameters (variables). APDL also encompasses a wide range of other features such as repeating a command, macros, if-then-else branching, do-loops, scalar, vector, and matrix operations. Since the ANSYS

solver cannot account for resin cure shrinkage strain and elastic constitutive model for laminate sequence with $[\pm\theta]$, the thermomechanical properties of the plies and effective thermal strain of the composite were obtained using a separate material module. The material module has been written using FORTARN 77 and interfaced with the stress module. The modules were solved sequentially in the following order thermo-chemical module, material module, and stress module. The result of thermochemical module is analyzed through the time history postprocessor, while the results of stress module is analyzed through the general postprocessor of ANSYS.

3.1 INPUT MODULE

This module provides the input required for the process model to predict process-induced residual stress and warpage. The tool-part geometry and finite element mesh for thermochemical and stress module was generated using GUI of the ANSYS. A typical finite element mesh for tool-part used in thermochemical module is shown in Appendix A. The part alone was modeled for stress module. The element type is changed through GUI depending on the module. Figure 3.2 shows the schematic and details of elements used in each of the modules. The composite properties were used in each module as a function of temperature and degree of cure, while the properties of the tool material was assumed to be function of temperature only. Since ANSYS GUI does not have functions to input composite material properties as a function of temperature and degree of cure, APDL batch file was written for this purpose. Similar to the composite material properties, the lay-up sequence, cure cycle, cure kinetics and boundary condition equations were read into the ANSYS program through the APDL batch files.

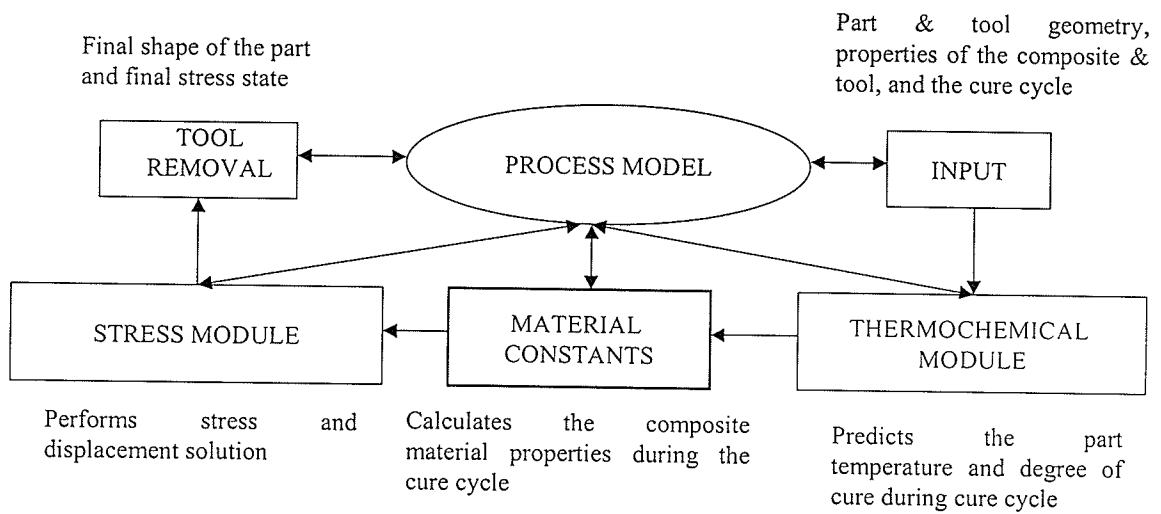
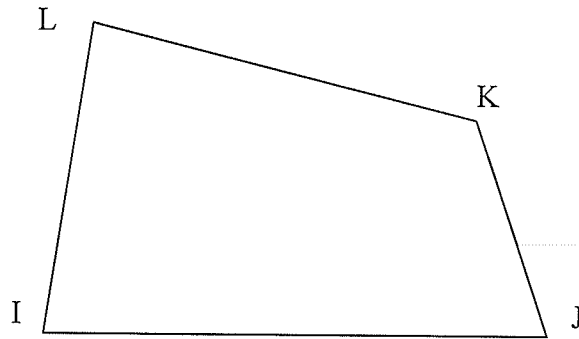


Figure 3.1 ANSYS based process model



PLANE 55 (Thermal Solid): Thermochemical module

Nodes: I, J, K, L

Degree of freedom: Temperature

Material Properties: KXX, KYY, DENS, C,

Surface Loads: Convections - face 1 (J-I), face 2 (K-J), face 3 (L-K), face 4 (I-L)

Body Loads: Heat Generations - HG(I), HG(J), HG(K), HG(L)

PLANE 42 (2-D-Structural Solid): Stress & tool removal module

Nodes: I, J, K, L

Degree of freedom: Translation in element x & y direction

Material Properties: EX, EY, EZ, NUXY, NUYZ, NUXZ, ALPX, ALPY, ALPZ, DENS,

GXY

Body Loads: Temperatures - T(I), T(J), T(K), T(L)

Element capability: Large deflection, large strain, plasticity, creep and stress stiffening

Figure 3.2 Schematic & details of elements used in the ANSYS based process model

[Courtesy: Reference (40)]

3.2 THERMOCHEMICAL MODULE

This module predicts the part temperature and resin degree of cure throughout the cure cycle. In addition, the temperature distribution within the part and tool, at any given cure time can also be obtained from time history post-processor. This module stores the predicted part temperature and degree of cure for each time step and for each ply of the composite part as an array of parameters. These stored parameters used as input to the material module to predict the continuous evolution of composite thermomechanical properties and effective CTE for each time step and for each ply of the laminate. Figure 3.3 shows the functional structure of the thermochemical module. The tool/part geometry, finite element mesh, thermophysical properties of the composite and tool is used as input to this module. The autoclave heat transfer boundary conditions provided by the SIMCLAVE model were used for the heat transfer analysis. During the analysis cure cycle is divided into a number of equal time steps. In the current analysis a time step of one minute was used. During the analysis the batch file was read through GUI and the frontal solver of ANSYS was invoked for transient thermal analysis. The predicted part temperature and degree of cure was analyzed using time history post processor.

The governing differential equation used for the 2-D transient heat transfer analysis is given by,

$$\frac{\partial}{\partial t}(\rho C_p T) = \frac{\partial}{\partial x} \left(K_{xx} \frac{\partial T}{\partial x} \right) + \frac{\partial}{\partial y} \left(K_{yy} \frac{\partial T}{\partial y} \right) + 2 \frac{\partial}{\partial x} \left(K_{xy} \frac{\partial T}{\partial y} \right) + \frac{dH}{dt} \quad (3.1)$$

Where,

ρ - mass density of the composite, kg/m³

C_p - specific heat capacity of the composite as a function of temperature, J/kg K

K_{ij} – thermal conductivity of the composite as a function of temperature, W/m K

$\frac{dH}{dt}$ – rate of heat generation within the composite, J/m³/sec

The exothermic heat generated within the composite is given by,

$$\frac{dH}{dt} = \frac{d\alpha}{dt} \rho_r (1 - V_f) H \quad (3.2)$$

where,

ρ_r - resin density, kg/m³

V_f – fiber volume fraction

H – total heat of reaction, J/kg

$\frac{d\alpha}{dt}$ – rate of degree of cure, 1/sec

The temperature dependence of rate of degree of cure is determined using the Differential Scanning Calorimeter. The rate of degree of cure might follow nth order or autocatalytic reaction. The material used in the current study was found to follow the nth order reaction.

The rate of degree of cure for an nth order reaction is given by,

$$\frac{d\alpha}{dt} = ze^{(-E/RT)}(1 - \alpha)^n \quad (3.3)$$

where,

E – activation energy, J/mol

T – absolute temperature, K

R – gas constant, J/mol K

z – Arrhenius constant, 1/sec

n – reaction order

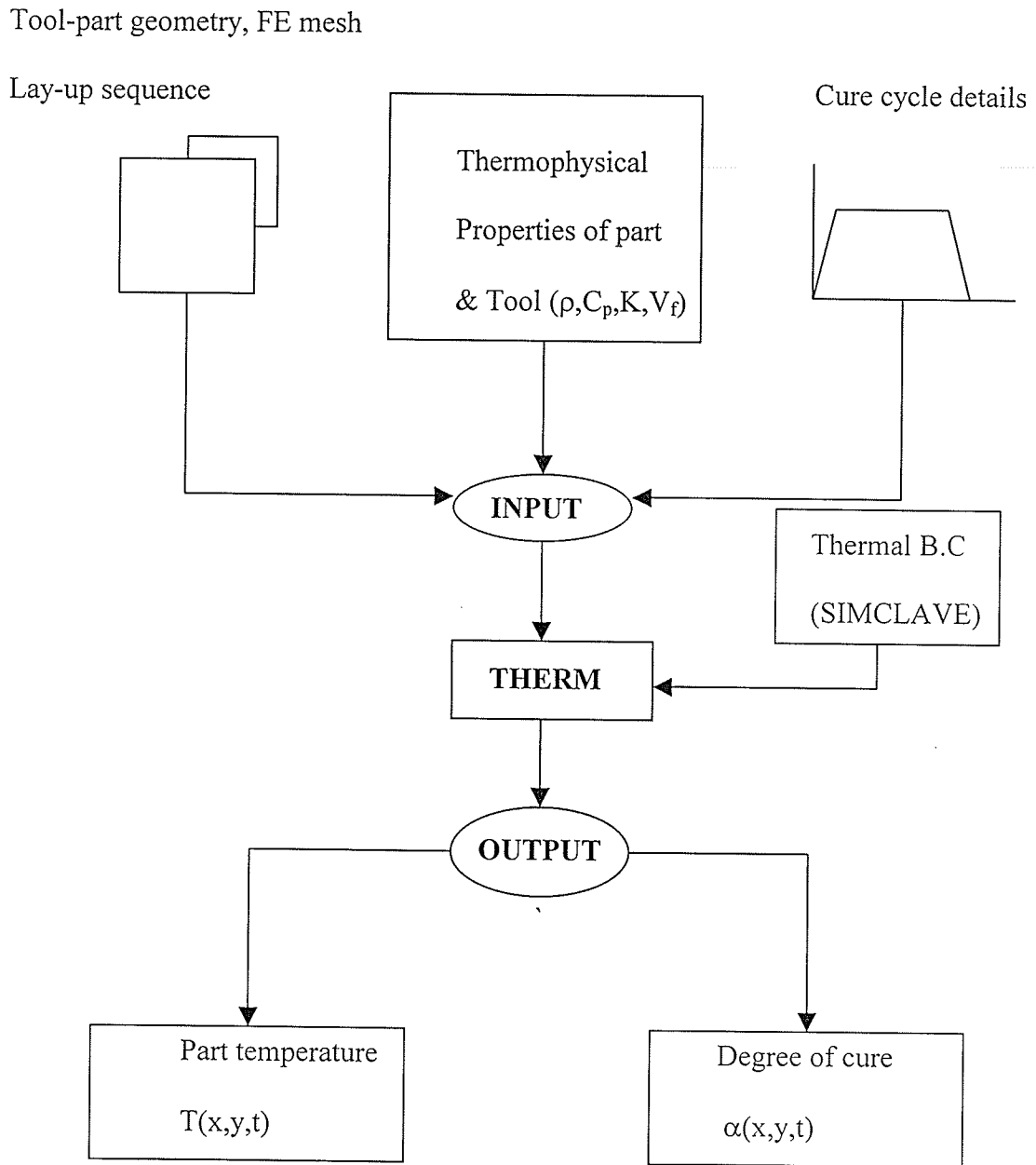


Figure 3.3 Functional structure of thermochemical module

Autoclave curing of composite laminates involves transfer of heat from the autoclave environment to the composite during processing. The temperature and degree of cure within the part, during processing, affects the process-induced residual stress and warpage in composite laminates. Therefore accurate prediction of part temperature and degree of cure is very important in the prediction of process-induced warpage. In order to accurately predict part temperature and degree of cure, it is necessary to predict accurately the amount of heat transferred from autoclave environment to the composite/tool assembly. In the current study, the exact convective heat transfer boundary conditions for the transient thermal analysis were obtained using SIMCLAVE developed by Mike et.al. [10]. The autoclave convective heat transfer is given by,

$$h = C \left(\frac{P}{T} \right)^{0.8} \quad (3.4)$$

Where,

C – effective autoclave constant

P – applied pressure, Pa

T – absolute temperature, K

The convective heat transfer for each time step is calculated using the autoclave air temperature and pressure cycle. During the transient heat transfer analysis, the equation for heat transfer and cure kinetics has decoupled by assuming constant temperature and thermophysical properties of the composite within the time step. Thus coupled problem is simplified to an uncoupled simple problem. Frontal solver of ANSYS performs non-linear analysis to predict degree of cure for each time step using the cure kinetics equation (3.3). Using equation (3.2) and the predicted degree of cure the exothermic heat generated within the composite was determined for each time step. The predicted degree

of cure and heat generated within the composite for a time step is used to predict the part temperature for next time step. The governing equation (3.1) along with exothermic heat generated within the composite (as a body load), composite thermophysical properties, and autoclave convective heat transfer (as surface load) were used for transient heat transfer analysis to predict part temperature at each time step.

The cure kinetics data required as an input to the thermochemical module is measured using a DSC. By performing the dynamic scan and isothermal measurements using DSC, the cure kinetics model is obtained. The measured data for these parameters used in the thermochemical module are discussed in detail in chapter 5. The thermophysical properties required as input to the thermochemical module such as density, thermal conductivity and specific heat capacity of the composite were measured as explained in chapter 4. Overviews of the equations used in the thermochemical module are given here. The measured data can be found in chapter 5.

The density of the composite is calculated using the rule of mixtures which is given by,

$$\rho_c = \rho_f V_f + \rho_r (1 - V_f) \quad (3.5)$$

where,

ρ_c is density of the composite in kg/m^3

ρ_f is density of the fiber in kg/m^3

ρ_r is density of the resin in kg/m^3

V_f is the fiber volume fraction

The specific heat capacity of the composite is calculated using rule of mixtures as,

$$C_{p_c} = \frac{C_{p_f} \rho_f V_f + C_{p_r} \rho_r (1 - V_f)}{\rho_c} \quad (3.6)$$

where,

C_{p_c} , C_{p_f} & C_{p_r} are specific heat capacity of composite, fiber and resin, J/kg K

The thermal conductivity of the composite in longitudinal and transverse direction was measured as a function of temperature. The equation is given by,

$$K_{ij} = AT + B \quad (3.7)$$

where,

K_{ij} is thermal conductivity of the composite in each direction, W/m K

T is temperature, K

A & B are constants

3.3 MATERIAL MODULE

The material module predicts the composite thermomechanical properties and effective CTE for each time step and for each ply of the composite laminate. The predicted thermomechanical properties and effective CTE for each ply is used as an input to the stress module by the process model. Figure 3.4 shows the functional structure of a material module. Since ANSYS cannot account for cure shrinkage strain as well as elastic constitutive model for laminate sequence with $[\pm\theta]$, this module was written using FORTAN 77 and interfaced with the stress module of the process model. The predicted part temperature and degree of cure from thermochemical module along with the

measured composite CTE, cure shrinkage and elastic and shear modulus was used as input to the materials module.

The equation used for the calculation of effective CTE in each ply of the composite is given by,

$$\bar{\alpha}_i = \alpha_i + \frac{\Delta \varepsilon_i}{\Delta T} \quad (3.8)$$

where,

α_i – CTE of composite in each direction, $^{\circ}\text{C}$

$\Delta \varepsilon_i$ – linear cure shrinkage strain increment in each direction

ΔT – temperature increment, $^{\circ}\text{C}$

The material constants in the x & y direction of the ply was determined using the ply orientation and the measured materials constant of the composite as a function of degree of cure. Figure 3.5 shows the schematic of the transformed material constants from the measured material constants. The composite material properties required as input to the material module are CTE, cure shrinkage and elastic and shear modulus of the composite. The Poisson's ratio of the composite was taken from reference (14,15). The procedures for measurement of these parameters are given in detail in chapter 4. The results of the measured properties are presented in chapter 5. Overviews of the equations used in this module are given here. CTE and cure shrinkage were measured using Thermo Mechanical Analyzer (TMA). The cure shrinkage of the composite in the through-the thickness direction is given by,

$$\varepsilon_{ij} = A\alpha + B \quad (3.9)$$

The elastic and shear modulus of the composite were measured using Dynamic mechanical analyzer (DMA) and Rheometer respectively. The longitudinal and transverse modulus as a function of degree of cure is given by,

$$E_{ij} = A\alpha + B \quad (3.10)$$

where,

α is degree of cure

A & B are constants

3.4 STRESS MODULE

This module predicts the thermal stress development throughout the cure cycle and final state of deformation in the tool/part assembly at end of cure cycle. In addition, this model predicts the process-induced warpage and residual stress due to anisotropy in CTE and cure shrinkage, when analysis is performed without the tool. Thus ANSYS based process model can predict the process-induced warpage and residual stress only due to anisotropy. However the process model also has capability to predict the process-induced warpage and stress due to tool/part interaction along with warpage due to anisotropy in CTE & cure shrinkage, when this stress module is used along with the tool removal simulation module. Figure 3.6 shows the schematic of the functional structure of the stress module. The predicted part temperature from thermochemical module, and predicted thermomechanical properties and effective CTE for each ply of the composite from material module, are used as input in this module. During each time step of the analysis the composite materials constants for each ply is assumed to be constant. The governing equilibrium equations with displacement boundary conditions are used to

predict the development of residual stress and final state of deformation in composite-tool assembly. The governing strain-displacement equation is given by,

$$\{\delta_i\} = [K]^{-1} \{F_i\} \quad (3.11)$$

Where,

$\{\delta_i\}$ – nodal displacement vector during each time step

$[K]$ – global stiffness matrix

$\{F_i\}$ – global load vector during the time step

The element nodal force vector for each time step is given by,

$$\{f\}^e = \int_{\Omega^e} [B]^T [D] \bar{\alpha} d\Omega \quad (3.12)$$

where,

$\{f\}^e$ is element nodal force vector at that time step

$[B]$ – strain-displacement matrix

$[D]$ – ply stiffness matrix

$\bar{\alpha}$ – effective CTE

The total displacement at the end of module time step is given by,

$$\{\delta\} = \sum_{i=1}^l \{\delta_i\} \quad (3.13)$$

The mechanical boundary conditions are applied using GUI. In addition to fixed or free boundary conditions for nodal x and y translation, the sliding boundary conditions can be specified at the node. These boundary conditions are applied based on the type of analysis. The boundary conditions used in the stress module for the current study on process-induced warpage in angle laminates are explained in chapter 4.

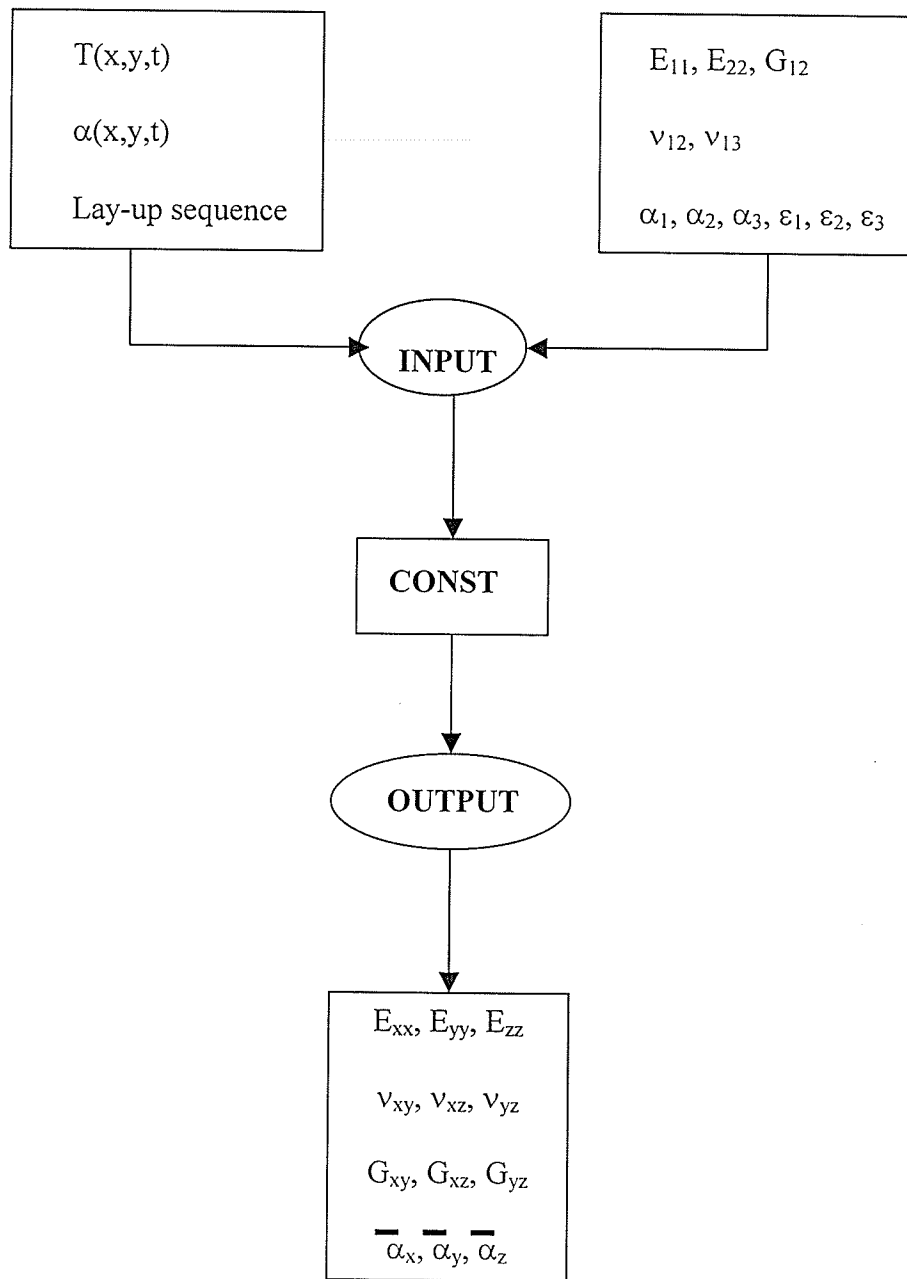


Figure 3.4 Functional structure of the material module

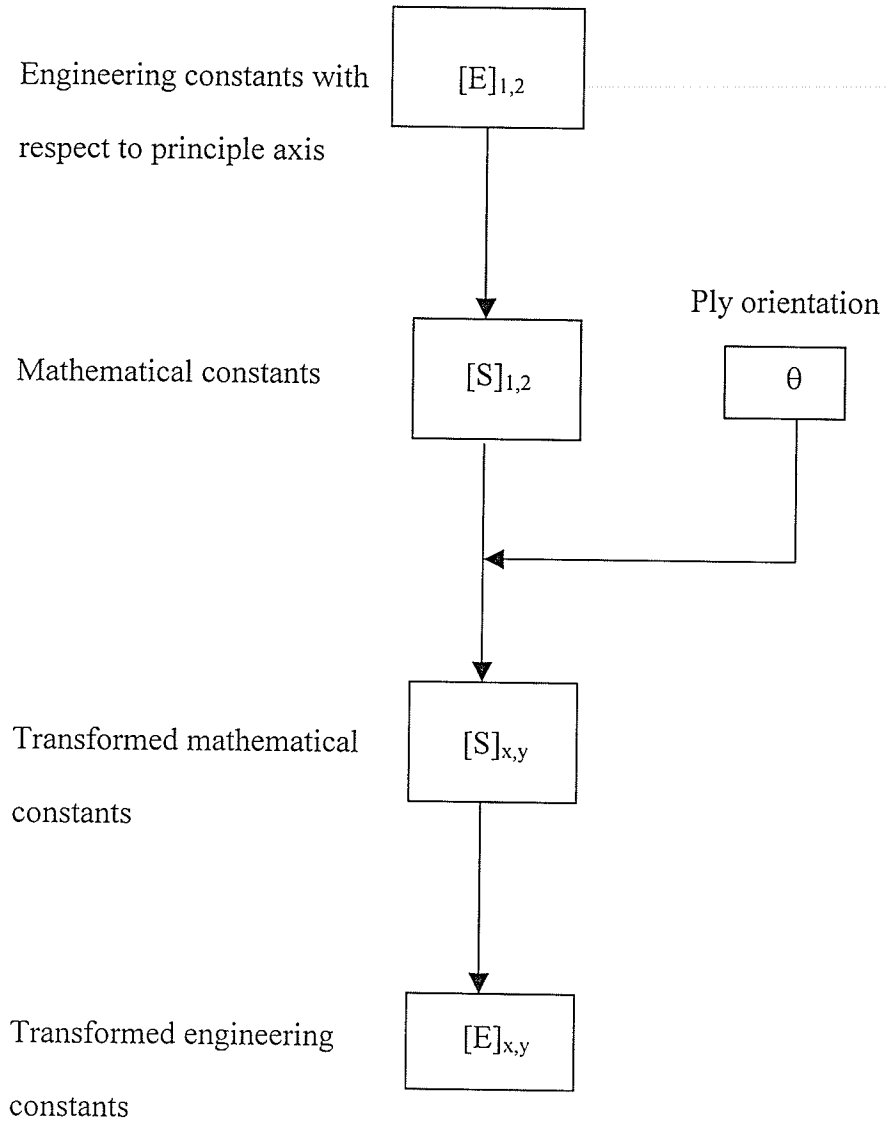


Figure 3.5 Schematics of determination of materials constants

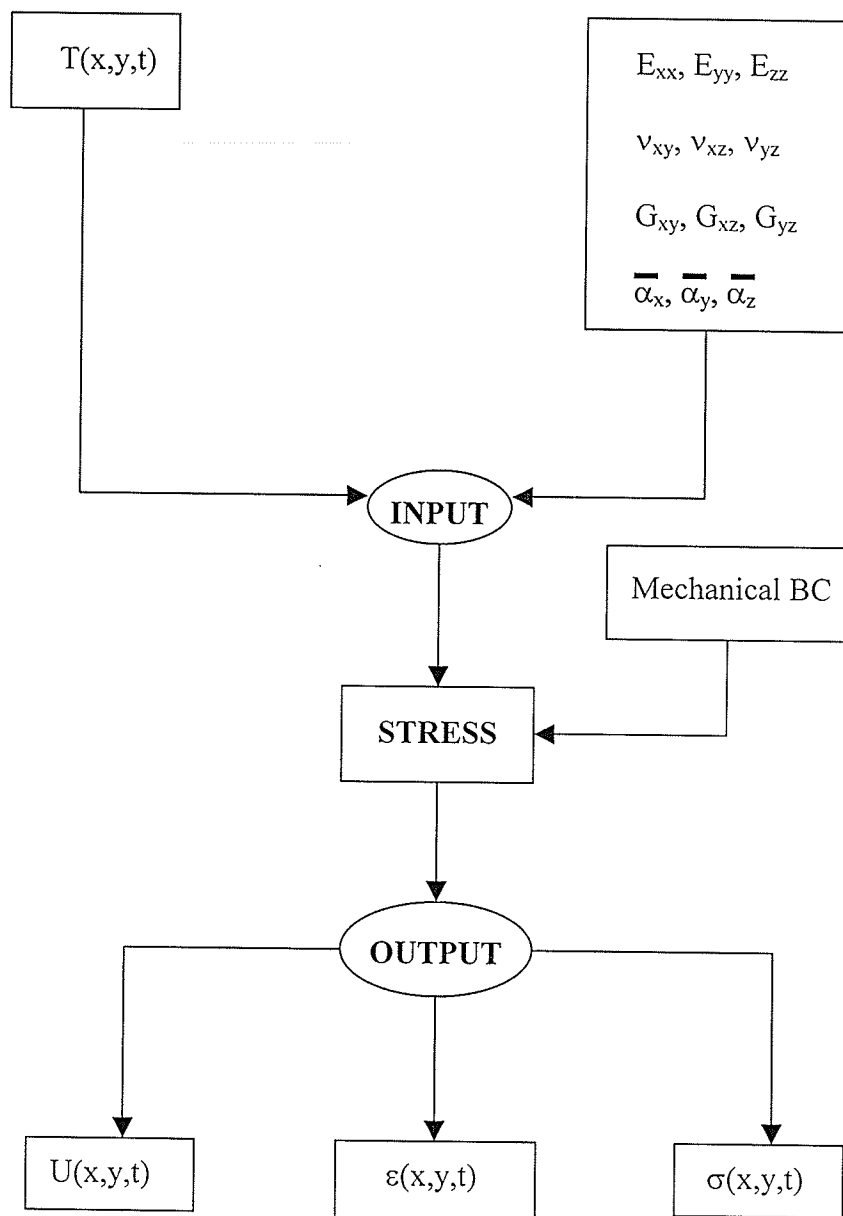


Figure 3.6 Schematic of functional structure of stress module

3.5 TOOL REMOVAL MODULE

The tool removal module predicts the final state of residual stress and warpage in the composite and tool assembly. Similar to the previous models (6,8) tool-part interaction effect is accounted for by varying the modulus of the shear layer placed between the tool and part to predict the process-induced warpage due to tool-part interaction. In addition, similar to the previous models there is a need to calibrate the shear layer modulus to predict the warpage due to tool/part interaction. However since the mechanism of tool-part interaction is not clearly understood till today, and since the shear layer approach cannot be used for reliable predictions the tool removal module was not used in the current study.

During autoclave processing of composites, the laminate is cooled down to room temperature as a final step of the cure cycle. This is followed by removal of the laminate from the tool. The stress due to thermal strains will be partially recovered while the rest will be frozen-in, while the stress due to cure shrinkage strain will be cured-in. When the tool is removed, this stress is relieved through warping of the laminate. To predict the final state of deformation and residual stress in the composite laminate, a tool removal process is simulated. For this purpose equilibrium of the final deformation state of the shear layer is analyzed using the displacement results obtained from the stress module. The force required to keep the shear layer in equilibrium is calculated using the finite element formulation,

$$\{F\}^e = \iint_{\Omega_e} [B]^T [D] [B] \{\delta\}^e d\Omega \quad (3.14)$$

Where,

$\{F\}_e$ – element nodal force vector

$[B]$ – strain-displacement matrix

$[D]$ – ply stiffness matrix

$\{\delta\}_e$ – element nodal displacement vector

This force required to maintain the final deformation state of shear layer in equilibrium is equal to the residual force exerted by the tool on the composite part (6). Figure 3.7 shows the schematic of the tool removal simulation module. The predicted thermomechanical properties of the composite and the residual force in the tool is used as input to the tool removal module. Figure 3.8 shows the mechanism of tool removal simulation. The negative of the residual force exerted by the tool on the composite part is applied in the new finite element model of the part alone to predict the final shape of the part. The mechanical boundary conditions similar to those explained in the stress module can be used in this module. Similar to the previous process models, the shear modulus of the imaginary shear layer is calibrated to predict the process-induced warpage due to the mechanism of tool/part interaction.

3.6 MODEL VALIDATION

3.6.1 Validation of Thermochemical Module:

The predicted part temperature and measured part temperature for aluminium low mass tool (ALL) for cycle 1 (45 Psi pressure without dwell) is as shown in Figure 3.9. The part temperature and degree of cure during entire cure cycle was predicted using the thermochemical module for cycle 1. From this figure it could be observed that the

predicted part temperature and measured part temperature matches very well. Similar results were observed for other cure cycles as well as tools. A maximum error of about 7° in the predicted part temperature was observed. This validates the accuracy of the model to predict the part temperature during entire cure cycle. The details of the simulation study can be found in section 4.4.

3.6.2 Stress Module Validation:

Comparing the predicted warpage using an analytical solution with that using the process model validated the stress module of the ANSYS-based process model. The spring-back angle for the right angle laminate was predicted using ANSYS based process model for the case of cooling a cured angle laminate from cure temperature of 177 °C to room temperature. In addition, the analytical solution for the process-induced spring back in angle laminates is given by,

$$d\theta = (\alpha_l - \alpha_r)\Delta T\theta + (\varepsilon_l^c - \varepsilon_r^c)\theta \quad (3.15)$$

where,

α_l – longitudinal CTE in the laminate

α_r – through-the-thickness CTE in the laminate

ε_l^c – cure shrinkage strain of the composite in longitudinal direction

ε_r^c – cure shrinkage strain of the composite in through the thickness direction

ΔT – difference between room temperature and cure temperature

θ - included angle of the angle laminate

Table 3.1 shows the cured composite properties used for finite element and analytical solution. Figure 3.10 shows the boundary conditions used in the finite element analysis.

The predicted process-induced warpage (spring back angle) from analytical solution was found to be 1.98° while from stress module was found to be 1.92° . This validates the accuracy of the stress module in predicting the warpage due to the mechanism of anisotropy in CTE and cure shrinkage.

3.7 SUMMARY

Preliminary finite element (ANSYS) based process model developed at UM by Zeng and Raghavan (38) has been improved through refinement of sub-models to predict the process-induced stress and warpage due to the mechanism of anisotropy in composite laminates. The process model includes thermochemical module, material module, stress module and tool removal simulation module. APDL was used for thermochemical, stress and tool removal modules while FORTRAN 77 was used for material module. Unlike most of the previous process models, this model uses sophisticated SIMCLAVE model for the prediction of exact thermal boundary conditions in the thermochemical module for accurate prediction of part temperature and degree of cure throughout the cure cycle. In addition, materials module predicts the continuous evolution of composite thermomechanical properties and effective CTE in each ply throughout the process cycle for accurate prediction of the process-induced residual stress and warpage. Besides since stress module is independent of tool removal module, the process-induced warpage due to anisotropy in CTE & cure shrinkage can be easily delineated from the warpage due to tool/part interaction. However the model lacks the capability to predict the laminate compaction and influence of resin flow on process-induced warpage due to the unavailability of the resin flow module.

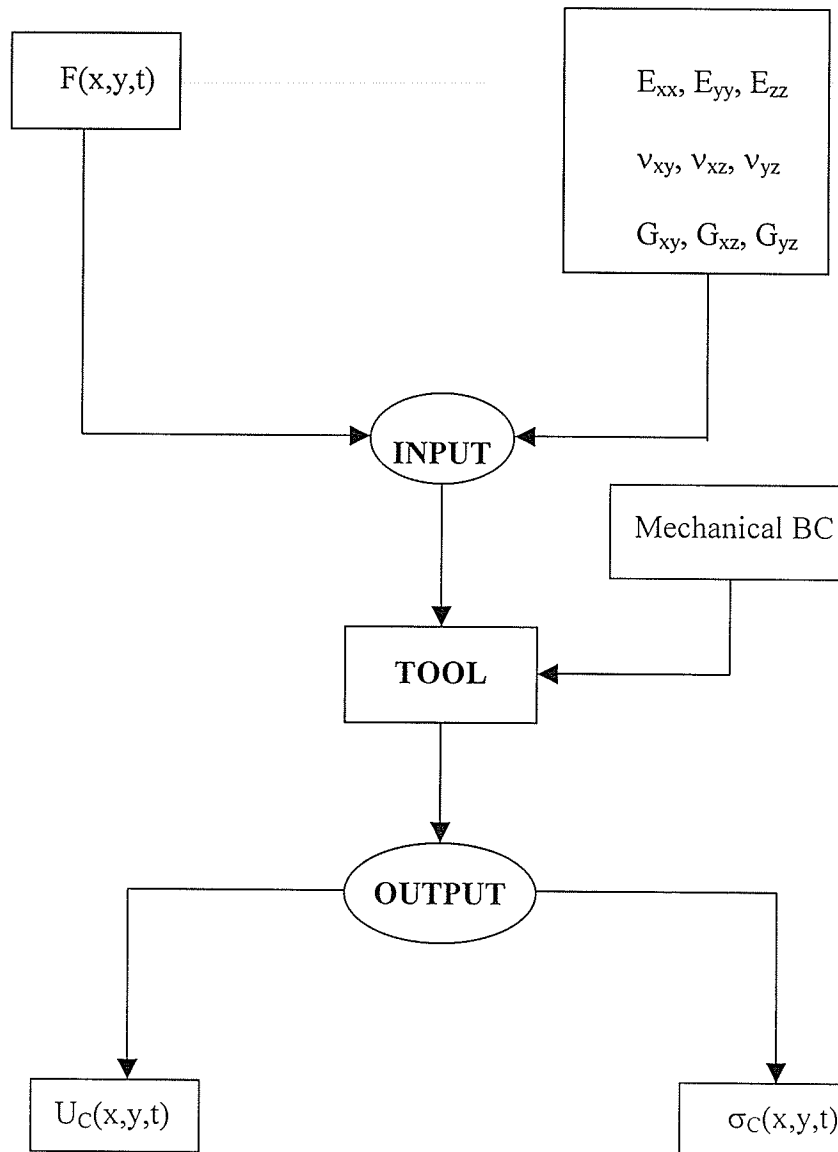
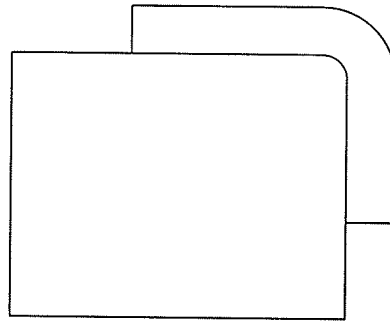
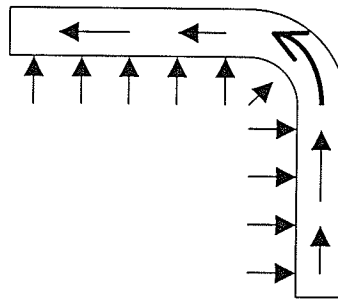


Figure 3.7 Schematic of Prediction of residual stress and warpage in the part

Tool-Part configuration



Residual force applied by the tool



Negative of the residual force
applied on the part

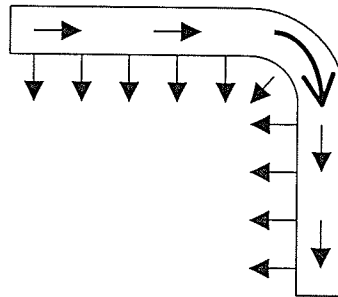


Figure 3.8 Tool removal simulation

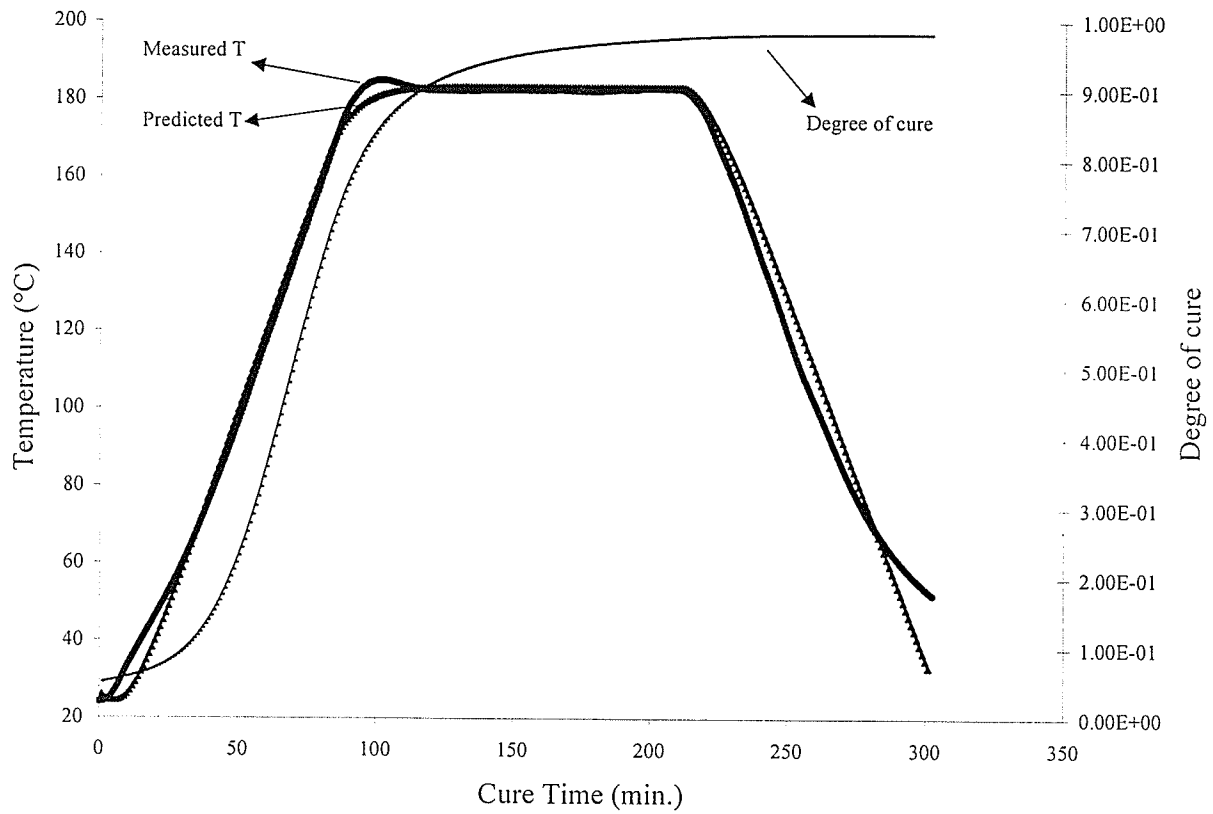


Figure 3.9 Validation of thermochemical module

Table 3.1 Properties of the cured composite used in ANSYS and analytical solution

| Composite Properties | E_{11} GPa | E_{22} GPa | G_{12} GPa | ν_{12} | ν_{13} | α_1 $^{\circ}\text{C}$ | $\alpha_2=\alpha_3$ $^{\circ}\text{C}$ | ϵ_1^c | $\epsilon_2^c=\epsilon_3^c$ |
|----------------------|-----------------|-----------------|-----------------|------------|------------|----------------------------------|---|----------------|-----------------------------|
| | 126.53 | 6.07 | 4.6 | 0.25 | 0.3 | 3.5 | 36.5 | 0.00048 | 0.0249 |

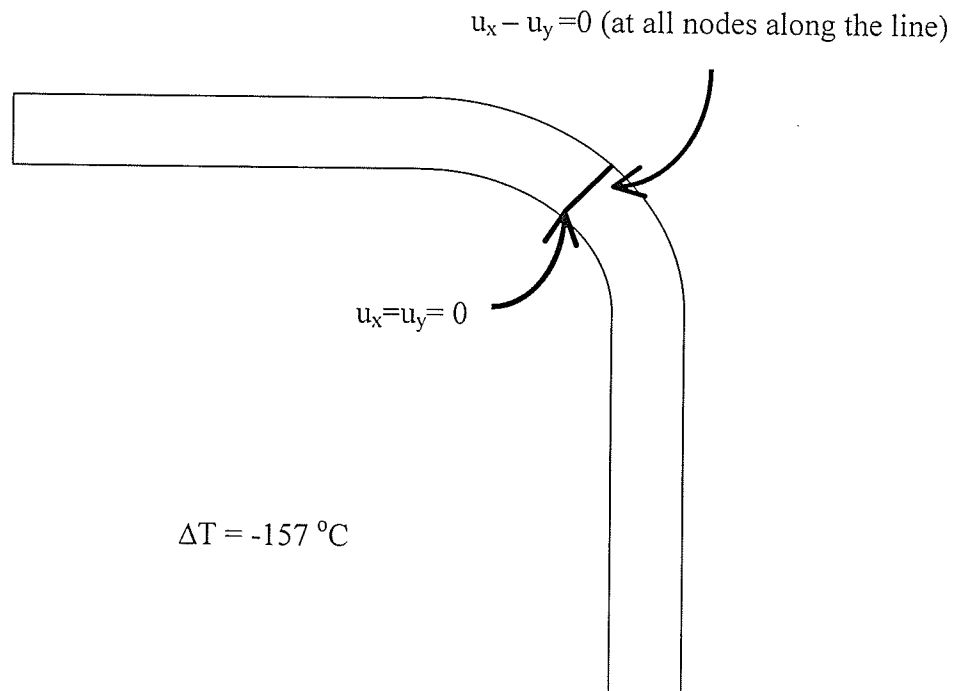


Figure 3.10 Boundary conditions used for Finite Element Analysis

CHAPTER 4

EXPERIMENTAL & SIMULATION DETAILS

This chapter provides details on the experimental and simulation work performed in this study. Experimental work involved (a) characterization of the material used in this study for its properties, and (b) study on the influence of process and material parameters on process-induced warpage in angle and flat laminates. Simulation study involved study on the influence of process and material parameters on process-induced warpage in angle laminates using the ANSYS-based process model. The material characterization was carried out at the University of Manitoba. Manufacturing of angle and flat laminates and the measurement of process-induced spring back were carried out at Boeing Canada Technology, Winnipeg division.

4.1 MATERIAL CHARACTERIZATION

Material characterization is one important component of this study to predict process-induced stress and warpage in composite laminates. Accurate measurement of properties of the composite is a priori for accurate prediction of the warpage. Many research studies in the past used the properties of completely cured composite while predicting the warpage. Those studies that used the more accurate relationship between composite properties and degree of cure obtained this relationship using simplified rule of mixtures. Since rule of mixtures has been proven to give only approximations for all properties except longitudinal modulus and physical properties, all composite properties were directly measured and used in the prediction of warpage.

The material used in this study is Cytec-Fiberite 934 neat resin and Cytec-Fiberite HMF 5-322/34C carbon fiber composite. This composite consists of Cytec-Fiberite 934 resin and Toray T300 carbon fibers as reinforcement. Boeing Canada Technology, Winnipeg division, supplied both the resin and prepreg. The prepreg used was fabric with volume fraction of 57.3% as stated by the manufacturer. The material was stored in a freezer at -18 °C until usage. The resin was stored in small vials and prepreg was stored in vacuum tight bags. A single vial of resin and small quantity of prepreg was taken out of the freezer at any given time for testing. After removing the material, the material was thawed for about one and half hour at room temperature and kept in a vacuum desiccators for about additional one and half hour to remove any condensed moisture or air bubble in the sample. Both resin and composite panels used for material characterization were cured in a vacuum oven or hot press using the manufacturer recommend cure cycle given in Figure 4.1. The samples with intermediate degree of cure were made using the cure kinetics data. The required physical, cure kinetics, thermo-physical, rheological and mechanical properties of the material are given in Figure 4.2. Details on characterization of each of these properties are given in subsequent sections.

4.1.1 PHYSICAL PROPERTIES

The required physical properties were composite density and fiber volume fraction. While the former was calculated using rule of mixtures using the physical properties of the constituents of the composite, the latter was obtained from the material suppliers data sheet.

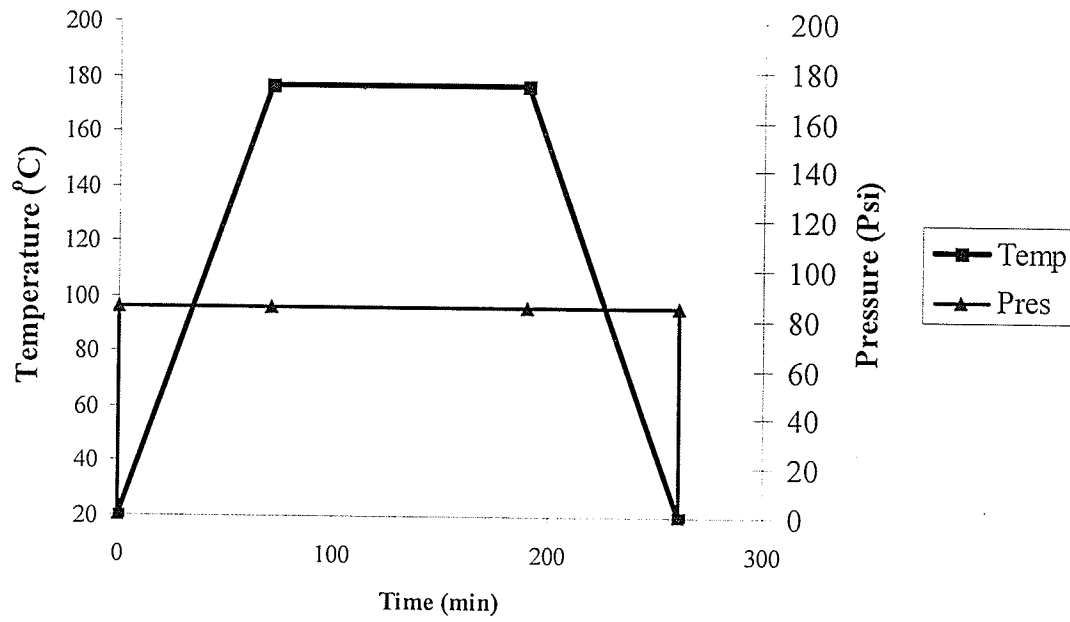
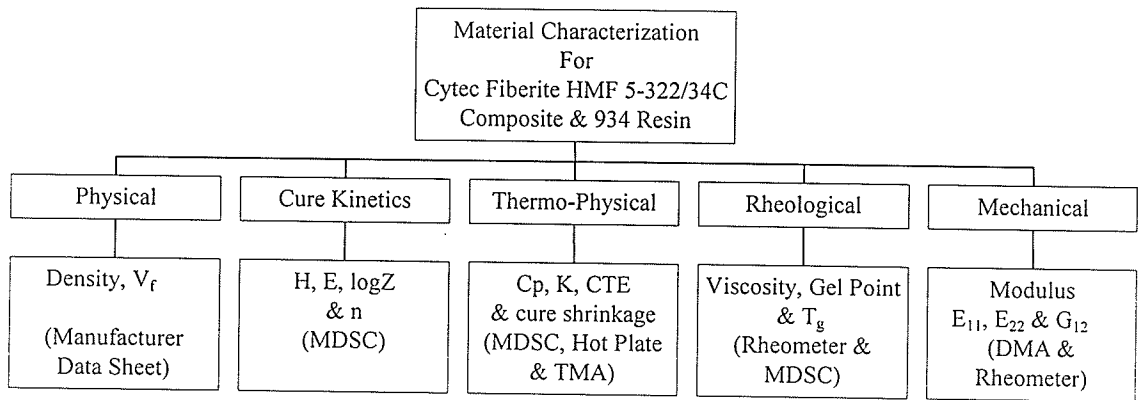


Figure 4.1. Manufacturer recommended cure cycle for Cytac Fiberite HMF 5-322/34C
Carbon Fiber Composite and 934 neat resin



4.2 Required material properties

The density of the 934-resin and the T300 fiber was found to be 1300 kg/m³ and 1760 kg/m³ respectively (41). In addition, the fiber volume fraction of the supplied prepreg was given to be 57.3 %. Using rule of mixtures equation,

$$\rho_c = \rho_f V_f + \rho_r (1 - V_f) \quad (4.1)$$

density of the un-cured HMF 5-322/34C composite prepreg with 57.3% volume fraction was calculated to be 1563.6 kg/m³. This is consistent with the density of 1555.5 kg/m³ given in the material data sheet. In the current study manufacturer supplied constant density of the composite is used. It is essential to use the equation (4.1) for the calculation of composite density if the process model includes the flow module and is capable of predicting the fiber volume fraction variation with respect to process time. However in the current study a constant composite density was used as an input parameter to the thermochemical module.

4.1.2 CURE KINETICS PARAMETERS

The cure kinetics parameters such as heat of reaction (H), Arrhenius constant (k), reaction order (n), activation energy (E), and pre-exponential factor (Z) for resin and composite were obtained using TA Instruments 2910 Modulated Differential Scanning Calorimeter (MDSC). A brief account of sample preparation and test procedure is given below.

The material was thawed and kept in vacuum for about an hour before testing. A resin sample of about 5-10 grams was placed in aluminum hermetic pans and crimped. In the case of prepreg, a sample of about 10-15 mg was placed in an aluminum non-hermetic

pan and crimped. The sample pan with sample, and reference pans were approximately of equal weight. Dynamic scans were carried out at heating rates of 5, 10 and 15 °C/min heating rate to obtain the total heat of reaction. Figure 4.3 shows a plot of dynamic scan result. The total area under the curve gives the total heat of reaction. Since the peak temperature was not constant for different heating rate, B & D kinetics or ASME method could not be used for the measurement of activation energy and pre-exponential factor. Hence, isothermal kinetics was used for this purpose. Figure 4.4 shows a sample isothermal scan. Isothermal scans were performed at peak temperature 190 °C and at range of temperatures between 100 °C and 190 °C. The dynamic scan data was used along with isothermal data to solve equation 4.2, in isothermal kinetics, to obtain the Arrhenius constant and reaction order at various cure temperature. In addition, from equation 4.3 by plotting (1/k) with respect to cure temperature in a logarithmic scale, the activation energy and pre-exponential factor were obtained.

$$\frac{d\alpha}{dt} = k(1 - \alpha)^n \quad (4.2)$$

Where,

$d\alpha/dt$ - rate of degree of cure

α - degree of cure

n - reaction order, and

k - reaction rate constant (1/min)

The temperature dependence of this rate constant is given by,

$$k = z e^{(-E / RT)} \quad (4.3)$$

Where,

E - activation energy (J/mol)

R - gas constant (8.314 kJ/kg K)

T - absolute temperature (K)

z – pre-exponential factor (1/min)

4.1.3 THERMO-PHYSICAL PROPERTIES

Thermophysical properties such as specific heat capacity, thermal conductivity, coefficient of thermal expansion and cure shrinkage of the composite were measured as a function of temperature and degree of cure.

4.1.3.1 Specific Heat Capacity

The specific heat capacity of the composite was used as an input to the thermochemical module. The specific heat capacity of the fiber and resin were measured directly using MDSC. The heat capacity of the composite was also measured using MDSC.

The sample preparation in this case was similar to the cure kinetics measurement. However in order to measure the differential heat flow between the sample and reference pans the weights of the reference pan, and sample pan with sample were not made equal. In addition, the specific heat capacity of the composite was also measured as a function of cure. However the trend in the measured specific heat capacity for composite as a function of cure was not observed due to the large scatter in the measured data as explained in chapter 5. Hence, specific heat capacity of composite was calculated using rule of mixture (equation 4.4) and above results for resin and fiber,

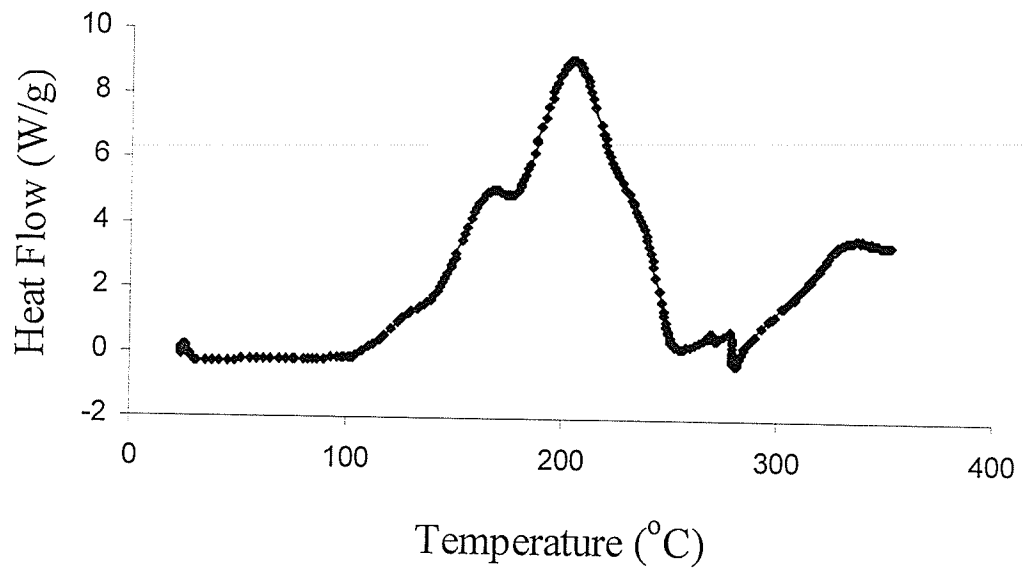


Figure 4.3. Raw data for a DSC dynamic scan

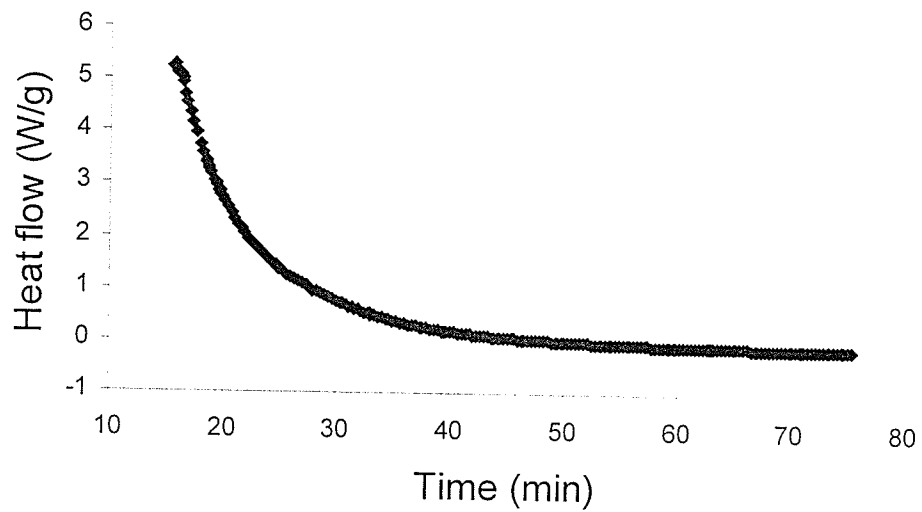


Figure 4.4. Isothermal DSC data for 934-resin

$$Cp_c = \frac{Cp_f \rho_f V_f + Cp_r \rho_r (1 - V_f)}{\rho_c} \quad (4.4)$$

where,

Cp_c is specific heat capacity of the composite J/kg K

Cp_r is specific heat capacity of the resin J/kg K

Cp_f is specific heat capacity of the fiber J/kg K

ρ_c is density of composite kg/m³

ρ_r is density of resin kg/m³

ρ_f is density of fiber kg/m³

V_f is fiber volume fraction

4.1.3.2 Thermal Conductivity:

Thermal conductivity of the composite was used as an input to the thermochemical module. Thermal conductivity of the fully cured composite in longitudinal and through-the-thickness direction was measured as a function of temperature using a hot plate. The change in the thermal conductivity of the composite with respect to resin degree of cure was assumed to be negligibly small based on the literature review (6). Composite samples of eight plies thickness (≈ 1.6 mm) and 1" diameter were used for through-the-thickness thermal conductivity measurement. Samples of 6x10x10 mm were used for longitudinal thermal conductivity measurement.

Figure 4.5 shows the schematic of the experimental set-up used for the thermal conductivity measurement. Two thermocouples were placed on the top and bottom

surfaces of the sample as shown in Figure 4.5. Alumina fiber insulation was used around the sample and hot plate surface in order to minimize the convection and radiation heat flow from surface of the hot plate and the sample. Thus a 1-D heat flow in the sample was achieved. Initially, the heat flow into the composite sample was calibrated using a steel sample of known thermal conductivity and dimension. The dimension of the steel sample was 1" diameter and 1" long. And thermal conductivity of the steel standard was 15 W/m K. At three isothermal temperatures the temperature gradient across the thickness of the specimen was recorded. The thermocouple readings were noted down at three temperatures. Using the temperature gradient data and thermal conductivity of the steel specimen, the heat flow per unit area into the specimen was calculated using Fourier conduction equation. Fourier equation for conductive heat transfer is given by,

$$Q = kA \frac{dT}{dl} \quad (4.5)$$

Where,

Q - amount of heat flow, W

k - thermal conductivity, W/ m K

A - cross sectional area of the sample, m²

dT/dl - temperature gradient across the thickness of the sample

The similar procedure was repeated for composite samples in through-the-thickness and longitudinal direction. Using the recorded temperature gradient data and heat flow per unit area, the thermal conductivity of the composite was calculated as a function of temperature using equation (4.5).

4.1.3.3 Coefficient of Thermal Expansion (CTE):

The CTE of the composite was used as an input to the material module. The CTE of the composite in the longitudinal and through-the-thickness direction was measured using TA Instruments' Thermo Mechanical Analyzer (TMA) 2940 at Boeing Canada Technology, Winnipeg division. Composite samples of 6mm diameter with eight plies thickness (1.6mm) were used for through-the-thickness CTE measurement. The prepreg plies were layed-up and cut into 6mm diameter samples. These samples were first debulked using a vacuum pump. Samples were then cured to three degrees of cure values, 32% (below gel point), 57 % (above gel point) and 100% using a vacuum oven. Samples of dimension 6x6mm and a thickness of 32 plies were prepared for CTE measurement in the longitudinal direction. For longitudinal CTE measurement samples were cured for two degrees of cure values, 32% (below gel point) and 100 %. Three samples per degree of cure and two samples per degree of cure were tested for the measurement of through-the-thickness and longitudinal CTE respectively.

A normal expansion probe of 0.1" diameter with 5gm static force was used to measure CTE of the composite as a function of temperature. The rate of heating was 2 °C/min. The temperature scan was performed from room temperature to the temperature, which initiates additional curing of the sample. The temperature range used for three degree of cure samples are, 32 % - RT to 100 °C, 57% - RT to 130 °C, and 100% - RT to 180 °C. A typical result is shown in Figure 4.6. Slope of this curve yielded CTE. In the case of unidirectional composites CTE in the transverse direction is equal to CTE in the through-the-thickness direction.

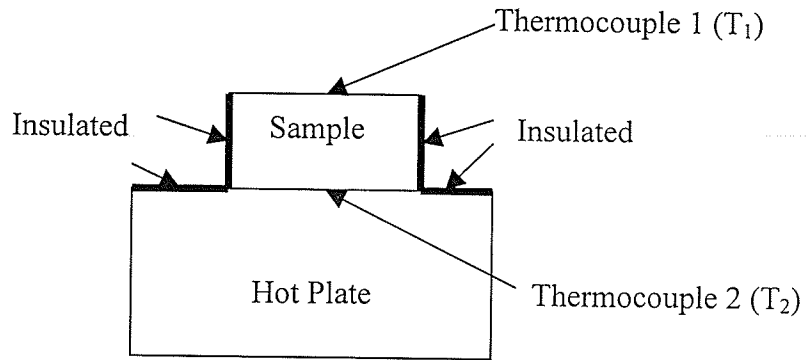


Figure 4.5 Schematic diagram of set-up for thermal conductivity measurement

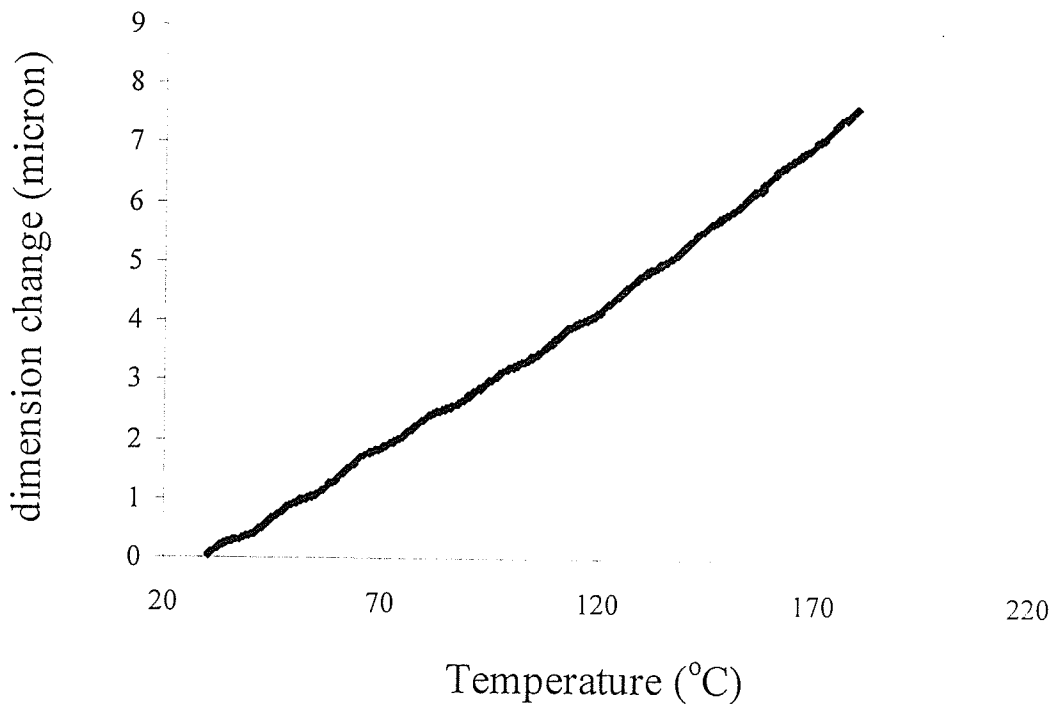


Figure 4.6 Raw TMA data obtained during the measurement of through-the-thickness

CTE

4.1.3.4 Cure Shrinkage Coefficient:

The cure shrinkage of the composite was used as an input to the material module. The cure shrinkage in the through-the-thickness and longitudinal direction were measured as a function of degree of cure using the TA Instruments' TMA 2940 at Boeing Canada Technology, Winnipeg division. The composite samples of 6mm diameter with eight plies thickness were used for cure shrinkage measurement in the through-the-thickness direction. The plies were laid-up and cut into 6mm diameter samples using a punch and die. The samples were then debulked using a vacuum pump at room temperature. For cure shrinkage measurement in the longitudinal direction samples of 6x6mm cross section with 32-ply thickness were prepared. Three samples were tested for through the thickness cure shrinkage measurement. Only one sample was tested for cure shrinkage in longitudinal direction due to the difficulty with sample preparation.

The macro expansion probe of 0.25" diameter with static force of 5gm was used in the measurement of cure shrinkage. The isothermal tests were performed at 160 °C and 177 °C for two hours until complete curing was achieved. Figure 4.7 shows the change in sample's linear dimension as a function of time in the thickness direction due to cure shrinkage. The cure shrinkage of the composite as function of degree of cure was calculated using the raw data and cure kinetics model. The cure shrinkage was found to be linear function of degree of cure as shown in Figure 4.8. Cure shrinkage coefficient is the slope of this plot. In the case of unidirectional composites cure shrinkage in the transverse direction is equal to cure shrinkage in the through-the-thickness direction. The temperature dependence of cure shrinkage was observed. However, due to the difficulty

in the availability of TMA, only two tests were performed and the measured shrinkage data at 177 °C was used in process model.

4.1.4 RHEOLOGICAL PROPERTIES

Rheological properties such as viscosity and gel point of the resin were measured using Bohlin CVO 120 Rheometer. The glass transition temperature (T_g) was measured as a function of cure using the TA Instruments MDSC.

4.1.4.1 Gel Point:

Gel point is the degree of cure when the polymer matrix transforms from liquid state to a gel state. Even though gel point is not used as an input to the process model directly, gel point is useful to decide,

- (a) The minimum cure level to test samples for mechanical properties since samples with cure levels below gel point will not be able to sustain the applied load,
- (b) To design the cure cycle for simulation parametric study

The gel point of the 934-resin was measured using Rheometer parallel plate fixture in oscillation mode. The parallel plate fixture used was 1" diameter. The resin sample in the small vial was thawed for about one hour and kept under vacuum for about one and half hour. To facilitate easy handling of the sample, the sample was heated at about 60 °C in an oven until the viscosity of the resin starts dropping. The resin sample was then placed between the parallel plates and a gap of about 1mm was set. During the test the gap is maintained constant by changing the normal force. A shear stress of 800 Pa at a

frequency of 1 Hz was used. The temperature scans were performed at a heating rate of 2 °C/min from room temperature to 200 °C. The elastic and viscous moduli were measured as a function of temperature. When the resin gels, the elastic and viscous modulus curve cross-over as shown in Figure 4.9. The cure extent corresponding to this cross-over point is the gel point and it is calculated using the temperature corresponding to this cross-over point, heating rate and resin cure kinetics. Two resin samples and a composite sample was tested.

4.1.4.2 Viscosity of Resin:

The viscosity of the resin is used as an input to the flow module. In the current study the viscosity data was not used since the process model does not include a flow module. The viscosity of resin was measured as a function of temperature and degree of cure using Rheometer parallel plate fixtures in Viscometry mode. The sample preparation for viscosity measurement was similar to that of the gel point measurement.

The resin sample was placed between the parallel plates of Rheometer and a gap of 1mm was set in the Viscometry mode. The constant gap was maintained by changing the normal force. Shear stress of 1 Pa was applied to the sample. The temperature scan was performed from room temperature to 200 °C at heating rates of 2, 3 and 5 °C/min. Figure 4.10 shows a typical result for viscosity as a function of temperature for three different heating rates. Two trails were performed for each heating rate. The modeling of the viscosity data can be found in Chapter 5.

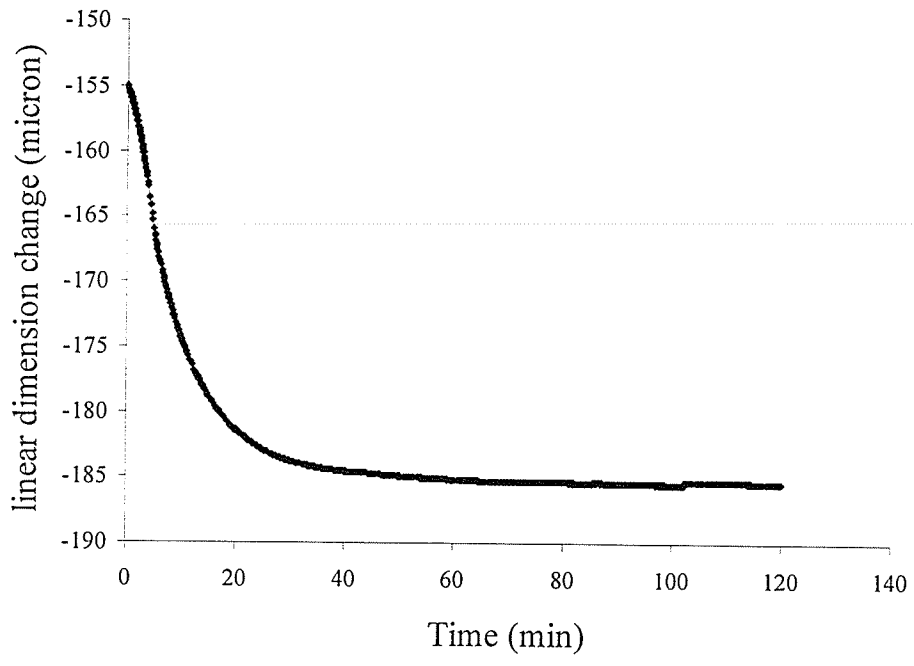


Figure 4.7 Cure shrinkage raw data from TMA

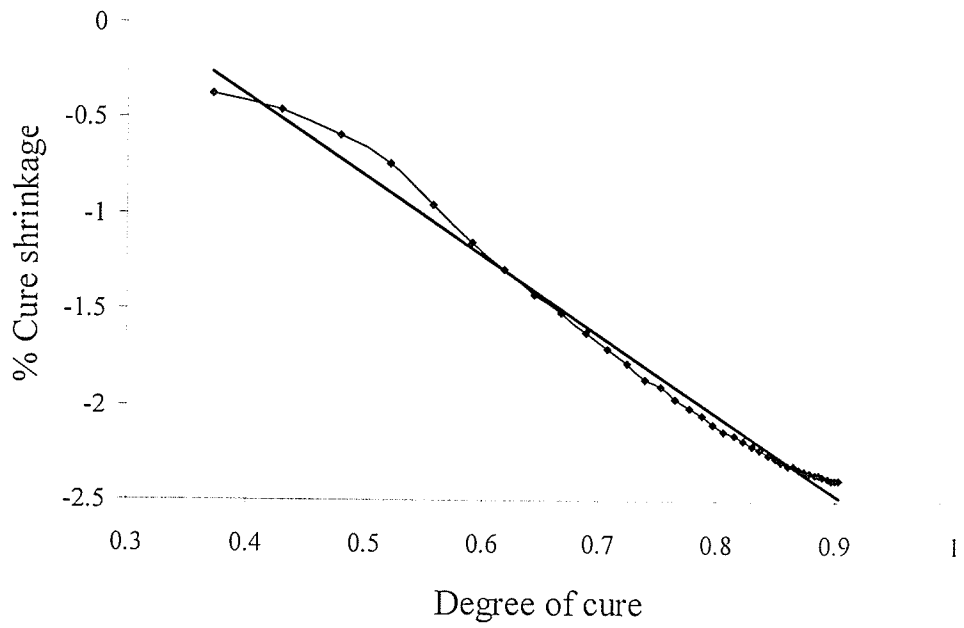


Figure 4.8 Through the thickness cure shrinkage as a function of degree of cure

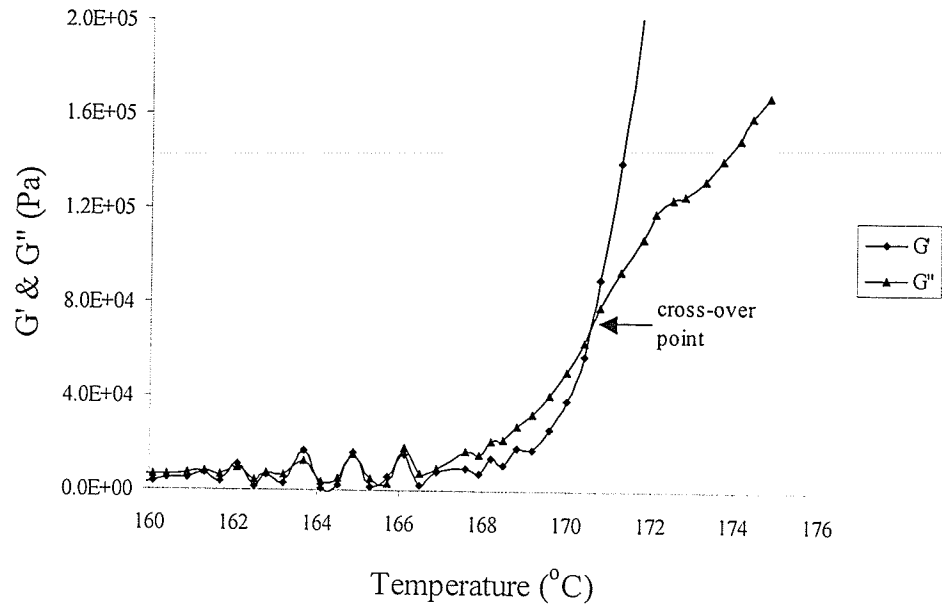


Figure 4.9 Gel point of 934-neat resin

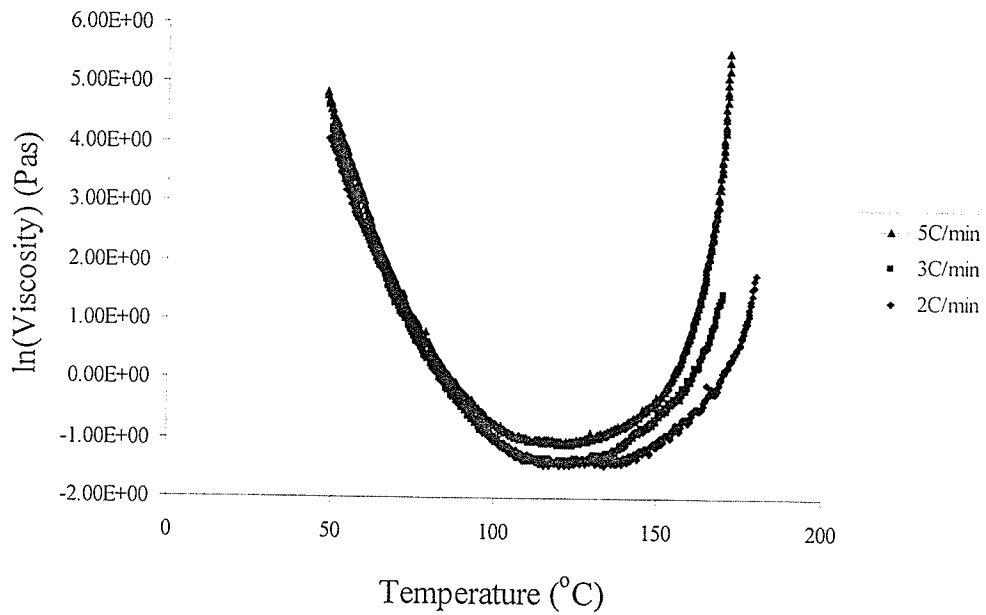


Figure 4.10 Viscosity of 934-resin at three different heating rates

4.1.4.3 Glass Transition Temperature (T_g):

The glass transition temperature of the 934-resin was measured using MDSC. The glass transition temperature helps to delineate the role of cure kinetics from diffusion during the polymerization reaction. Five samples with a range of degree of cure between uncured state and complete degree of cure were used to measure the glass transition temperature as a function of cure temperature. The sample was cured isothermally using MDSC at cure temperature of 177 °C for different time periods to achieve five degree of cure from uncured state to complete degree of cure. The glass transition temperature of these samples was measured using MDSC by performing dynamic scan from sub zero temperature to 300 °C. The temperature at which reversible heat flow path changes sharply is the glass transition temperature of the sample as shown in figure 4.11. The measured glass transition temperatures can be used to delineate the diffusion from cure kinetics as explained in chapter 5.

4.1.5 MECHANICAL PROPERTIES

4.1.5.1 Longitudinal (E_{11}) & Transverse Moduli (E_{22} , E_{33}):

The longitudinal and transverse moduli of the composite was used an input to the material module. The longitudinal and transverse moduli of the composite were measured using TA Instruments 2980 Dynamic Mechanical Analyzer (DMA). The eight unidirectional prepreg was layed-up and cut into samples of dimension 2mmx0.8mmx40mm. The samples were pre-cured isothermally at 130 °C for two hours using a vacuum oven to achieve 35% (slightly less than the gel point) degree of cure so that they could take the applied load.

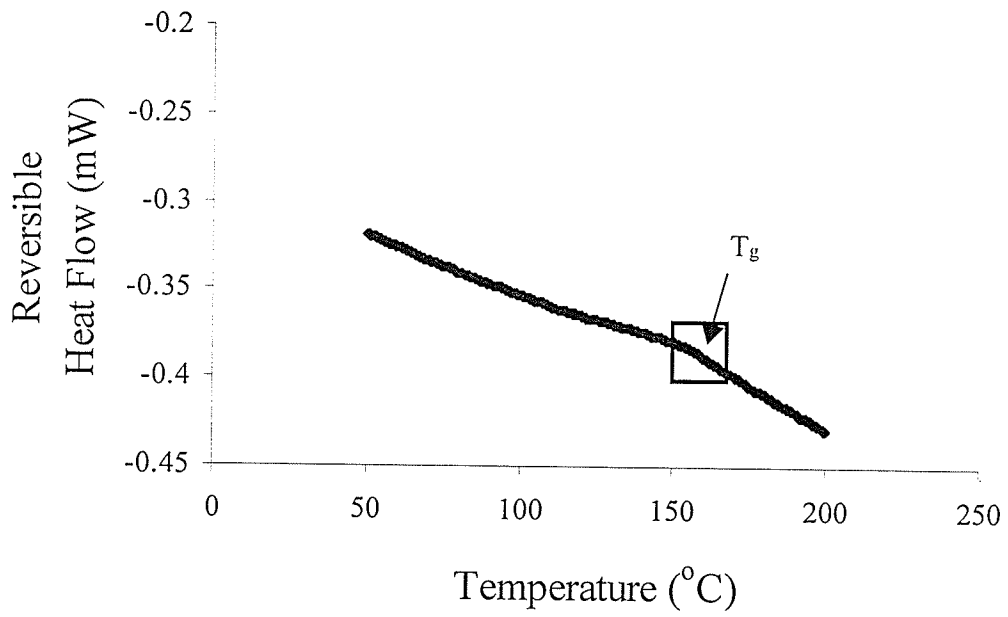


Figure 4.11 T_g of 88% cured composite measured from DSC

Isothermal tests were performed at 130 °C, 160 °C and 177 °C for two hours using a frequency of 1 Hz. A strain of 0.005 % was applied during the test. Two samples were tested for each temperature. Figure 4.12 shows the raw data of longitudinal moduli as a function of time at 177 °C. The moduli as a function of degree of cure at three temperatures were calculated using cure kinetics model. The three curves were superimposed to obtain longitudinal moduli as a function of degree of cure from 35 % cure to complete cure state. The curves were found to superimpose very well and hence the influence of temperature was found to be relatively negligible as compared to degree of cure on longitudinal modulus. Similar to longitudinal moduli transverse moduli (E_{22}) was measured using DMA at 160 °C and 177 °C. In addition, E_{33} was taken to be equal to E_{22} assuming that this composite was transversely isotropic. The details of modulus model used in this study are explained in chapter 5.

4.1.5.2 Shear Modulus:

The shear modulus of the composite was used as an input to the material module. The composite shear modulus was measured using the Rheometer. Four unidirectional prepreg was layed-up and were debulked using a vacuum pump. The samples were then cut into dimension of 5x40 mm. The samples were subjected to torsion test at isothermal temperature of 130, 160 and 177 °C using solid fixture. Frequency was set to 1 Hz and shear stress of 1000 Pa was applied during the test. The shear modulus (G_{12}) of the sample was measured through out the cure. Figure 4.13 shows the sample plot of measured shear modulus. Using the cure kinetics model and measured shear modulus as a function of time, the shear modulus of the composite was calculated as a function of

degree of cure. Similar to the longitudinal and transverse moduli, the step model for shear modulus of the composite was made and used in the material module. In addition, due to the scatter in the measured data, the measured shear modulus at 177 °C was used in the model. The effect of temperature on shear modulus was not taken into account.

4.2 EXPERIMENTAL PARAMETRIC STUDY

4.2.1 Reasons For Experimental Parametric Study:

In the current study experimental parametric study was performed to:

- (i) Provide part temperature data to validate process model
- (ii) Understand how and why the process-induced warpage was influenced by various parameters studied

4.2.2 Parameters Used in Experimental Parametric Study:

In the experimental parametric study the influence of parameters, which could be studied experimentally were studied through experiments. Hence, tool material CTE, thermal mass of the tool and process cycle parameters are chosen as parameters in the experimental parametric study. Three tools were used in the current study to manufacture the angle laminates as well as flat laminates. The effect of CTE of the tool on process-induced warpage was studied by using Aluminum (ALH & ALL) and Invar (INV) tools with CTE, 22.14 and 1.7 $\mu\text{°C}$ respectively. The influence of tool thermal mass on process-induced warpage was studied using Aluminum tools (ALH & ALL) of two different thermal masses. The thermal mass of ALH tool is about four times that of the ALL tool.

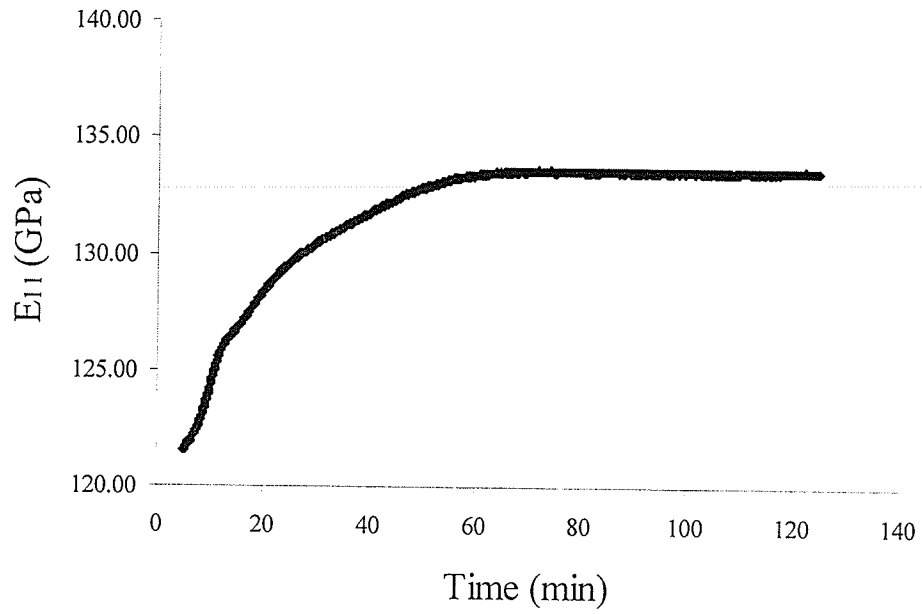


Figure 4.12. Longitudinal modulus measured from DMA

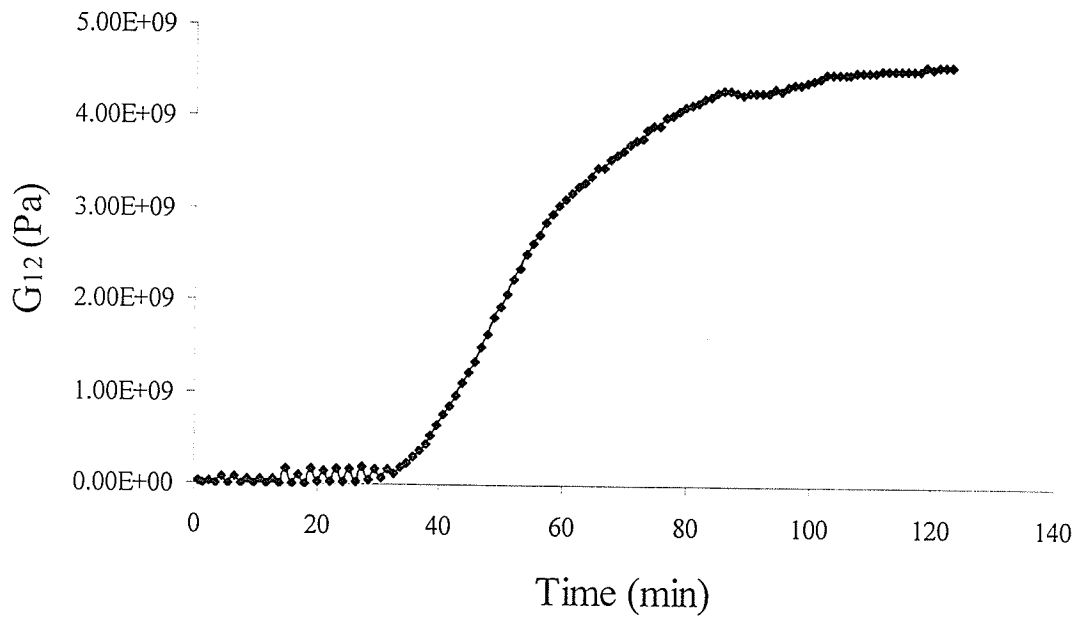


Figure 4.13 Shear modulus of the composite measured from Rheometer

The influence of process cycle parameters on process-induced warpage was studied by changing the cure cycle parameters in the manufacturing of angle and flat laminates. The compaction pressures of 45 Psi and 85 Psi were used in the current study. The cycles with and without dwell were used to understand the influence of application of dwell on process-induced warpage. This leads to four different process cycles as shown in figure 4.14.

The four different process cycles used in the manufacturing of angle and flat laminates are:

- Cycle 1 - Manufacturer recommended cycle with 45 Psi pressure
- Cycle 2 - Modified cycle with 45 Psi pressure
- Cycle 3 - Manufacturer recommended cycle with 85 Psi pressure
- Cycle 4 - Modified cycle with 85 Psi pressure

In the modified process cycle dwell was applied at 121 °C to see the effect of dwell on process-induced warpage. In addition, application of dwell changes the cure path and hence the influence of cure path on process-induced warpage could be studied using modified cure cycle.

4.2.3 Manufacturing of Angle Laminates and Flat Laminates:

In order to understand the influence of above parameters on process-induced warpage the twelve angle laminates and flat laminates were manufactured using three tools and four process cycles using an autoclave at Boeing Canada Technology Ltd Winnipeg division. The parts were manufactured using Cytec Fiberite HMF 5-322/34C plane weave fabric

yielding a laminate sequence of $[0,90,45,-45,90,0,45,-45]_s$. The laminate sequence was kept as a constant parameter in the current study. The dimensions of the manufactured angle laminates and flat laminates were 8.5"x14" and 3.5"x14" respectively. In addition, the cured laminate thickness was about 3.2mm. The three tools used in the manufacturing of parts are of different geometry and thermal mass. The geometry and properties of the tools used in the current study are given in Appendix B.

During manufacturing of angle laminates and flat laminates the plane weave fabric prepregs were cut into the desired dimension and orientation. The tools were coated with three sets of non-stick agent with an interval of 15 minutes between successive coats. The plies were layed-up on each tool in a desired laminate sequence. During the lay-up process, the vacuum was applied after every four plies in-order to ensure proper compaction of the laminate during lay-up process. Two thermocouples were placed diagonally opposite in the mid plane of the part in order to record the part temperature during entire cure cycle. This data is also useful in validating the accuracy of process model in predicting the part temperature throughout the cure cycle. Once the part was completely layed-up the final vacuum tight bag was prepared and the tool/part with bag was tested for leak proof. Three parts were cured at a time using an autoclave at Boeing Canada Technology Ltd Winnipeg division. The dimension of the autoclave used was 4' diameter and 8' long. The location of the tool/part assembly in each case was kept constant during each cure cycle. Figure 4.15 shows the location of the tools in the autoclave. The location of thermocouples can also be seen from this figure. In addition, the autoclave pressure and temperature was recorded during entire cure cycle.

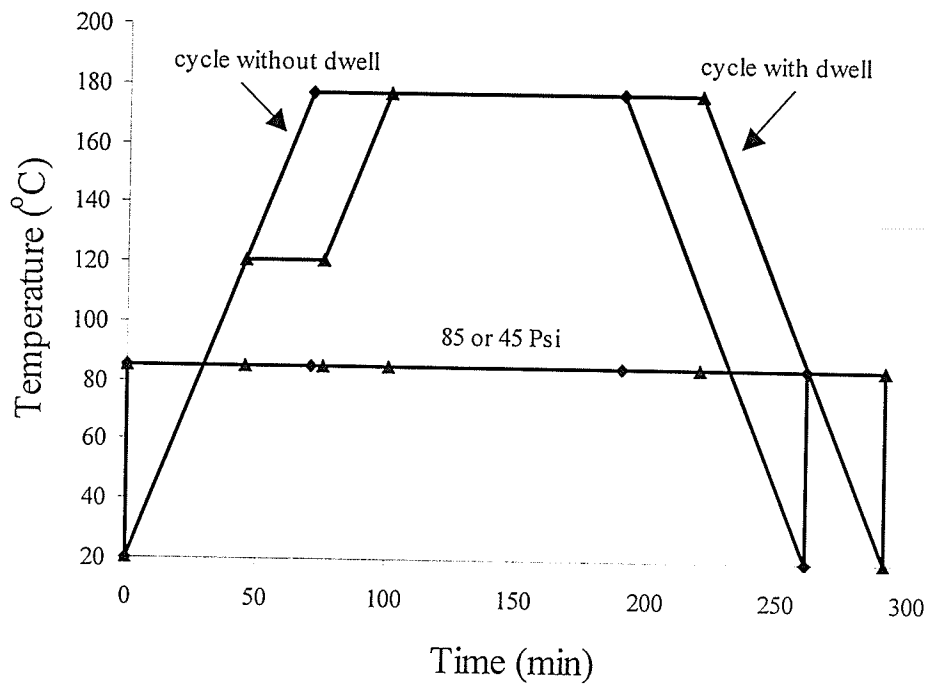


Figure 4.14 Cure cycles used in the manufacturing of angle and flat laminates

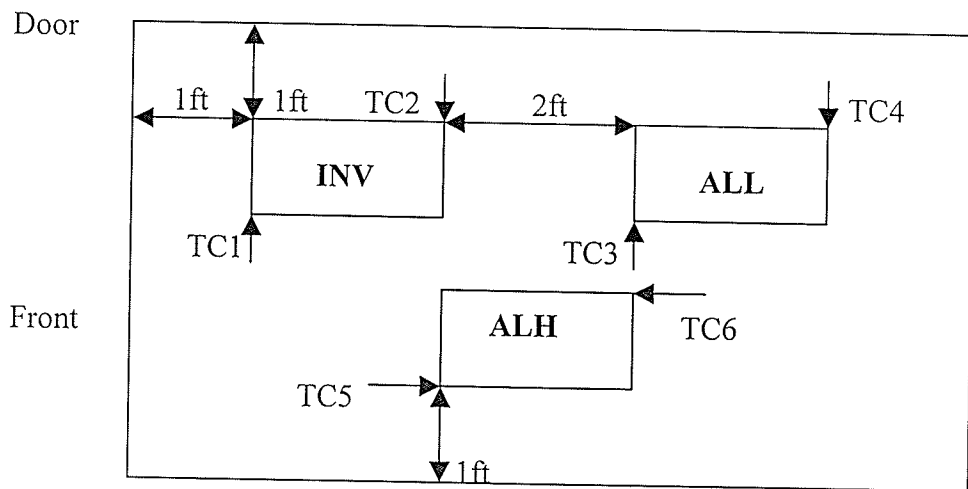


Figure 4.15 Location of the tools in the autoclave during processing

4.2.4 Warpage Measurement:

The parts were debugged after the curing process and trimmed to measure the process-induced warpage. The warpage (spring back angle) in the case of angle laminates was measured using ROMER Super Tech Arm system at Boeing Canada Technology Ltd Winnipeg division. The process-induced warpage (deflection) in the case of flat laminates was measured using a precision dial gauge at the University of Manitoba.

The ROMER instrument can measure the location of a point with an accuracy of 0.008". Using this instrument the locations of 15 points along the cross section of angle laminate was measured. The similar data was collected at four different planes along the length of the each part. Figure 4.16 shows a sample plot of the data obtained from the ROMER instrument for an angle laminate at one plane. The spring back angle was calculated by determining the slope (m) of the straight arms portion of the angle laminates. The spring back angle was calculated as,

$$\theta = 2 \tan^{-1}(m) \quad (4.6)$$

The average of the calculated spring back angles at four planes was used as measure of the process-induced warpage. The measured warpage in the case of angle laminates includes contribution from two mechanisms namely, anisotropy in CTE and cure shrinkage and tool-part interaction. Hence, in order to understand to the contribution of tool-part interaction to warpage 12 flat laminates of 3.5"X14" were manufactured using flat arm portion of the three tools and four process cycles. The laminate sequence was same as that used in the case of angle laminates. The process-induced warpage in the case of flat laminates was measured using a precision dial gauge with magnetic stand. The dial

gauge can measure deflection in the plates or beams with an accuracy of 0.001". Figure 4.17 shows a sample plot of the profile of the processed laminate. The maximum deflection of the part is used as a measure of the process-induced warpage. In addition, the warpage in the arm of the angle laminate was also measured using the ROMER data. This data was useful for understanding the error in the measured spring back angle due to warping of the arm.

4.3 SIMULATION PARAMETRIC STUDY

Since the tool-part interaction has not been satisfactorily understood and modeled till today, the warpage of the part was predicted ignoring the tool part interaction i.e. warpage due to anisotropy in CTE and Cure shrinkage (spring back) alone was predicted.

This was accomplished as follows:

- (a) At the outset, thermo-chemical module was run using FE mesh of part and tool together
- (b) Using the temperature and cure predictions from this module, material properties were calculated using the Material module
- (c) Another mesh of the part alone was created. Using this mesh and the properties calculated using the material module, the spring back of the part was predicted. The predicted warpage due to anisotropy in CTE and cure shrinkage was subtracted from the experimental warpage to obtain the contribution due to tool-part interaction. Since gradient in temperature and fiber volume fraction wasn't observed in experimentally manufactured composite laminates, it is believed that the total experimental warpage is entirely due to these two mechanisms.

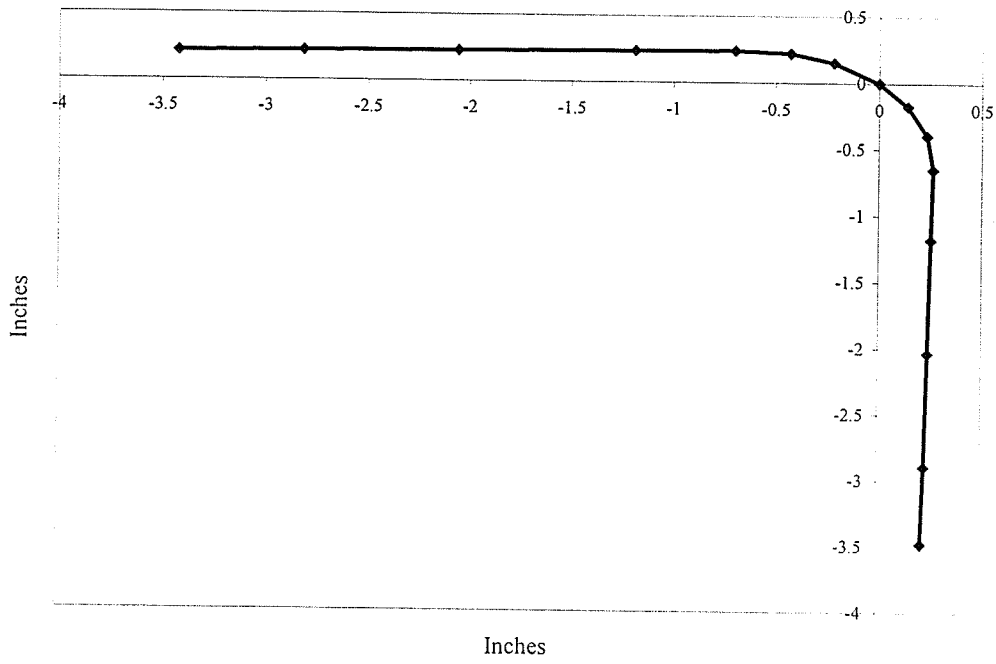


Figure 4.16 Data collected using ROMER for an angle laminate

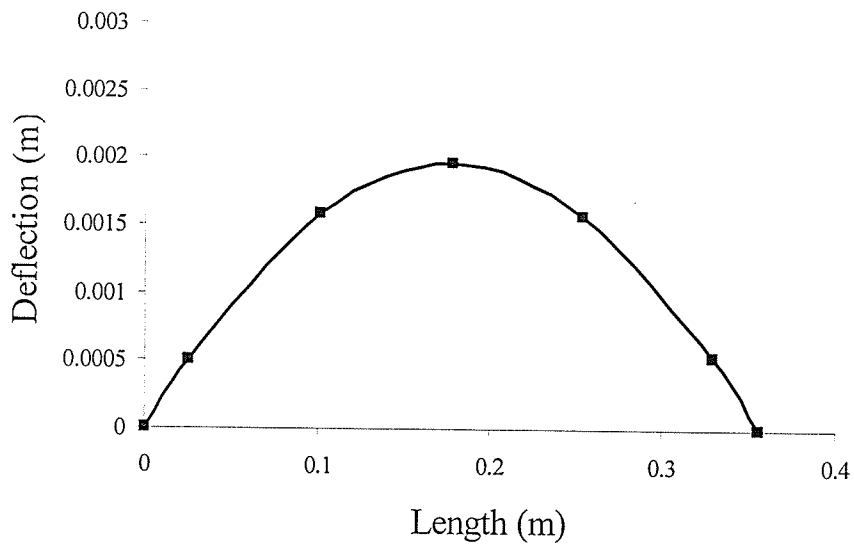


Figure 4.17 Measured warpage in flat laminate

Details on material, and thermal and stress boundary conditions used in the simulation as well as various parameters studied are given in subsequent sections.

4.3.1 Material:

The material used in this study is Cytec-Fiberite HMF 5-322/34C carbon fiber composite. The details of material properties can be found in next chapter.

4.3.2 Thermal Boundary Condition:

Information on autoclave convective heat transfer boundary condition within the accuracy was required for thermochemical module. The exact thermal boundary condition for thermochemical module was obtained from SIMCLAVE developed by Mike et.al.(10). The effective autoclave heat transfer is given by equation 3.4. The effective “c” values used in this equation for various boundaries is given in Table 4.1. Figure 4.18 shows the corresponding boundaries of the tool/part configuration. The effective “c” values used have been corrected for the influence of location and orientation of the part/tool in the autoclave.

4.3.3. Stress Boundary Conditions:

The boundary condition used in the stress module for the prediction of process-induced warpage due to anisotropy in CTE and cure shrinkage is as shown in Figure 4.19. The UM process model can also predict the warpage due to mechanism of tool-part interaction which is modeled using a calibrated shear layer. However, due to the

inadequate understanding of the tool-part interaction, and lack of accuracy in predictions warpage due to tool-part interaction was not simulated in this study.

4.3.4 Simulation Study Parameters:

4.3.4.1 Material Parameters:

The two materials parameters studied in the simulation parametric study are CTE of tool material and thermal mass of the tool. The properties of the tool material can be found in Appendix B. The thermal mass of ALH tool is about four times that of ALL and thermal mass of INV tool is about twice that of the ALL tool. The thermal analysis as well as the prediction of process-induced warpage due to anisotropy in CTE and cure shrinkage was performed for three tools.

4.3.4.2 Geometric Parameters:

In the current study the influence of two major geometry parameters on spring back was studied. The autoclave heat transfer and part thickness were the two geometry parameters studied in the current simulation study. The autoclave heat transfer was found to vary along the length of the autoclave based on the experiments performed by Mike et.al.(10). The scatter of about 30% in the autoclave heat transfer was observed. Hence, $\pm 30\%$ change in the autoclave heat transfer was used in the simulation parametric study.

In order to understand the influence of laminate thickness on process-induced spring back, the simulation was performed for three different laminate thicknesses. In this case all the parameters were kept constant, only the laminates thickness was varied. The

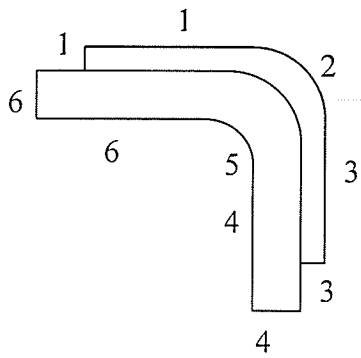
analysis was performed for three different laminates thickness as original thickness, twice the original thickness and triple the original thickness. The predicted part temperature, degree of cure and spring back were compared in all the three cases to understand the influence of laminate thickness on these parameters.

4.3.4.3 Cure Cycle Parameters:

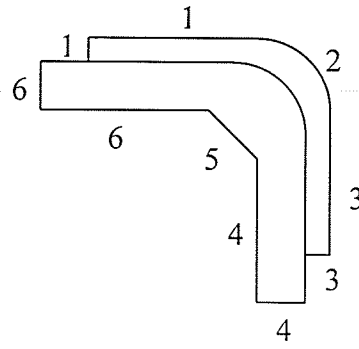
The influence of the cure cycle parameters on process-induced spring back was also studied through simulation parametric study in addition to experimental parametric study. The analysis was performed for three tools and five process cycles. The five cycles used for this purpose are four measured autoclave temperature cycles and a manufacturer recommended cycle. Figure 4.20 shows the cycles used in the simulation study. The compaction pressure was varied during the simulation study. In addition, cycles with and without dwell were used for simulation study.

This leads to total of five process cycles, one manufacturer recommended cure cycle and four-measured autoclave air temperature cycles as given below.

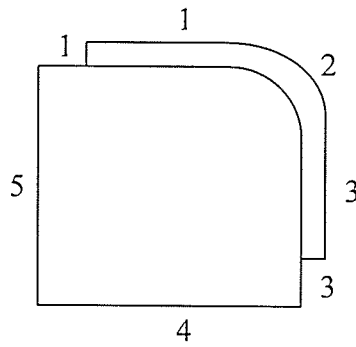
- MR Cycle - 45 Psi Manufacturer recommended cycle
- Cycle 1 - 45 Psi pressure without dwell
- Cycle 2 - 45 Psi pressure with dwell
- Cycle 3 - 85 Psi pressure without dwell, and
- Cycle 4 - 85 Psi pressure with dwell



Tool - A (ALL)



Tool - B (INVAR)



Tool - C (ALH)

Figure 4.18 Thermal BC's used in simulation study

Table 4.1 Effective “c” values used as thermal BC’s during simulation

| Boundary (Fig. 4.18) Tool | 1 | 2 | 3 | 4 | 5 | 6 |
|---------------------------------|-------|-------|-------|-------|--------|-------|
| ALL | 0.125 | 0.123 | 0.121 | 0.375 | 0.368 | 0.361 |
| INVAR | 0.179 | 0.172 | 0.165 | 0.515 | 0.5135 | 0.512 |
| ALH | 0.12 | 0.12 | 0.12 | 0.246 | 0.39 | - |

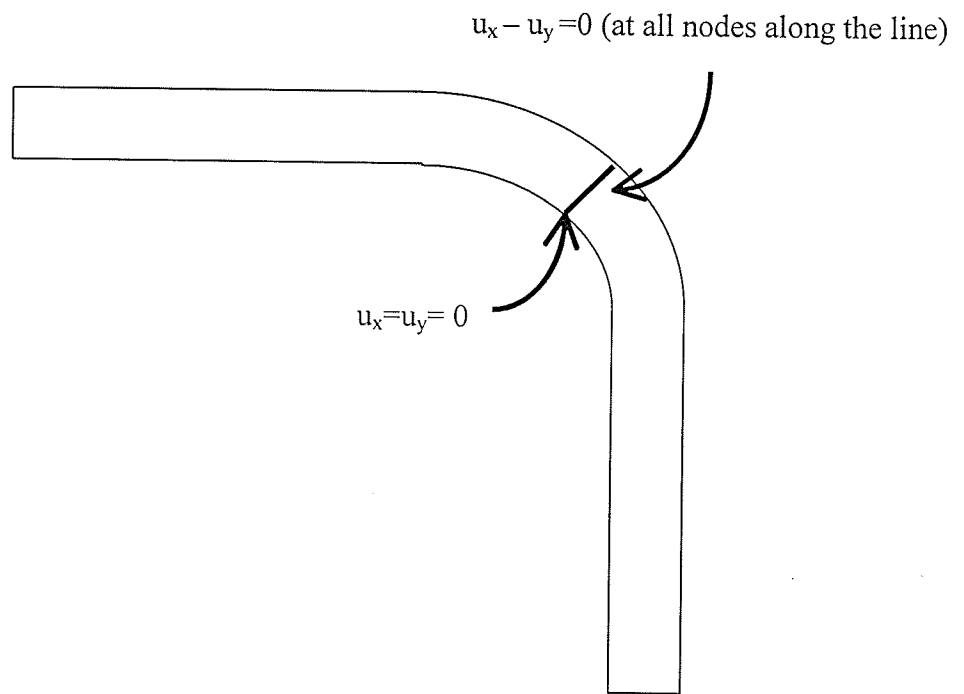


Figure 4.19 Boundary conditions used for Finite Element Analysis

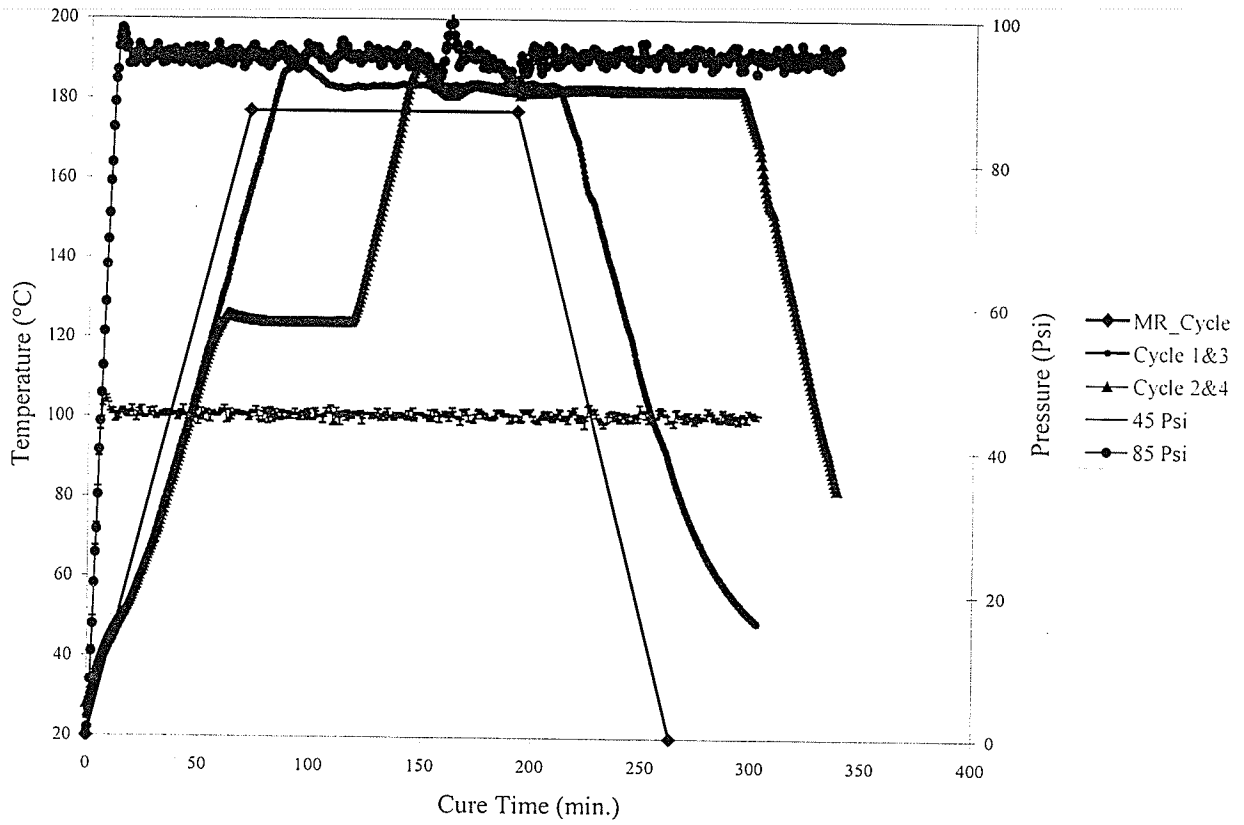


Figure 4.20 Cure cycles used in the simulation study

The summary of material, geometric and process parameters used in the simulation study are shown in Table 4.2. In addition, the influence of gel time and cure path on process-induced warpage was studied by changing the dwell temperature in the process cycle. Figure 4.21 shows the cure cycles used to understand the influence of dwell temperature and cure path on spring back. Cycle 1 was used to understand the effect of gel time on warpage through simulation study. For this purpose the dwell temperature was varied to 80 °C and 140 °C from 121 °C.

4.3.4.4 Thermo-Physical properties:

The influence of thermophysical properties on spring back was found to be insignificant based on the literature review. Hence, in the current study only the specific heat capacity of the composite value was varied by 10% in the simulation study to ensure the similar trend. The extensive simulation parametric study of thermophysical properties was not performed in this study.

4.3.4.5 Cure-Kinetics Parameters:

Based on literature review the cure kinetics parameters were found to be the most important parameters in the prediction of process-induced warpage. Hence, a greater attention was given to these parameters in the current study. Table 4.3 shows the cure kinetics parameters used in the simulation parametric study. In addition to initial degree of cure, heat of reaction, activation energy, the influence of cure kinetics reaction order model constant on predicted part temperature, degree of cure and spring back was studied through the simulation study.

4.3.4.6 Mechanical Properties:

In the current study the effect of composite modulus on spring back was studied using the process model. From the previous studies it was found that the composite modulus models plays an important role in the prediction of warpage. Hence, in the current study a grater attention was paid to these parameters. Table 4.4 shows the mechanical properties used in the current study. In addition, the combined effect of cure kinetics and mechanical properties were studied in the current simulation parametric study.

4.4 SUMMARY

The details on material characterization, experimental and simulation parametric study were focused in this chapter. An extensive material characterization of Cytec Fiberite 934 neat resin and composite were performed as an input to the process model to predict the warpage. The experimental parametric study was performed through the angle laminates and flat laminates to understand the effect of process cycle and tool material on process-induced warpage. The effect of parameters such as cure kinetics, autoclave heat transfer, cure shrinkage, gel time, cure path and modulus of the composite were studied through simulation using ANSYS based process model.

Table 4.2 Material, Geometric and Process parameters used in simulation study

| Parameter | Nominal | Maximum | Minimum |
|-------------------------|--|---------|---------|
| Material Parameters | | | |
| Tool Material | Two materials: Aluminum & Invar | | |
| Thermal Mass | Three different thermal mass: ALL, INVAR & ALH | | |
| Geometric parameter | | | |
| Autoclave heat transfer | $h = C (P/T)^{0.8}$ | +30 % | -30 % |
| Part Thickness | 2xt | 3xt | 1xt |
| Process Parameters | | | |
| Process cycle | Five cycles (Figure 4.20) | | |

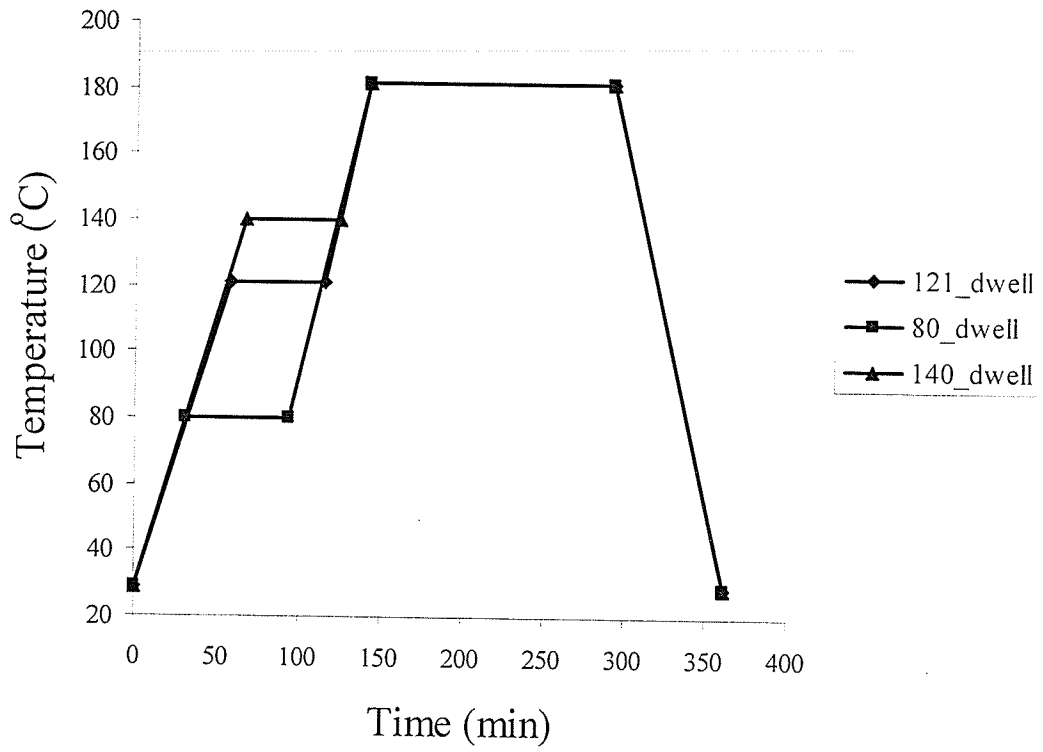


Figure 4.21 Cycles used in the simulation study of gel time and cure path

Table 4.3 Cure kinetics parameters used in the simulation parametric study

| Parameter | Nominal | Maximum | Minimum |
|-----------------------------|---------|---------|---------|
| Cure Kinetics | | | |
| Initial degree of cure | 0.05 | 0.1 | 0.01 |
| Heat of reaction kJ/kg | 483.4 | 531.74 | 435.06 |
| Activation energy kJ/mol | 34.88 | 38.36 | 31.39 |
| Reaction order parameters | | | |
| n_0 | 14.95 | 16.4 | 13.45 |
| T_0 (°C) | 139.2 | 160 | 120 |
| A | -13.2 | -11.9 | -14.56 |
| B | 9.95 | 11.75 | 8.15 |

Table 4.4 Mechanical properties used in the simulation study

| Parameter | Nominal | Maximum | Minimum |
|----------------------------|---------------------|---------|---------|
| Mechanical Properties | | | |
| Modulus of composite (GPa) | | | |
| E_{11} | $38.57\alpha+87.96$ | +10 % | -10% |
| E_{22} | $2.44\alpha+3.62$ | | |
| G_{12} | $31.7\alpha-27.1$ | | |

CHAPTER 5

RESULTS

Results from material characterization, experimental and simulation parametric study are presented in this chapter.

5.1. MATERIAL CHARACTERIZATION

The results of material characterization that are used as input for the process model for prediction of process-induced warpage is presented in this section. The details on individual runs are given in Appendix C.

5.1.1 Cure Kinetics:

The cure reaction for Cytac Fiberite 934 resin and composite was found to be an n^{th} order reaction. This reaction was empirically modeled using the relation,

$$\frac{d\alpha}{dt} = k(1 - \alpha)^n \quad (5.1)$$

Where,

$d\alpha/dt$ - rate of degree of cure

α - degree of cure

n - reaction order, and

k - reaction rate constant (1/min)

The temperature dependence of this rate constant is given by,

$$k = z e^{(-E/RT)} \quad (5.2)$$

Where,

E - activation energy (J/mol)

R - gas constant (8.314 kJ/kg K)

T - absolute temperature (K)

z – pre-exponential factor (1/min)

The isothermal experimental MDSC data for resin and composite was analyzed using equations 5.1 and 5.2 and values for the constants of these equations are tabulated in Table 5.1. Unlike most of the other resin systems, for this resin system, the reaction order “n” was found to be function of cure temperature as shown in Table 5.2. In the current study resin data was modeled and used in the thermochemical module. The temperature dependence of the reaction order “n” for resin was modeled as,

$$n = n_o + \frac{A}{1 + e^{\frac{-(T-T_o)}{B}}} \quad (5.3)$$

Where,

n_o , A, T_o and B are the model constants, and

T is temperature

It can be inferred from Figure 5.1 that equation 5.3 fitted the data very well to the measured value. The values of these model constants are,

$$n_o = 14.953$$

$$A = -13.244$$

$$T_o = 139.218, \text{ and}$$

$$B = 9.951$$

Table 5.1 Cure Kinetics parameters for Cytec Fiberite 934 Resin and composite

| 934 System | E (kJ/mol) | LogZ 1/min | H kJ/kg |
|------------|------------|------------|---------|
| Resin | 34.88 | 3.11 | 483.1 |
| Composite | 36.42 | 3.32 | 176.4 |

Table 5.2 Reaction order for resin and composite as a function of temperature

| Temperature (°C) | 100 | 130 | 160 | 177 | 190 |
|------------------|-------|-------|------|------|------|
| n | | | | | |
| Resin | 14.16 | 10.94 | 3.17 | 1.63 | 1.79 |
| Composite | 8.36 | 9.93 | 1.76 | 1.84 | 2.63 |

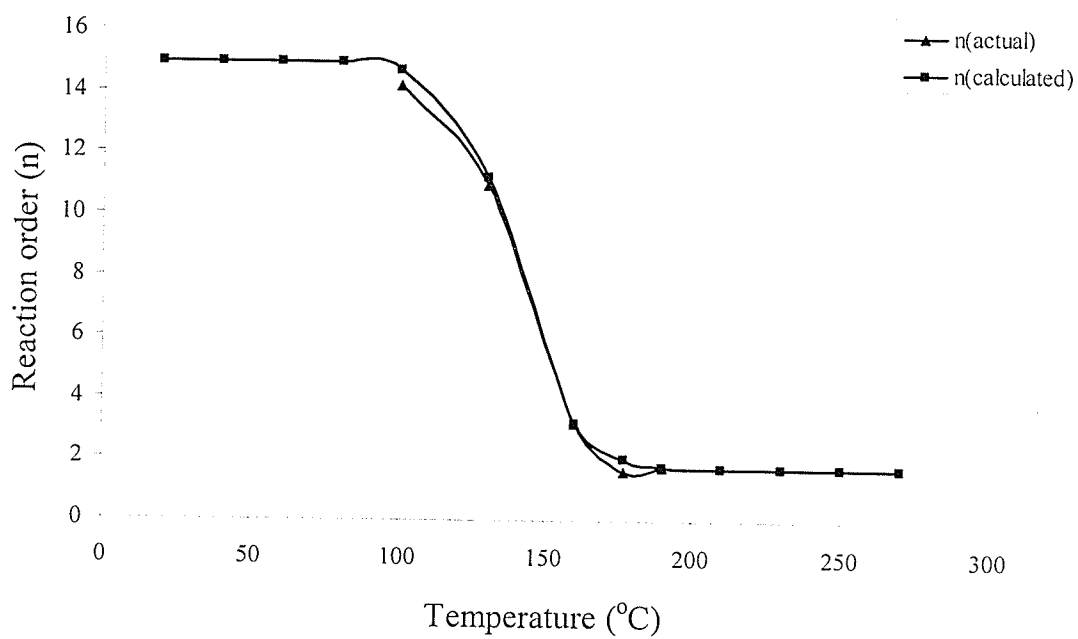


Figure 5.1 Reaction order “n” as a function of Temperature

5.1.2 Thermo-Physical Properties:

5.1.2.1 Specific heat capacity:

Figure 5.2 shows the measured heat capacity of the uncured composite. The heat capacity of uncured composite is given by (kJ/kg °C),

$$C_{p_c} = 0.003 T + 1.475 \quad (5.4)$$

The material exhibited a glass transition at about 15°C and hence there was a jump in the specific heat capacity of composite by 0.124 kJ/kg °C. Figure 5.3 shows the measured specific heat capacity of the composite as a function of degree of cure. However, due to the scatter in the measured data at different isothermal temperatures a trend in the measured data was not observed. Hence, this data was not used in the process model for the prediction of warpage. Instead the specific heat capacities of uncured 934-resin and T300 fiber were used in the thermochemical module. The specific heat capacity of uncured resin and fiber were found to be (kJ/kg °C),

$$C_{p_r} = 0.0027 T + 0.2 \quad (5.5)$$

$$C_{p_f} = 0.0011 T + 1.560$$

The specific heat capacity of the composite was calculated using rule of mixture as defined in chapter 4 section 4.1.3.1. From literature review (13) it was found that the effect of 10 % scatter in specific heat capacity on predicted warpage is insignificant. From Figure 5.3 we can observe that change in heat capacity, as a function of cure, for composite is less than 10 %. Hence, in the current model the influence of cure on specific heat capacity of the resin was assumed to be negligible. This assumption does not affect the accuracy of warpage prediction.

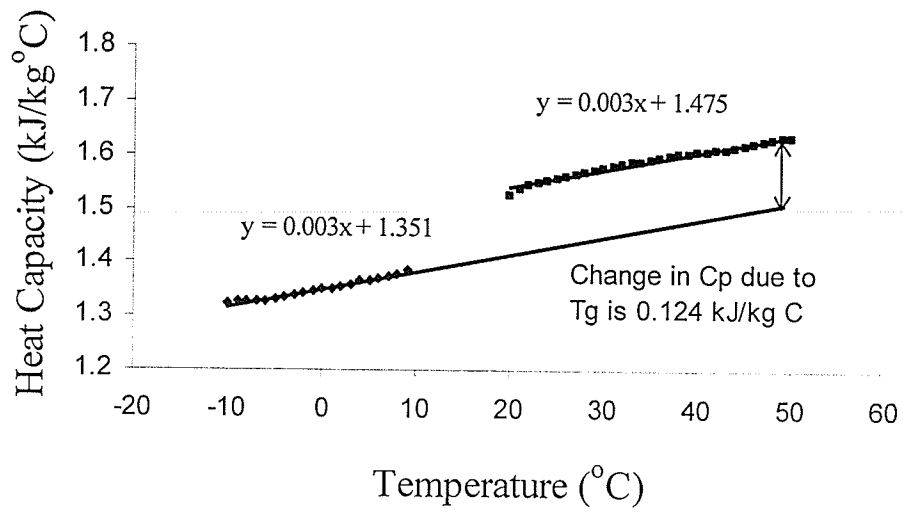


Figure 5.2 Heat capacity of uncured composite showing effect of T_g

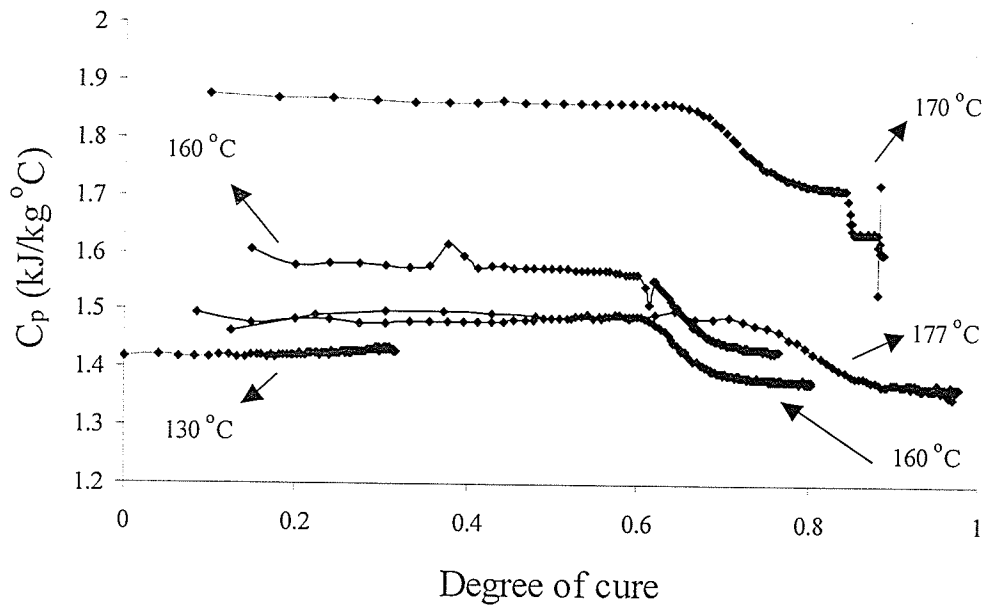


Figure 5.3 Heat capacity change as a function of degree of cure of the composite

5.1.2.2 Thermal conductivity:

Figure 5.4 shows the measured longitudinal and transverse thermal conductivity. The longitudinal and transverse thermal conductivity of composite was found to increase with increase in temperature. This temperature dependence was modeled using a linear relation and was found to be (W/m °C),

$$k_{11} = 5.27 + 0.0389 T \quad (5.6)$$

$$k_{22} = k_{33} = 2.567 + 0.0131 T$$

At any temperature the conductivity in the longitudinal direction was found to be higher than transverse conductivity. A review of published data on thermal conductivity of other composite systems indicated that change in thermal conductivity of the composite with degree of cure is negligibly small. Hence, in the current study the thermal conductivity of the composite was measured to be the function of temperature only.

5.1.2.3 Coefficient of Thermal Expansion (CTE):

Figure 5.5 shows the change in through-the-thickness dimension of composite cured to three different degree of cure during temperature scan. The slope of the best-fit line represents the CTE of composite in through-the-thickness direction (α_{33}). By comparing the slopes of the best fit lines for three degrees of cure it can be observed that CTE is nearly independent of degree of cure and temperature in the tested temperature range. A shift in the curves along the temperature and thickness axis can be observed in Figure 5.5. This shift is due to the slight change initial temperature and original dimension of the sample.

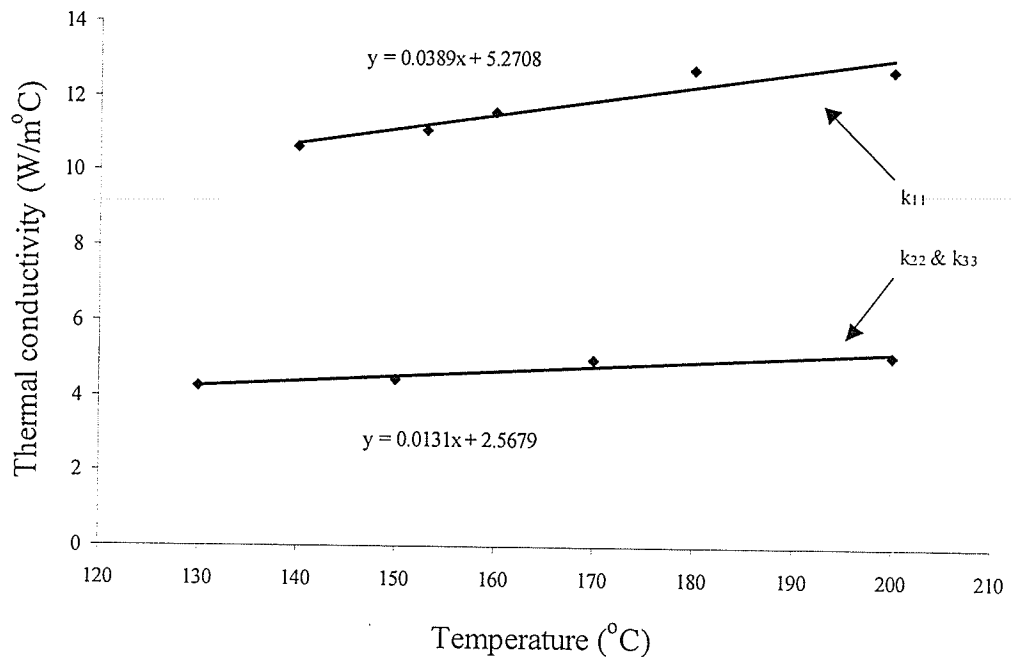


Figure 5.4 Thermal conductivity of the composite

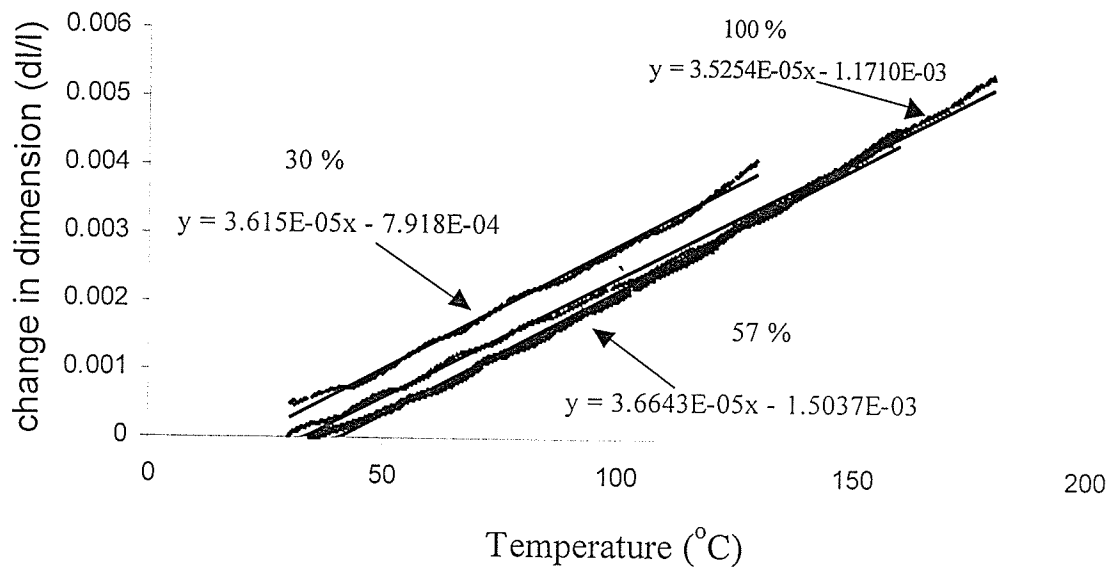


Figure 5.5 TMA result for composites cured to different degree of cure

The CTE in the transverse direction (α_{22}) was assumed to be equal to that of through-the thickness direction for a transversely isotropic material. The results for individual runs can be found in Appendix C. A scatter of about 10 % is observed in the CTE measurement. The average CTE was found to be,

$$\alpha_{11} = 3.5E-06 /^{\circ}C,$$

$$\alpha_{22} = 36.5E-06 /^{\circ}C, \text{ and}$$

$$\alpha_{33} = 36.5E-06 /^{\circ}C$$

This result was found to be contrary to results in reference (15), in which CTE for this material was found to be, $\alpha_{11} = -0.8E-06 /^{\circ}C$, and $\alpha_{22} = \alpha_{33} = 27.62E-06 /^{\circ}C$. However, in the previous study (15) the CTE of the composite was not measured directly, instead they calculated the CTE of the composite using CTE of the resin and fiber using approximate micro-mechanics relations.

5.1.2.4 Cure Shrinkage:

The cure shrinkage was approximated to be linear function of degree of cure as shown in Figure 5.6, though it exhibited a non-linear dependence. The data in Figure 5.6 was fitted to a linear relation as shown below.

$$\varepsilon_{22}^c = \varepsilon_{33}^c = -4.1882 \alpha + 1.3005 \quad (5.7)$$

This equation applies only to the measurement range of degree of cure of 37% to 100%. Due to the experimental measurement procedure the shrinkage data during initial four-five minutes could not be obtained from TMA. Hence, using test temperature and cure kinetics model degree of cure during initial five minutes was calculated and used while

calculating shrinkage as a function of degree of cure. Similar to cure shrinkage in through-the-thickness direction, the cure shrinkage in the longitudinal direction is given by,

$$\varepsilon_{11}^c = -6.924 \times 10^{-4} \alpha + 9.122 \times 10^{-6} \quad (5.8)$$

The cure shrinkage in the longitudinal direction was found to be a linear function of cure as given in equation 5.8 until a degree of cure of 71%. In addition, longitudinal shrinkage beyond this cure extent was found to be negligibly small. The temperature dependence of cure shrinkage was observed in the current study as shown in Figure 5.7. However, due to the difficulties with availability of TMA equipment the temperature dependence of cure shrinkage could not be resolved in the current study. The results for individual runs can be found in Appendix C. A scatter of about 7% in the measured data was observed. The total cure shrinkage in the longitudinal and transverse directions are found to be,

$$\varepsilon_{11}^c = -0.048 \%,$$

$$\varepsilon_{22}^c = -2.49\%, \text{ and}$$

$$\varepsilon_{33}^c = -2.49 \%$$

This result was found to be different from that in reference (15), in which cure shrinkage for this material was found to be, $\varepsilon_{11}^c = -0.0125 \%$, and $\varepsilon_{22}^c = \varepsilon_{33}^c = -0.7056 \%$. However, in the previous study (15) the cure shrinkage of the composite was not measured directly, instead it was calculated using approximate micro-mechanics relations using the shrinkage data for the resin. In addition to this approximation, in the previous study, the cure shrinkage of the resin was assumed to be -1.5% and no measurement was performed.

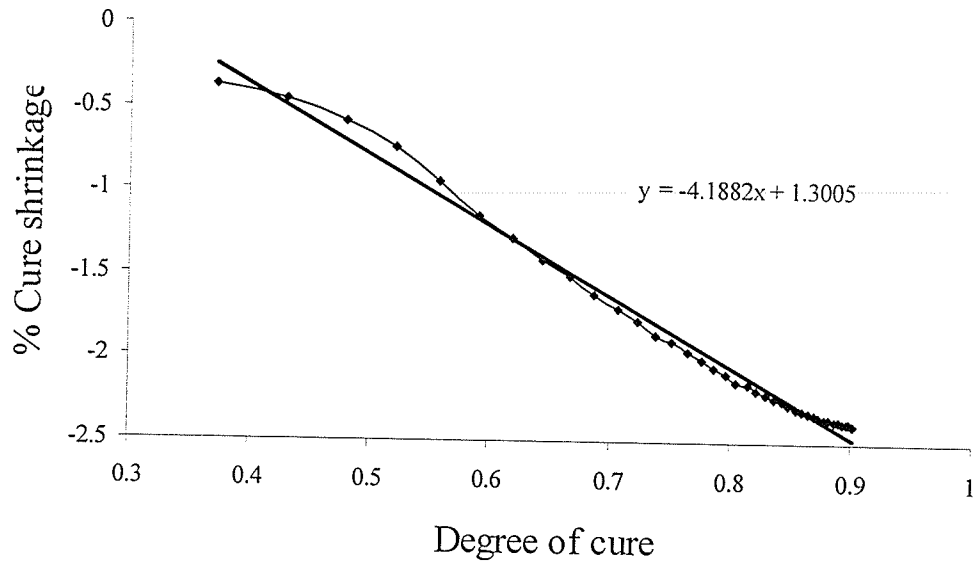


Figure 5.6 Cure shrinkage in thickness direction as a function of degree of cure at 177°C

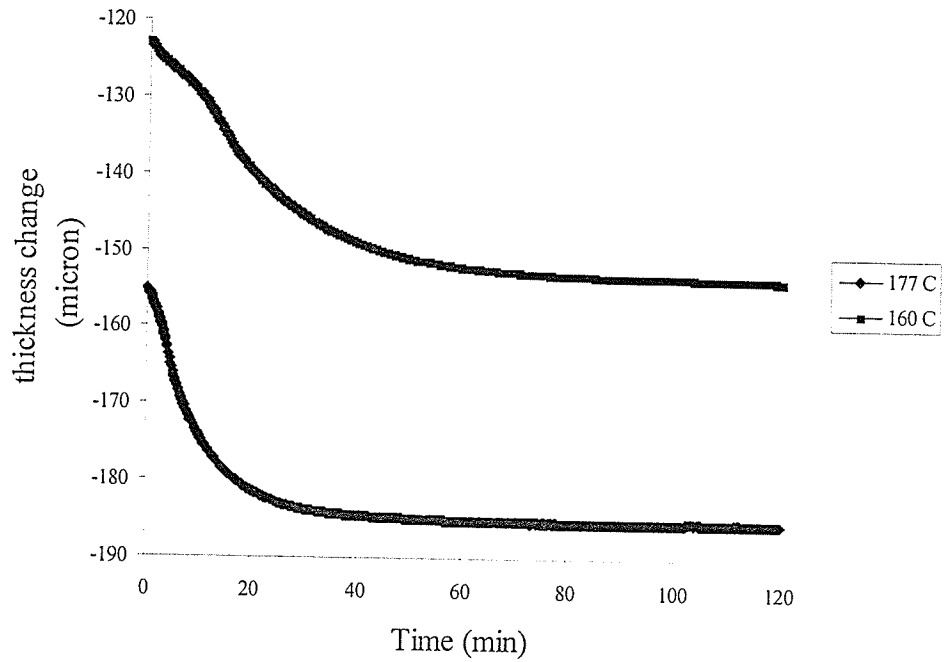


Figure 5.7 Illustration of temperature dependence of cure shrinkage profile

5.1.3 Rheological Properties:

5.1.3.1 Gel Point:

Figure 5.8 shows the elastic and viscous moduli curves for 934 - resin. The highlighted cross-over point is the gel point. The gel point temperature was found to be 171.4 °C, which corresponds to degree of cure of 41% for a heating rate of 2°C/min. The gel point was found to be same for composite and resin. The gel point was not used as input to the process model. However, it was used to pre-cure the samples for modulus test and was used in the design of the cure cycle as explained in chapter 4. A scatter of about 3 % in the measured data was observed.

5.1.3.2 Viscosity:

The viscosity data was modeled using an empirical equation given in reference (9),

$$\mu = \mu_{\infty} e^{(k\alpha)} e^{\left(\frac{U}{RT}\right)} \quad (5.9)$$

The fitted model constants are,

$$\mu_{\infty} = 8.858 \times 10^{-16} \text{ Pas,}$$

$$k = 28.264, \text{ and}$$

$$U = 103.309 \text{ kJ/mol}$$

The viscosity model is very important in the prediction of resin flow and laminate thickness during the composite processing. However, in the current study the viscosity data was not used since the process model used in the prediction of warpage and residual stress does not include a resin flow module.

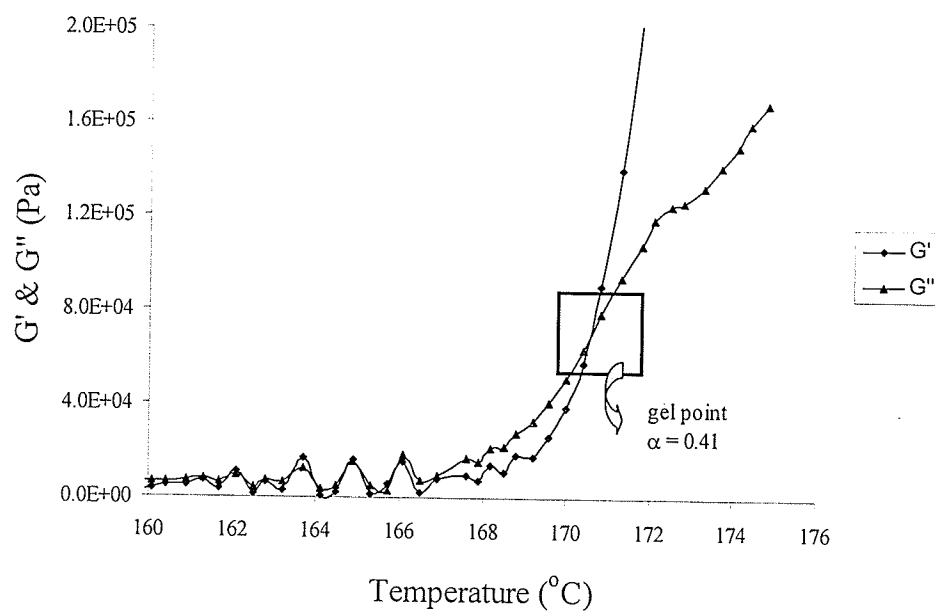


Figure 5.8 Gel Point for 934-resin

5.1.3.3 Glass Transition Temperature (T_g):

Figure 5.9 is a MDSC plot showing a transition in heat flow due to glass transition for 88% cured composite. The T_g for this sample was found to be about 154 °C. The T_g data helps in understanding the time or degree of cure at which diffusion takes over the cure kinetics reaction during a isothermal DSC test. For example, from Figure 5.9 for 88% cured composite the T_g is around 154 °C. Hence, when we use a cure temperature of 154 °C we can cure the material up to a degree of cure of 88 %. Above this cure or corresponding cure time the diffusion takes over the cure kinetics. For cure kinetics analysis our data up to this curve should be used. Similarly, the T_g of the composite was measured for a range of cure extent, plotted, and fitted to an exponential function based on literature review as shown in Figure 5.10. The glass transition temperature (°C) for this material as a function of degree of cure is given by,

$$T_g = 19.538 e^{2.3705\alpha} \quad (5.10)$$

5.1.4 Mechanical Properties:

5.1.4.1 Longitudinal & Transverse moduli:

Figure 5.11 shows the longitudinal modulus (E_{11}) of the composite as a function of degree of cure. The longitudinal modulus was found to be a linear function of the degree cure. In addition it can be observed in Figure 5.11 that the modulus curves at various test temperatures 130 °C, 160 °C and 177 °C were found to superpose very well. Hence, the effect of temperature on longitudinal modulus was taken to be negligible. The longitudinal modulus of the composite is given by (GPa),

$$E_{11} = 38.571 \alpha + 87.963 \quad (5.11)$$

This equation is good for measured range of degree of cure, 32 % to 100%. The longitudinal modulus below 32 % degree of cure, was assumed to be a constant value of 57 GPa that is approximately equal to the longitudinal modulus of uncured composite at room temperature.

Figure 5.12 shows the transverse modulus (E_{22}) of the composite as a function of degree of cure. Similar to the longitudinal modulus, the transverse modulus was found to be linear function of degree cure and influence of temperature on transverse modulus was found to be insignificant. The transverse modulus is given by (GPa),

$$E_{22} = 2.448 \alpha + 3.624 \quad (5.12)$$

This equation is good for measured range of degree of cure, 32 % to 100%. The transverse modulus below 32 % degree of cure was calculated using rule of mixture using fiber E_{22} of 3.21 GPa and uncured resin modulus of near zero value. This value was found to be 1.83 GPa. In addition, E_{33} was assumed to be equal to E_{22} for a transversely isotropic material.

The measured longitudinal modulus at the end of cure (100 % cure) was found to be 126.534 GPa, which matches very well with the cured composite modulus of 117-138 GPa provided by Cytec Fiberite manufacture data sheet (41). In addition, the measured longitudinal and transverse moduli of 126.5 and 6.072 GPa for the cured composite was found to be different from those found in reference (15) for this material. The cured composite E_{11} & E_{22} values found in literature (15) were 150.76 and 7.93 GPa respectively. However, the previous studies did not measure continuous modulus

development as a function of degree of cure. Besides they used moduli of fiber and cured resin in the prediction of composite modulus using approximated rule of mixtures.

5.1.4.2. Shear modulus:

Figure 5.13 shows the measured shear modulus of the composite as a function of degree of cure. The shear modulus of the composite was modeled as follows (GPa),

$$G_{12}=0.1125 \alpha - 0.0126, 0 \leq \alpha \leq 0.86 \quad (5.13)$$

$$G_{12}=31.7 \alpha - 27.1, 0.86 \leq \alpha \leq 1.0$$

The shear modulus of the composite was measured at 130, 160 and 177 °C. The measured shear modulus was found to be temperature dependent. However due to the large scatter in the measured data at 130 and 160°C, the effect of temperature on modulus was not studied in the current study. The measured shear modulus at 177 °C was used in the process model for the prediction of warpage. The shear modulus of fully cured composite was found to be 4.6 GPa, in contrast to the value of 3.7 GPa in literature (15), obtained using rule of mixtures.

5.1.5 Summary of Material Characterization:

The extensive material characterization on Cytec Fiberite 934 neat resin and composite was performed in the current study. Unlike most of the previous studies, in the current study direct composite properties measurement was performed. In addition, the properties were measured as a function of degree of cure and temperature. The summary of results of material characterization can be found in Table 5.3.

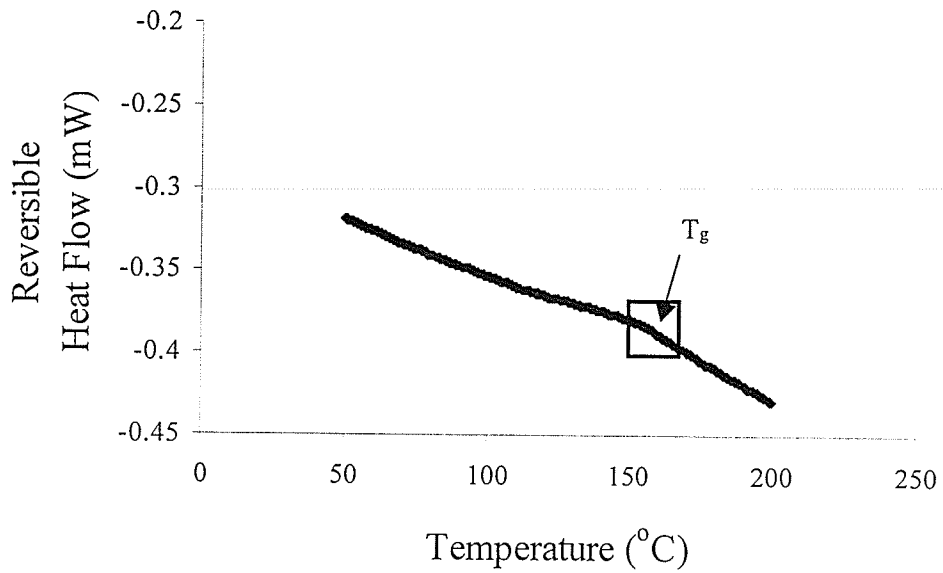


Figure 5.9 T_g of 88% cured composite measured from MDSC

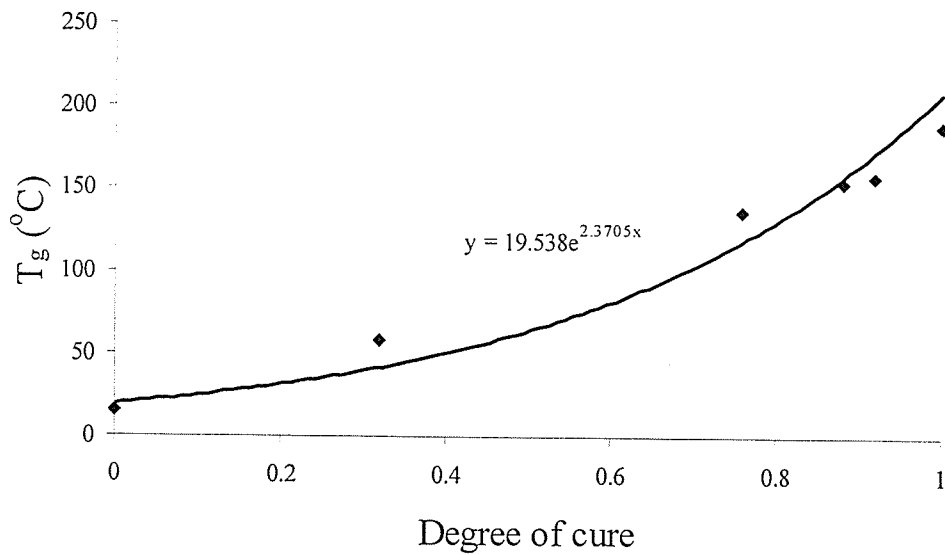


Figure 5.10 Glass transition temperatures as a function of degree of cure

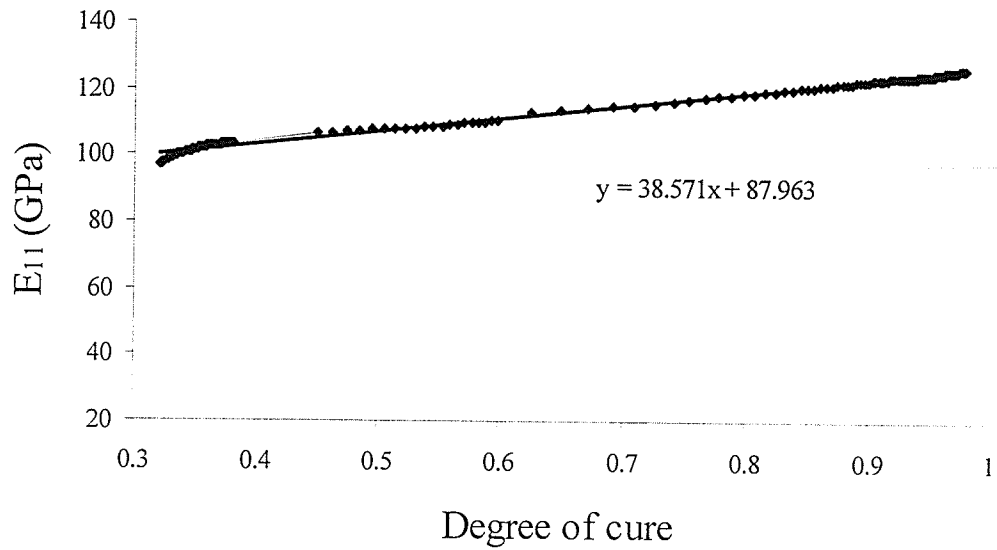


Figure 5.11 Longitudinal modulus of the Cyttec Fiberite composite during cure

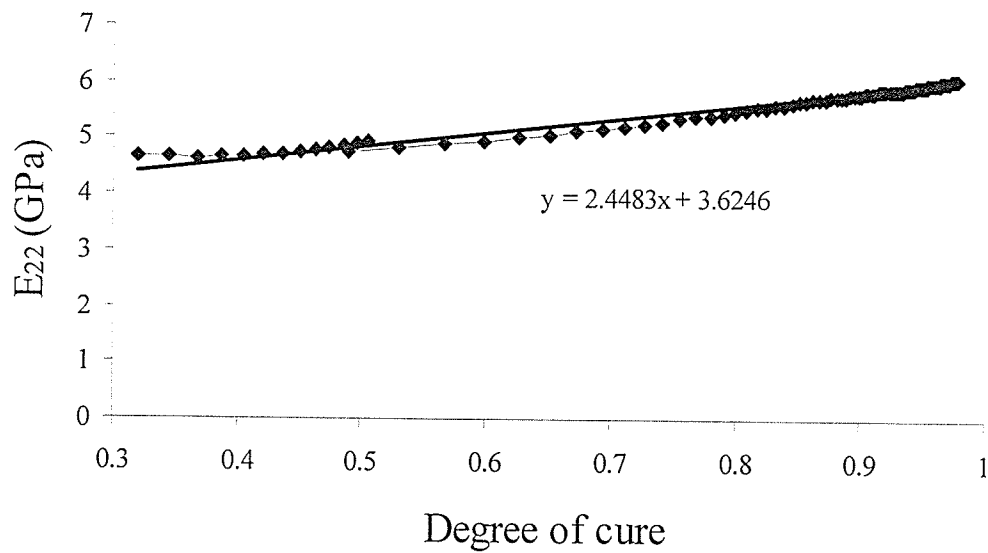


Figure 5.12 Transverse modulus of the composite as a function of degree of cure

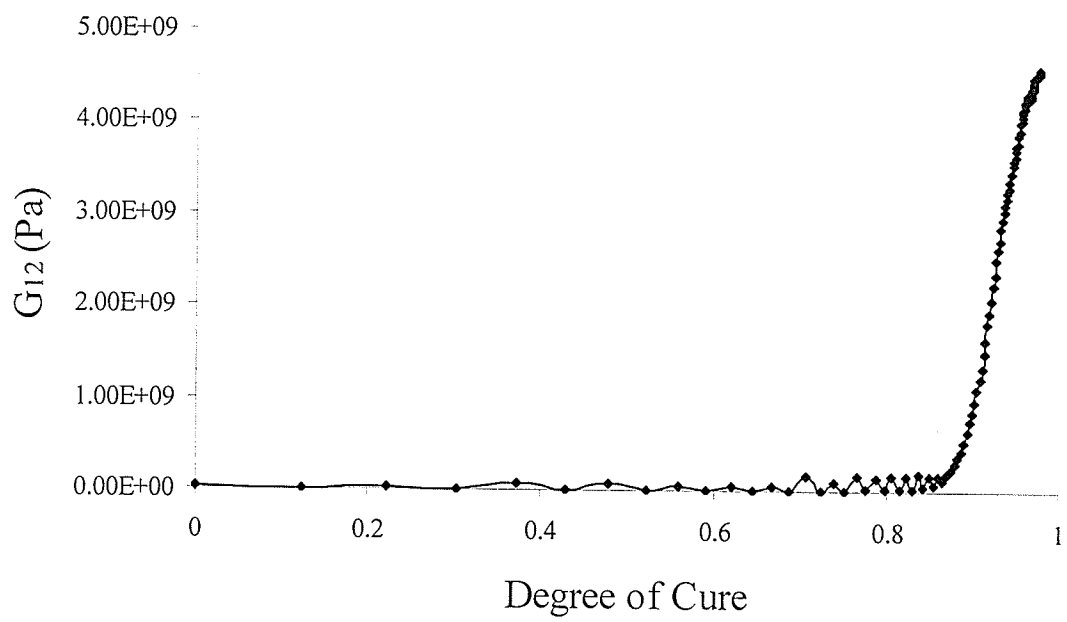


Figure 5.13 Shear modulus of composite as a function of degree of cure

Table 5.3 Summary of the results of Material Characterization

| Classification | Properties | Measured Values |
|-----------------|--|---|
| Physical | Density (kg/m ³) | Resin: 1300, Fiber: 1760 |
| | Fiber Volume Fraction | 57.3 % |
| Cure Kinetics | Total heat of reaction (kJ/kg) | H = 483.1 |
| | Activation Energy (kJ/mol) | E = 34.88 |
| | Log Z (1/min) | 3.11 |
| | Reaction order (n) | $n = n_0 + A/(1 + \exp(-(T - T_0)/B))$ $n_0 = 14.953$, $A = -13.244$, $T_0 = 139.218$, and $B = 9.951$ |
| Thermo-Physical | Specific heat capacity (J/kg °C) | Resin: $C_p = 2.7 T + 200.0$ Fiber: $C_p = 1.1 T + 1560.0$ |
| | Thermal conductivity (W/m °C) | $K_{11} = 5.27 + 0.0389 T$ $K_{22} = K_{33} = 2.567 + 0.0131 T$ |
| | CTE of Composite x 10 ⁻⁶ (/ °C) | $\alpha_{33} = \alpha_{22} = 36.5$ $\alpha_{11} = 3.5$ |
| | Coefficient of Cure shrinkage for Composite | $\epsilon_{33} = \epsilon_{22} = -0.0249$ $\epsilon_{11} = -0.000485$ |
| Rheological | Viscosity | $\mu = \mu_\infty \exp(k\alpha) \exp(U/RT)$ $\mu_\infty = 8.858E-16$ Pas, $k = 28.264$ $U = 103.309$ kJ/mol |
| | Gel Point | $T = 171.4$ °C, $\alpha = 0.41$ |
| | Glass Transition Temperature (T _g) | $T_g = 19.538 \exp(2.3705\alpha)$ |
| Mechanical | Modulus of Composite GPa | For, $0 \leq \alpha \leq 0.32$, $E_{11} = 57$ GPa & $E_{22} = 1.83$ GPa, For, $0.32 \leq \alpha \leq 1.0$, $E_{11} = 38.571\alpha + 87.963$ $E_{22} = 2.448\alpha + 3.624$ $G_{12} = 0.112\alpha - 0.0126$, $0.0 \leq \alpha \leq 0.86$ $G_{12} = 31.7\alpha - 27.1$, $0.86 \leq \alpha \leq 1.0$ |

- α is degree of cure and α_{ij} is CTE of the composite

5.2 RESULTS FROM EXPERIMENTAL PARAMETRIC STUDY

5.2.1 Introduction:

In the current study the experimental parametric study was performed in order to understand the effect of, (a) process cycle parameters, and (b) tool material CTE and thermal mass on process-induced warpage. The angle laminates were manufactured to understand the effect of these parameters on process-induced warpage due to the mechanisms of anisotropy in CTE and cure shrinkage, and tool-part interaction. The warpage due to tool-part interaction was delineated from the warpage due to anisotropy in CTE and cure shrinkage by subtracting the predicted warpage due to anisotropy from the measured warpage. The flat laminates were manufactured in order to, (a) compare the warpage in the arm of the angle laminate with the measured warpage due to tool-part interaction, and (b) compare the warpage due to tool-part interaction delineated from the total warpage of the angle laminate with the measured warpage of the flat laminate due to tool-part interaction.

5.2.2 Measured Autoclave Air Temperature and Part Temperature:

Figure 5.14 shows the measured autoclave air temperature and measured part temperature for cycle 1. From this figure it could be clearly observed that the autoclave air temperature, "Auto_Temp", lags considerably the set air temperature "MR_Cycle". The maximum temperature difference was about 27°C. Hence it is very important to predict the autoclave air temperature accurately based on autoclave set temperature. In addition, the measured part temperatures "ALH", "ALL" and "INV" for three tools lags the autoclave air temperature "Auto_Temp". The maximum temperature difference of about

50°C was observed in the case of ALH tool. Hence it is very important to predict the part temperature accurately based on the autoclave temperature and thermal boundary conditions. In addition, the part temperature for ALH tool lags much more than that of ALL and INV tools. This is due to the higher thermal mass of the ALH tool. The difference between measured part temperatures at two locations in the part was found to be negligibly small. Therefore temperature gradient within the part in our case study is insignificant and hence cannot be a source of process-induced warpage. The similar trend was also observed for other cure cycles.

5.2.3 Measured Spring Back Angle in Angle Laminates:

Figure 5.15 shows the summary of measured spring back angle in angle laminates for three tools and four process cycles. The measured warpage includes the warpage due to anisotropy in CTE and cure shrinkage and tool-part interaction. As mentioned in chapter 4, section 4.2.4, the spring back angle was calculated using slope of the line fitted to arm positional data. The effect of selected parameters on process-induced warpage is explained here.

5.2.3.1 Effect of Process Cycle Parameters:

From Figure 5.15 by comparing the spring back angle for cycle 2 and cycle 1 it can be observed that the spring back angle decreases with the application of dwell. But, a similar trend in spring back angle was not observed for cycle 4 and cycle 3. Comparing the spring back angles for cycles 4 and 2, it can be observed that the spring back angle increases with increase in compaction pressure. But, a similar trend was not observed for

cycles 3 and 1. Hence, based on the experimental spring back angle measurement the effect of process parameters on process-induced warpage could not be discerned.

5.2.3.2 Effect of Tool Material CTE and Thermal Mass:

From Figure 5.15 the spring back angle was found to be high for aluminum tools and low for Invar tool for cycles 1, 3 and 4. But spring back angle was found to be almost equal for three tools in the case of cycle 2. Therefore the actual impact of CTE of the tool material on warpage could not be understood with certainty based on measured spring back angle. In addition, lower spring back was observed for ALH tool as compared to that of ALL tool for cycles 1, 2 and 3. However, this trend was not observed in the case of cycle 4. Hence, the influence of thermal mass of the tool on the process-induced warpage could not be concluded based on measured spring back angle.

5.2.4 Error in The Measured Spring Back Angle Due To Warpage in The Arm:

As mentioned in section 5.2.3 the spring angle was measured by calculating the slope of the line fitted to the measured positional data along the arm of the angle laminate. However warpage of the arm of the angle laminate has been observed and this could be a source of error in the measured spring back angle. Hence, in order to account for this error the warpage in the arm of the angle laminate was calculated by joining the end points of the arm of the angle laminate as shown in Figure 5.16. Figure 5.17 shows the calculated warpage in the arm of angle laminates for three tools and four process cycles. Similar to the measured spring back angle the trend in the effect of process cycle parameters and thermal mass of the tool on warpage was not observed. However, the

warpage in the arm was found to be least for Invar tool compared to that for aluminum tools for all the process cycles.

In addition, the correct spring back angle was determined by calculating the slope of the straight line joining the end points of the arms of the angle laminate. The recalculated spring back angle, taking into account the warpage of the arm for three tools and four process cycles are shown in Figure 5.18. Based on the corrected spring back angle the effect of process and material parameters on process-induced warpage was analyzed again as explained in the following sections.

5.2.4.1 Process parameters:

From Figure 5.18 by comparing cycle 1 & 2 and 3 & 4 for ALH tool the spring back was found to increase with the application of dwell. However a similar trend was not observed in the case of ALL and Invar tools. Similarly with application of higher compaction pressure the spring back was found to decrease for ALL tool. However a similar trend was not observed in the case of ALH and Invar tools. In addition, from Figure 5.18 the measured spring back for Invar tool was found to be almost constant for various process cycles. Therefore based on the above observations the influence of process cycle parameters on process-induced spring back cannot be concluded at this point of time. Hence the effect of process parameters on warpage was studied further through the case of flat laminates as well as through simulation as given in sections 5.2.5 and 5.3.2 respectively.

5.2.4.2 Tool material CTE and thermal mass:

From Figure 5.18 the effect of tool material CTE on process-induced spring back could be clearly observed. The measured warpage for Invar tool was found to be less than aluminum tools for all the process cycles. This could be due to the low CTE mismatch between the tool and the part in the case of Invar tool when compared to that of aluminum tool. Hence it could be concluded that warpage decreases with decrease in CTE mismatch between the tool and composite part. This result is in agreement with the results found in references (8,13,14 & 17).

From Figure 5.18 a trend in the spring back was not observed as a function of tool thermal mass. The measured spring back was found to be high for ALH tool for cycles 2 & 4 when compared to that of ALL tool. On other hand the measured spring back was found to be high for ALL tool for cycles 1 & 3. Hence the effect of thermal mass on spring back could not be concluded based on experimental results. Besides no previous data is available on the effect of thermal mass on process-induced warpage. Therefore similar to the process cycle parameters the effect of thermal mass on spring back was studied through the case study of warpage measurement in flat laminates as well as through simulation parametric study.

5.2.4.3 Measurement Error of ROMER Instrument:

The accuracy of ROMER was found to be insufficient for spring back angle measurement of the order of 1-2°. The scatter of about $\pm 13\%$ in the measured data has been observed in data from one plane to another plane.

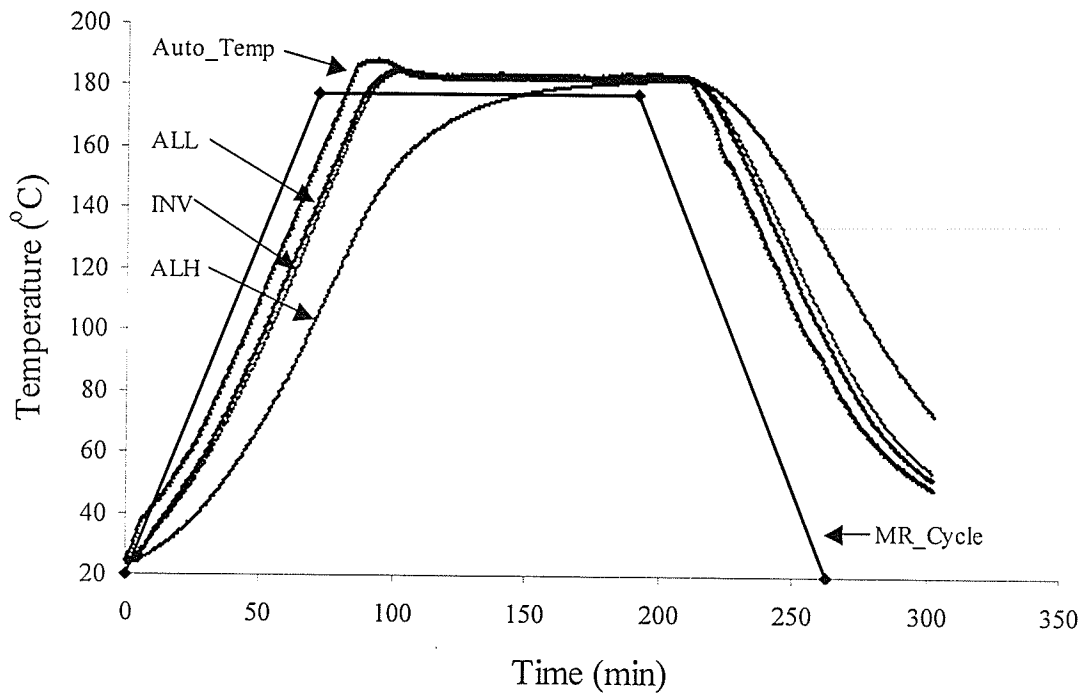


Figure 5.14 Measured autoclave temperature and part temperature

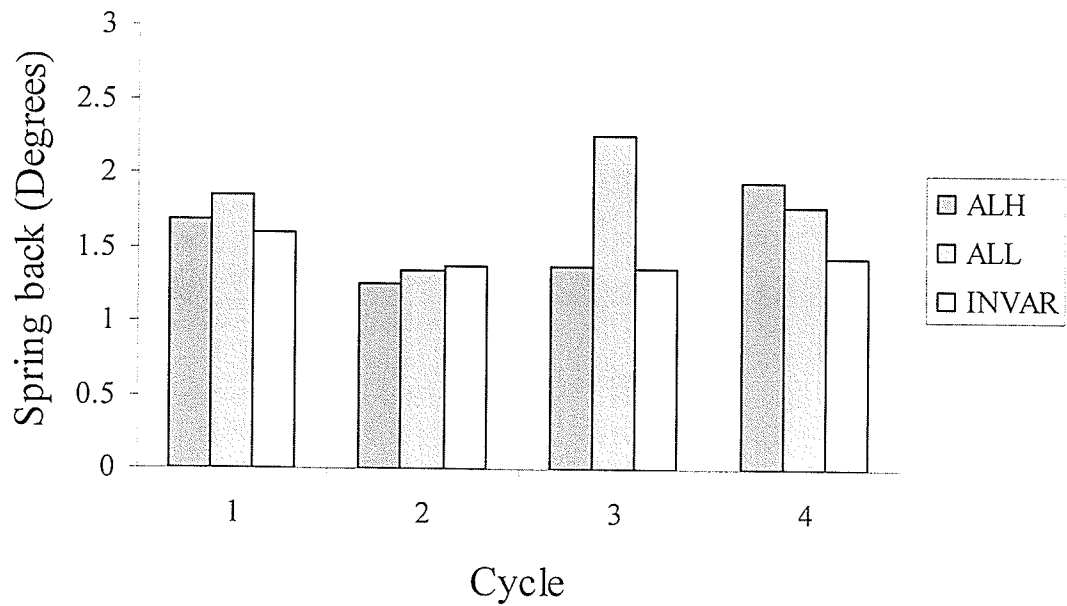


Figure 5.15 Measured spring back in angle laminates (based on slope of the fitted line)

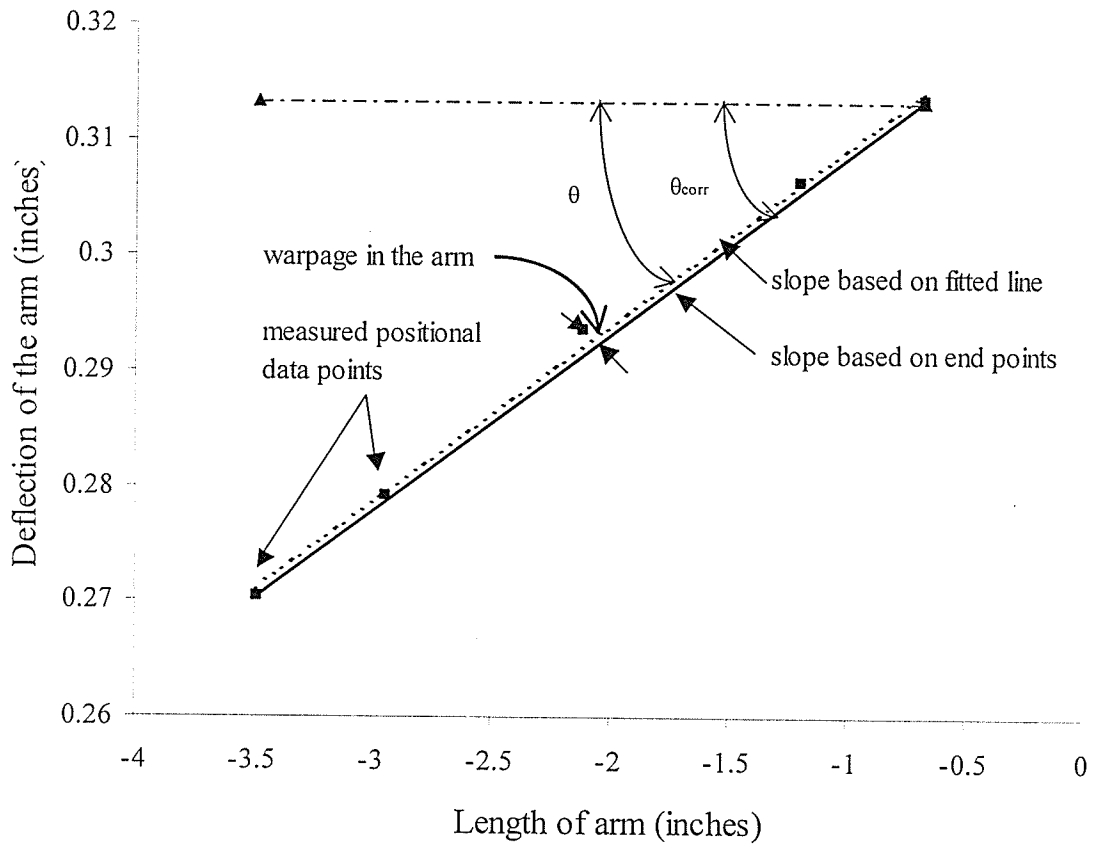


Figure 5.16 Warpage in the arm of the angle laminate and corrected spring back angle

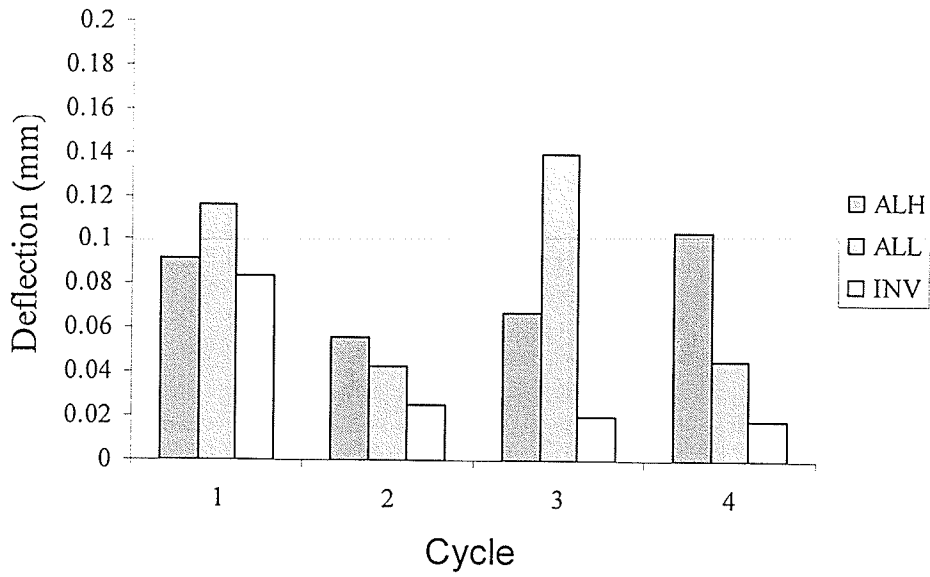


Figure 5.17 Warpage in the arm of the angle laminates for three tools and four process

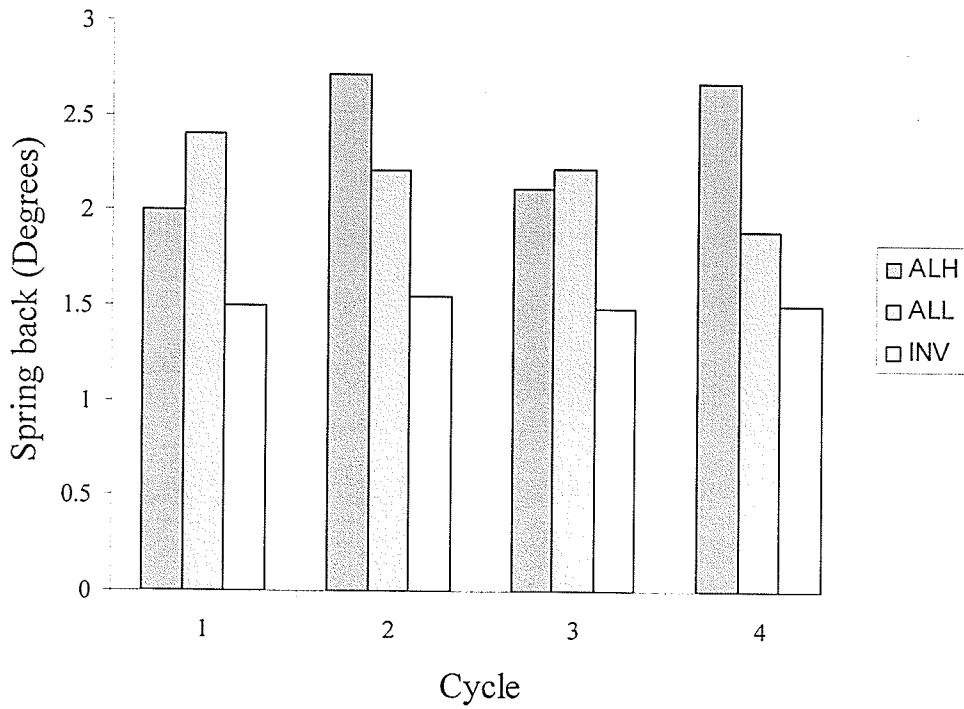


Figure 5.18 Calculated spring back angles (based on the slope of the line joining end points of the arm of the angle laminates)

5.2.5 Measured Warpage in Flat Laminates:

One of the reasons for manufacturing and measuring the warpage in flat laminates was to compare the warpage in the arm of the angle laminate with that of the flat laminate. In addition, the measured warpage in flat laminates may help to understand the effect of process cycle parameters, and tool materials CTE and thermal mass on process-induced warpage due to tool-part interaction. Figure 5.19 shows the summary of measured warpage in flat laminates for four process cycles and three tools. The warpage in the case of flat laminates is only due to mechanism of tool-part interaction. Since, there is no curved segment there is no warpage to the mechanism of anisotropy in CTE & cure shrinkage. The maximum deflection in the laminate was used as measure of process-induced warpage due to the mechanism of tool-part interaction.

By comparing Figures 5.17 and 5.19 we can observe similar trend between the warpage in the arm of the angle laminate and flat laminate for all the three tools and four process cycles. Hence, this study confirms that contribution of tool-part interaction results in warpage of the arm in angle laminates. The effect of process parameters and tool material parameters on warpage due to tool-part interaction is discussed as explained in the following sections.

5.2.5.1 Process parameters:

From Figure 5.19 by comparing cycles 1 & 2 and 3 & 4, it can be observed that with the application of dwell the warpage was reduced in the case of aluminum tools. However similar trend was not observed in the case of Invar tool. Similarly, with the increase in the

compaction pressure, the warpage due to tool-part interaction was found to increase in the case of aluminum tools. But a similar trend was not observed for invar tool. Hence, based on the measured warpage due to tool-part interaction, it could be concluded that, the application of dwell reduces the warpage and increase in pressure increases the warpage in the case of aluminum tool.

5.2.5.2 Tool material CTE and thermal mass:

From Figure 5.19 it is clear that the warpage due to tool-part interaction mechanism is minimum for invar tool when compared to the aluminum tools for all the cycles. This is due to the lower CTE mismatch between the invar tool and the composite as compared to that of the aluminum tool and the composite. In addition, the warpage in the case of ALH and ALL tools for four process cycles did not show any trend. Hence, the effect of thermal mass on warpage could not be concluded based on the experimental measurements.

5.2.6 Summary of Experimental Parametric Study:

In the current study the effect of process parameters, tool material CTE and tool thermal mass were studied experimentally. The angle laminate and flat laminate were used as case study.

Based on this study it could be concluded that,

- The effect of process parameters on spring back due to anisotropy in CTE and cure shrinkage as well as tool-part interaction could not be concluded based on the measured warpage.
- The warpage due to tool-part interaction was found to increase with increase in CTE mismatch between tool material and the composite. Invar tool with minimum CTE mismatch was found to produce least warpage.
- The influence of tool thermal mass on warpage could not be discerned based on the experimental measurement of warpage in the case of both angle laminates as well as flat laminates.
- Comparing Figures 5.17 and 5.19 we can observe similar trend between the warpage in the arm of the angle laminate and flat laminate. Hence, this study confirms that the observed warpage in the arm of angle laminate was due to the tool-part interaction.

5.3 RESULTS OF SIMULATION PARAMETRIC STUDY

Spring back due to anisotropy in CTE and cure shrinkage was predicted during this simulation study to understand the relation between various parameters and this mechanism. Various parameters studied were process cycle, tool material CTE and thermal mass, resin cure kinetics parameters, composite thermophysical and mechanical properties, autoclave heat transfer, and gel time. In addition, few combination runs were also performed in order to understand the combined effect of some of the above parameters.

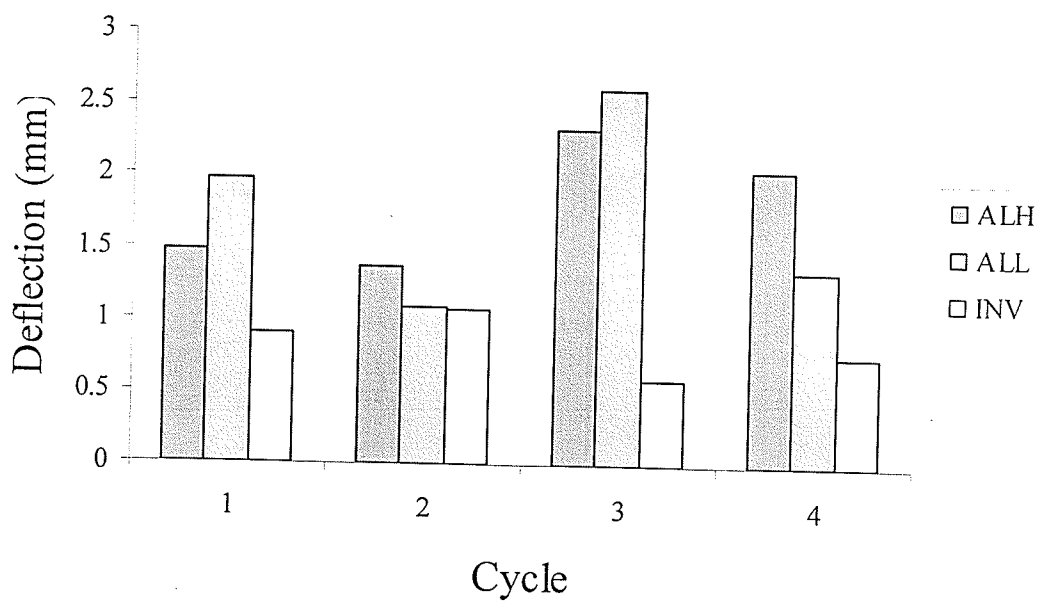


Figure 5.19 Measured warpage in flat laminates for four cycles and three tool materials

5.3.1 Predicted Part Temperature & Degree of Cure:

Figure 5.20 and 5.21 shows the autoclave air temperature, measured part temperature and predicted part temperature for ALH tool for process cycles 1 (45Psi without dwell) and 4 (85 Psi with dwell) respectively. "MR_Cycle" and "Mod_Cycle" in Figures 5.20 and 5.21 are the set autoclave temperature cycles. "Clave Temp" is the autoclave air temperature recorded during the cure cycle. The autoclave temperature lagged the manufacturer recommended cure cycle, "MR_Cycle", and modified cure cycle, "Mod_Cycle", significantly. The "TC5" and "TC6" are the part temperatures measured at the two corners (on either side of the length) of the laminate, at the mid plane, during the cure cycle. The measured part temperature was found to lag autoclave temperature considerably. The "Pred_Temp" in these figures shows the predicted part temperature for ALH tool based on measured autoclave air temperature cycle, which was found to match well with the measured part temperature. The maximum difference of about 7°C was observed between the measured and predicted part temperature. This difference could be due to the approximations used in decoupling the temperature and cure kinetics. Similar good agreement between the predicted part temperature and measured part temperature was observed for ALL and Invar tools as given in Appendix D. "MR_Pred" represents the predicted part temperature based on the manufacturer recommended cycle and modified cure cycle. The prediction based on these cycle were found to be far from the actual measured part temperature. This shows the importance of accurate prediction of autoclave air temperature based on autoclave set temperature and prediction of part temperature based on the autoclave air temperature using accurate thermal boundary

conditions. This also explains that approach used by many previous researchers of using autoclave set temperature in prediction is not correct.

Figure 5.22 shows the predicted part temperature degree of cure profile for three tools and cycle 1. Similar to the measured part temperature discussed in section 5.2.2, the predicted part temperature for ALH tool lags considerably the measured autoclave air temperature compared to that of ALL and Invar tool. We can also observe the change in the cure path for different tools. The cure path for ALH tool was found to lag that of ALL and Invar tool considerably. The change in temperature and cure path for ALL and Invar tools were found to be negligibly small. This large lag in the temperature as well as cure path for ALH tool is due to the higher thermal mass of the ALH tool. Figure 5.23 shows the predicted part temperature for ALH tool and cycle 1 at the middle of the cure cycle. The temperature gradient within the part was found to be negligibly small. Similar to ALH tool, the maximum temperature gradient within the part in the case of ALL and Invar tools was found to be about 1-2 °C. Hence, the temperature gradient within the part could not be a source of process-induced warpage in our case study.

5.3.2 Process-Induced Warpage Due To Anisotropy in CTE & Cure Shrinkage:

The predicted spring back angle through simulation study is only due to the mechanism of anisotropy in CTE and cure shrinkage. The effects of various parameters on spring back due to anisotropy in CTE and cure shrinkage are presented in the following sections. In addition, an effort is made to reason the higher impact of one parameter over another in the discussion section.

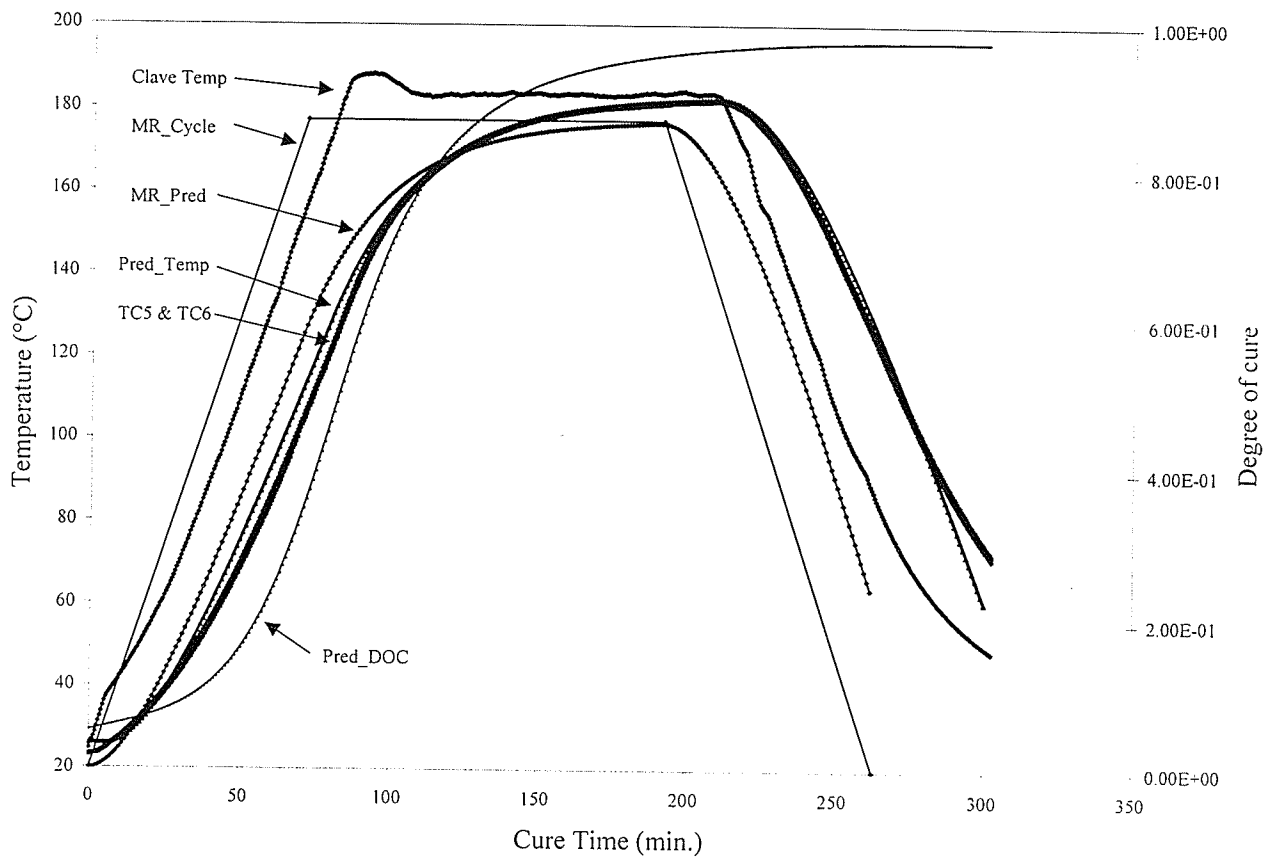


Figure 5.20 Predicted part temperature & degree of cure for cycle 1, ALH tool

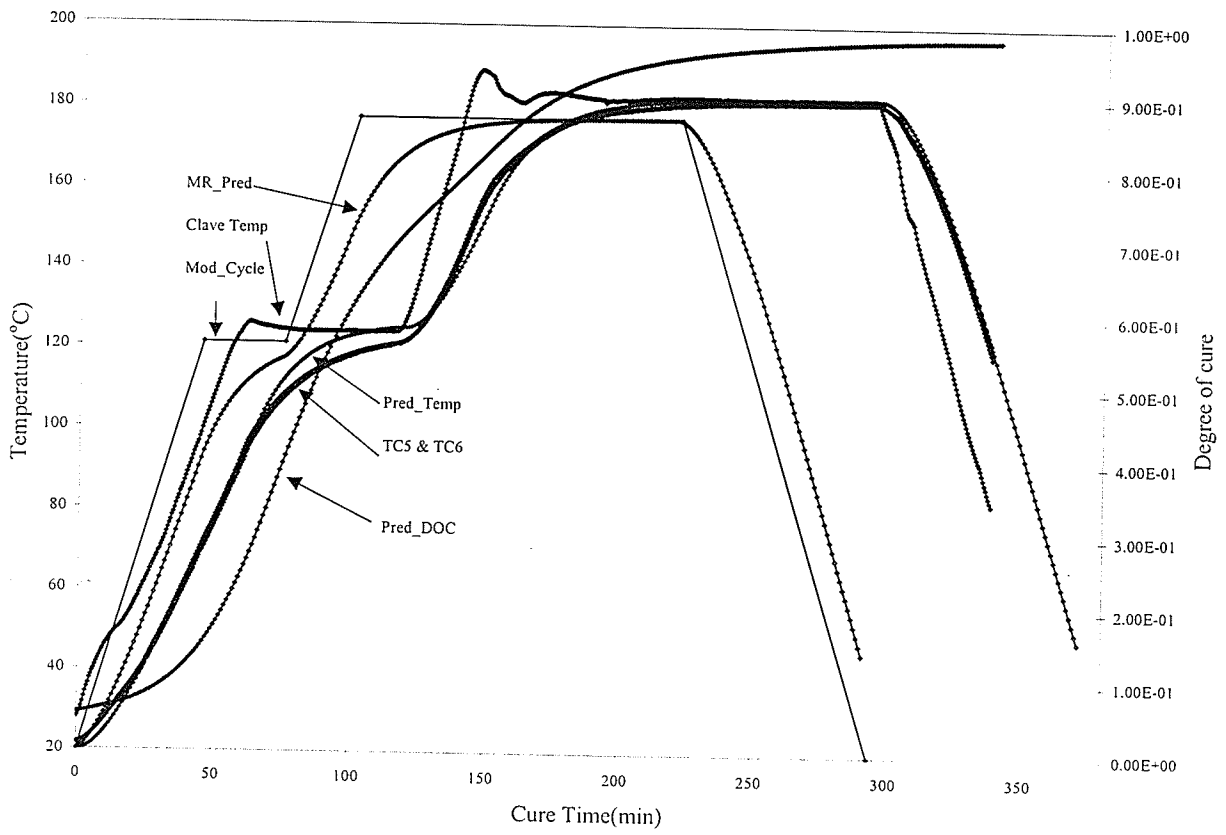


Figure 5.21 Predicted part temperature & degree of cure for cycle 4, ALH tool

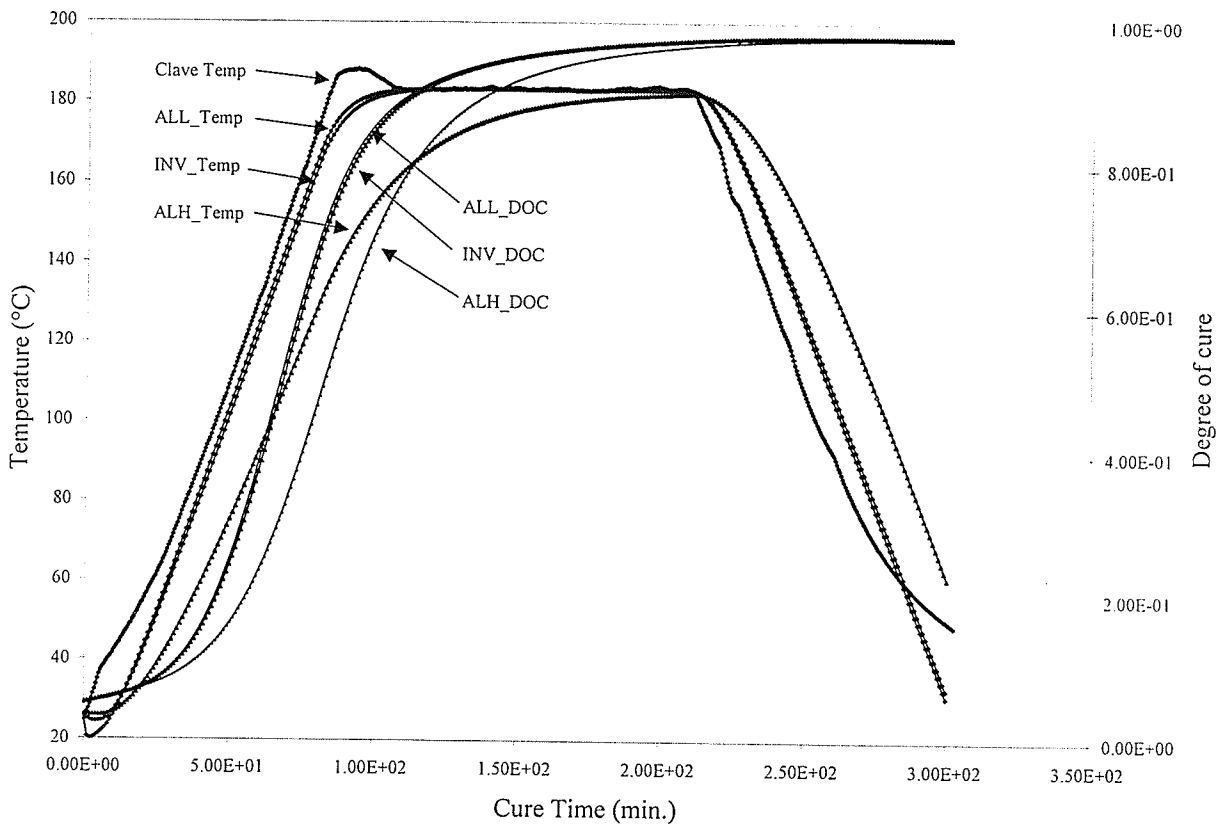


Figure 5.22 Comparison of predicted temperature & degree of cure for three tools and cycle 1

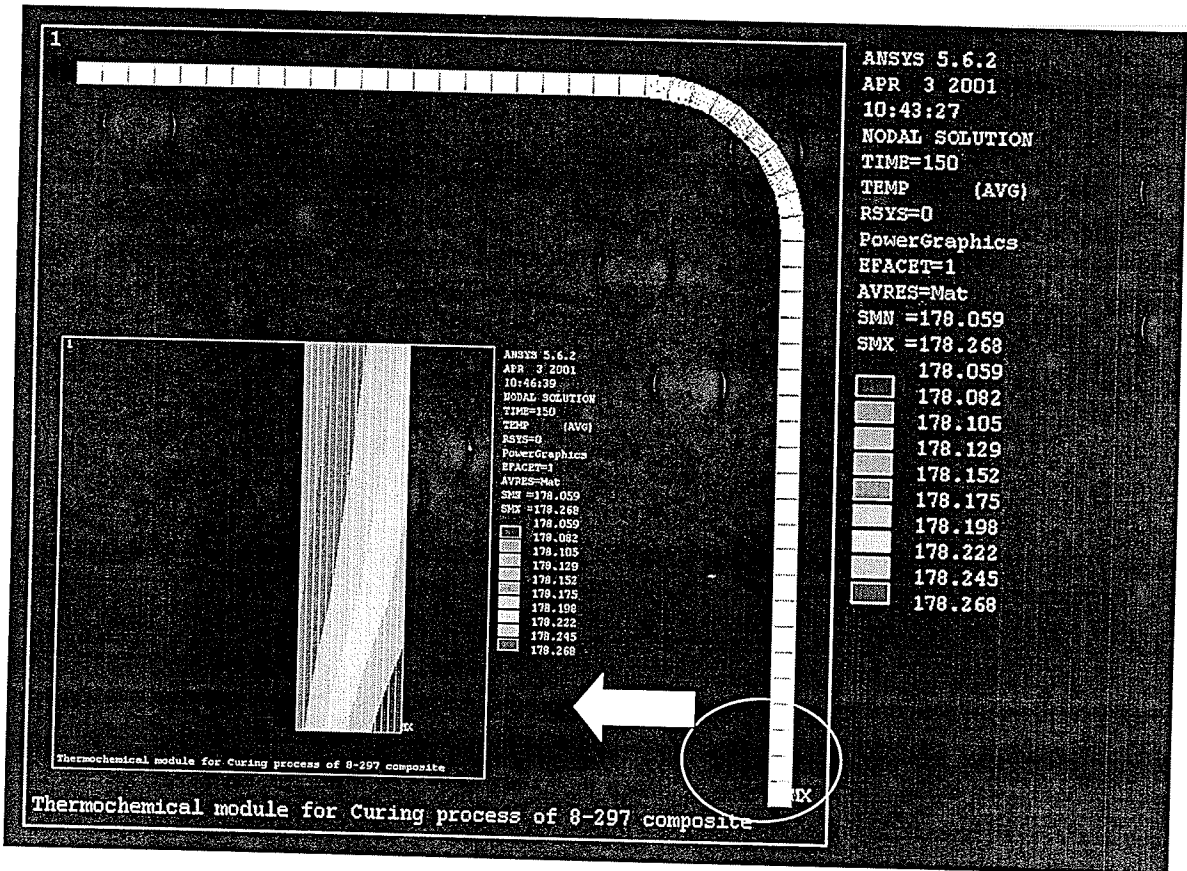


Figure 5.23 Predicted part temperature at the middle of the cure cycle for cycle 1 and

ALH tool

5.3.2.1 Effect of Process Cycle Parameters:

Table 5.4 gives the predicted spring back angle for three tools, four autoclave air temperature cycles and for a manufacturer recommended cycle. From Table 5.4 by comparing the spring back for cycles 1 & 2 and 3 & 4, the spring back was found to increase with the application of dwell. The observed trend was found to match with the experimental parametric study performed by Sarrazin et.al. (17). However an opposite trend was observed in references (7 & 8). By comparing the predicted spring back for cycles 1 & 3 and 2 & 4, we can observe that the effect of pressure on predicted spring back is negligibly small. Similar trend was also observed in a published experimental parametric study (17) and a simulation parametric analysis (13, 18).

Table 5.5 shows the predicted spring back angle for three tools and cycle 4 with dwell temperatures of 80, 121 and 140°C. From Table 5.5 it is clear that the predicted spring back decreases with decrease in the dwell temperature for all the three tools. However from Tables 5.5 by comparing the predicted spring back for cycle 4, it is clear that the influence of application of dwell at 121°C and above on predicted process-induced warpage is insignificant. It was also observed that the material has already gelled before reaching the dwell in the case of 121 and 140°C dwell cycles as explained in discussion chapter.

5.3.2.2 Effect of Tool Thermal Mass:

From Table 5.4 it can be observed that for all the five cycles the predicted spring back due to anisotropy in CTE and cure shrinkage was found to be the least for ALL tool and

highest for ALH tool. The thermal mass of the ALH tool is about 4 times that of ALL tool, and thermal mass of Invar tool is twice as much as that of ALL tool. Therefore from simulation parametric study it could be concluded that the warpage due to anisotropy in CTE and cure shrinkage increases with increase in the thermal mass of the tool.

5.3.2.3. Effect of Part Thickness:

Table 5.6 shows the predicted spring back angle for three different laminate thicknesses. It is clearly observed that the process-induced warpage decreases with increase in the laminate thickness. Similar observation was made in the previous studies (7,13,15, 17).

5.3.2.4 Effect of Autoclave Heat Transfer Coefficient:

Figure 5.24 shows the variation in the part temperature and degree of cure profile for high and low values of heat transfer coefficient. The influence of variation in the autoclave heat transfer coefficient on the prediction of part temperature was found to be relatively significant. A maximum of 15°C difference in the prediction of part temperature was observed for low autoclave heat transfer coefficient when compared to the nominal case. The predicted spring back was found to be 1.83 and 1.819° respectively for high and low autoclave heat transfer coefficient compared to nominal value of 1.83°. Hence influence of 30 % scatter in the autoclave heat transfer on prediction of warpage (spring back) is relatively low in our case study. This could be due to negligibly small temperature gradient within the part used in our case study. However predicted warpage could be sensitive to autoclave heat transfer in the case of complex structures where the temperature gradient within the part is a major source of process-induced warpage.

Table 5.4 Predicted spring back angle for three tools, four autoclave air temperature cycles and a manufacturer recommended cycle

| Cycle | MR | 1 | 2 | 3 | 4 |
|-------|-------|-------|-------|-------|-------|
| Tools | | | | | |
| ALL | 1.248 | 1.246 | 1.257 | 1.249 | 1.257 |
| INVAR | 1.348 | 1.323 | 1.325 | 1.336 | 1.339 |
| ALH | 1.865 | 1.83 | 1.851 | 1.835 | 1.863 |

Table 5.5 Effect of dwell temperature on spring back angle

| Dwell T (°C) | 80 | 121 | 140 |
|--------------|-------|-------|-------|
| Tool | | | |
| ALL | 1.243 | 1.257 | 1.259 |
| INVAR | 1.328 | 1.339 | 1.339 |
| ALH | 1.809 | 1.863 | 1.863 |

Table 5.6 Variation in the predicted spring back angle as a function of laminate thickness and autoclave heat transfer

| Parameter | Low | Nominal | High |
|--------------------------------------|-------|---------|-------|
| Part thickness ($t=3.37\text{mm}$) | 1xt | 2 x t | 3 x t |
| Spring back angle (degrees) | 1.83 | 1.328 | 1.227 |
| Autoclave Heat Transfer (degrees) | 1.819 | 1.83 | 1.83 |

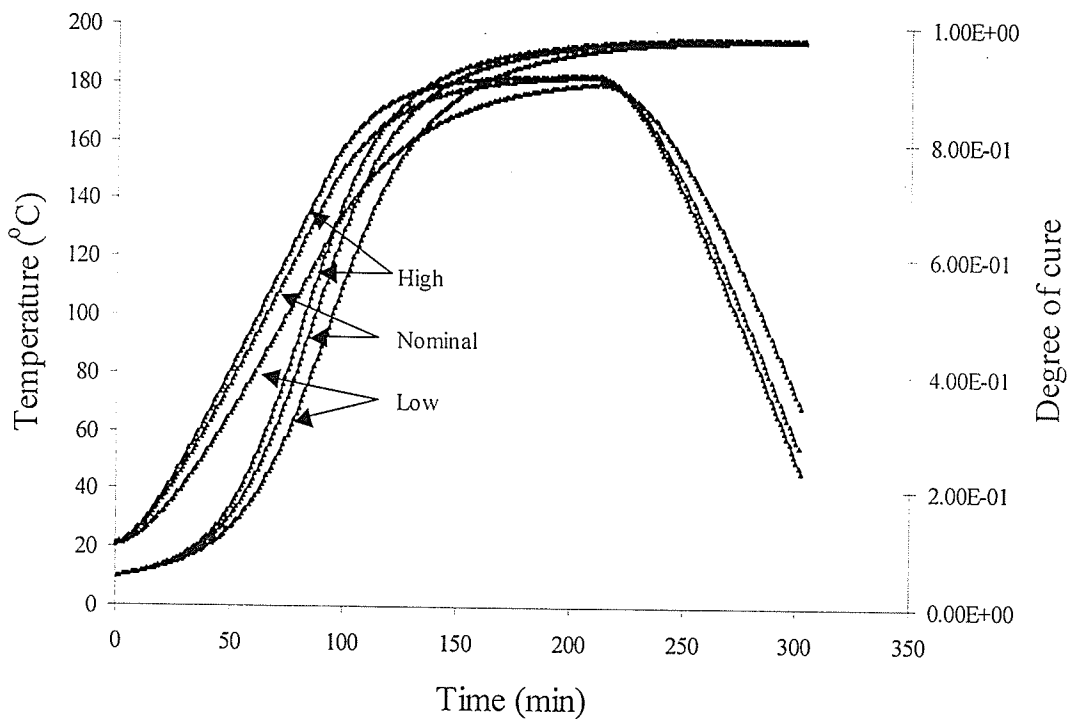


Figure 5.24 Predicted part temperature based on scatter in thermal boundary condition

5.3.2.5 Effect of Cure-Kinetics Parameters:

Table 5.7 shows the summary of effect of cure kinetics parameters on predicted spring back. From the table we can observe that the initial degree of cure, reaction order model constants A and n_0 are the most important cure kinetics parameters in the prediction of spring back. The effect of total heat of reaction and activation energy on spring back was found to be relatively low. The influences of reaction order model constants B and T_0 on predicted spring back are found to be insignificant. The similar results were observed in a previous parametric study (13). The spring back was found to decrease with decrease in the initial degree of cure. In addition, the spring back was found to decrease with either decrease or increase in the activation energy. Figure 5.25 shows the effect of reaction order model constants on reaction order. The constants n_0 and A , which, moves the curve along “ n ” axis, are found to be very important in the prediction of degree of cure as explained in next chapter. From Table 5.6 it can be observed that the predicted spring back decreases with increase in A and n_0 values. Hence higher the reaction order lowers the predicted spring back.

5.3.2.6 Effect of Thermo physical Parameters:

Table 5.8 shows the effect of thermo physical properties on predicted spring back. The effect of specific heat capacity on process-induced spring back was found to negligibly small. Similar result was observed in reference 13. The CTE was found to have little effect on spring back in contrast to that found in reference (13). In addition, the cure shrinkage coefficient was found to play an important role in the prediction of spring back.

Table 5.7 Influence of 10 % scatter in cure kinetics parameters on spring back angle

| Parameter | Maximum | Minimum |
|---------------------------------------|---------|---------|
| Cure Kinetics | | |
| Initial degree of cure (α_i) | 1.9 | 1.72 |
| Heat of reaction (H) kJ/kg | 1.835 | 1.826 |
| Activation energy (E) KJ/mol | 1.785 | 1.78 |
| Reaction order (n) | | |
| n_0 | 1.658 | 1.856 |
| T_0 (°C) | 1.83 | 1.83 |
| A | 1.688 | 1.845 |
| B | 1.83 | 1.83 |

Table 5.8 Effect of 10 % scatter in the thermo physical properties on spring back

| Parameter | Maximum | Minimum |
|---------------------------|---------|---------|
| Thermophysical Properties | | |
| C_p | 1.826 | 1.835 |
| α_{33} | 1.829 | 1.832 |
| ϵ_{33} | 1.895 | 1.768 |

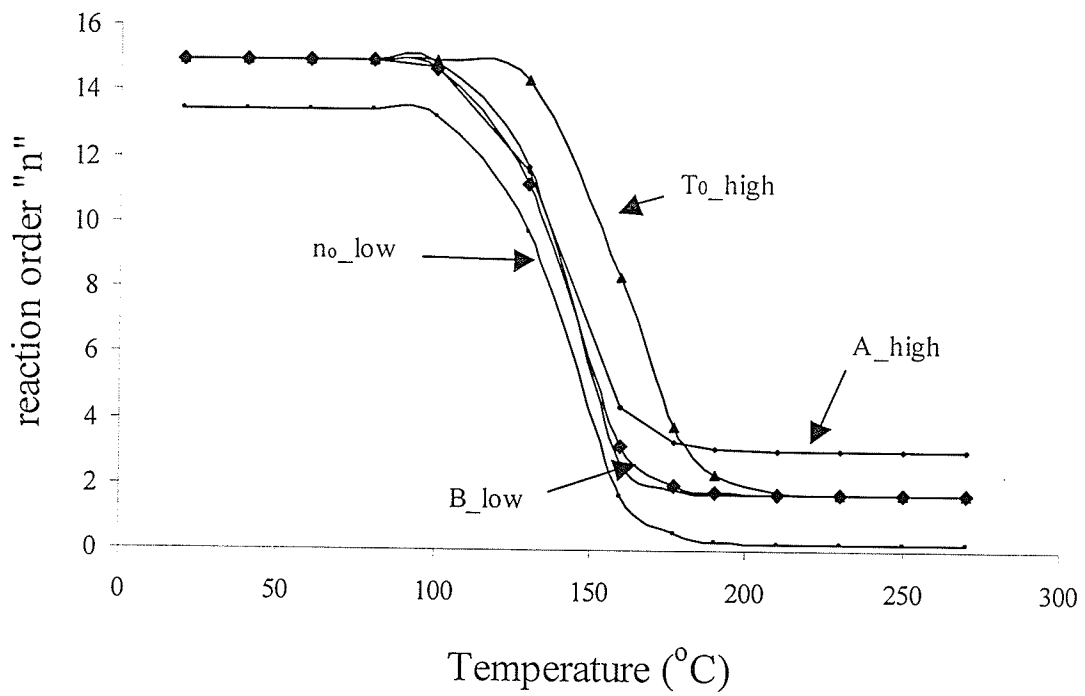


Figure 5.25 Variation in reaction order model as a function of model constants

5.3.2.7 Effect of Mechanical Properties:

Table 5.9 shows the effect of composite modulus on spring back. The longitudinal and transverse moduli of the composite play an important role in the prediction of spring back angle. The spring back was found to decrease with increase in the longitudinal modulus while spring back was found to decrease with decrease in the transverse modulus. In addition, the shear modulus of the composite has little effect on process-induced warpage. These results were found to be in agreement with the trend in the published literature (13).

5.3.2.8 Combination runs:

The combination runs were performed only on those parameters that were found to have large impact on the predicted spring back. Table 5.10 shows the predicted spring back angle for combination of cure kinetics, thermo physical and mechanical parameters. From the individual runs we know that spring back reduced from nominal case for A (high) and n_0 (high) values. From table 5.10 for combination of A (high) and n_0 (high) values the warpage reduced much more than that for individual cases. The similar trend was observed in the case of various combinations of parameters.

5.3.3 Summary of Simulation Parametric Study:

In the current study the warpage due to anisotropy in CTE and cure shrinkage was predicted using ANSYS based process model. The parametric study was performed in order to understand the impact of various process, geometry and material parameters on warpage.

Table 5.9 Effect of modulus of the composite on spring back

| Parameter | Maximum | Minimum |
|--|---------|---------|
| Mechanical Properties – Modulus of Composite | | |
| E_{11} | 1.78 | 1.879 |
| E_{22} | 1.879 | 1.77 |
| G_{12} | 1.829 | 1.832 |

Table 5.10 Combined effect of cure kinetics, thermo physical and mechanical properties on predicted spring back

| Combination Parameters | Spring back angle (degrees) |
|--|-----------------------------|
| Combination of cure kinetics parameters | |
| $A(\text{high}) + n_o(\text{high})$ | 1.52 |
| $A(\text{high}) + n_o(\text{high}) + \alpha_i(\text{low})$ | 1.42 |
| Combination of cure kinetics and thermo physical parameters | |
| $A(\text{high}) + n_o(\text{high}) + \alpha_i(\text{low}) + \epsilon_{33}(\text{low})$ | 1.38 |
| Combination of mechanical properties | |
| $E_{11}(\text{high}) + E_{22}(\text{low})$ | 1.726 |
| $E_{11}(\text{low}) + E_{22}(\text{high})$ | 1.956 |
| Combination of mechanical and thermo physical parameters | |
| $E_{11}(\text{high}) + E_{22}(\text{low}) + \epsilon_{33}(\text{low})$ | 1.66 |
| $E_{11}(\text{low}) + E_{22}(\text{high}) + \epsilon_{33}(\text{high})$ | 2.11 |

Unlike previous parametric analysis in this study the reasons for higher impact of one parameter over other was studied and explained in next chapter. The results of simulation study could be summarized as,

- The temperature gradient within the part was found to be negligibly small and hence, cannot be major source of spring back in our case study.
- The spring back due to anisotropy in CTE and cure shrinkage depends on the cure path as well as part temperature profile. The use of final cured composite properties in the prediction of spring back leads to erroneous results. Hence, it is essential to predict the spring back using resin and composite properties, which, were measured throughout the cure cycle.
- The spring back was found to increase with the application of dwell in the cycle.
- The effect of compaction pressure on spring back was found to be insignificant.
- The dwell temperature was found to play a major role in the prediction of spring back. Low dwell temperature results in low cure rate and hence low spring back.
- The tool thermal mass plays an important role in the prediction of spring back due to anisotropy in CTE and cure shrinkage. Higher thermal mass of the tool results in higher lag in the part temperature and degree of cure profile. The process-induced spring back due to the mechanism of anisotropy was found to increase with increase in the thermal mass of the tool.
- The spring back was found to decrease with increase in the thickness of the laminate.

- The parameters that alter the cure path such as cure kinetics reaction order model constants, through the thickness composite cure shrinkage coefficient, and composite longitudinal and transverse moduli are found to be the most important parameters in the prediction of spring back.
- From the combination runs it is obvious that the effect of combination of various parameters on spring back is linear combination of the predicted spring back for individual parameters.

CHAPTER 6

DISCUSSION

Unlike previous parametric study an effort was made in the current study to understand the reasons for higher impact of one parameter over other on spring back due to the mechanisms of anisotropy and tool-part interaction. This chapter explains the reasons for increase or decrease in the predicted spring back for various material, geometric and process parameters.

6.1 PREDICTION USING ANALYTICAL SOLUTION

In the section 3.6.2 the predicted spring back angle using analytical solution for this angle laminate was 1.98° . The analytical solution uses the cured composite properties, laminate sequence and the temperature gradient between cure temperature and room temperature. In addition, it does not take into account the effect of thermal boundary conditions, thermal mass of the tool and evolution of composite thermophysical and mechanical properties during cure. Therefore based on analytical solution predicted spring back angle for this angle laminate and material is always 1.98° , irrespective of process cycle parameters, tool material and tool thermal mass. However numerical solution, which takes into account the effect of all the above parameters, is far from the analytical solution. In addition, unlike analytical solution, the numerical solution varies widely from one cycle to other, and one tool material to other, as was discussed in 5.3.2. This emphasizes the point that the prediction using cured composite properties and final state of cure cycle would result in erroneous results. This could be one of the reasons for negligible effect of tool material on spring back observed in literature 14 & 15. In

addition, this study concludes that the warpage due to the mechanism of anisotropy is path dependent.

6.2 CURE KINETICS PARAMETERS

In the section 5.3.2.5 it was observed that the predicted spring back decreased with higher values of reaction order model constants A and n_0 . Figure 6.1 shows the effect of these model constants on predicted degree of cure during the entire cure cycle. In addition, the effect of these parameters on part temperature profile was found to be negligibly small as shown in Figure 6.2. From figure 6.1 it is clear that the rate of degree of cure for n_0 (low) is much greater than that for the nominal case. Similarly the rate of degree of cure for the nominal case is much higher than that of A (high). Therefore it can be inferred that when there is no variation in the part temperature profile or heating rate, low curing rate results in low process-induced warpage. This could be explained using equation for effective thermal strain in a laminate that is given by,

$$[\varepsilon_{th}] = [a] \sum Q_k e_k \quad (6.1)$$

and,

$$e_k = \Delta T \left(\alpha + \frac{\Delta \varepsilon}{\Delta T} \right) \quad (6.2)$$

where,

[a] matrix and Q_k depends on the modulus of the composite

e_k – effective thermal strain in each ply

k - ply number

α - CTE of the composite

ε - cure shrinkage of composite, and

ΔT – temperature gradient

From the above equations it is clear that the effective thermal strain is function of modulus, and CTE and cure shrinkage of the composite. In addition, from material property characterization tests have shown that CTE is independent of temperature and degree of cure. However cure shrinkage and modulus of the composite are function of degree of cure. Hence at any given time step, the cure shrinkage as well as the modulus depend on the cure path. In addition, the incremental temperature at any given time step is function of temperature profile. Therefore process-induced warpage is function of (a) cure path, (b) temperature profile, and (c) cure shrinkage and modulus of the composite. In the case of parametric study on the influence of cure kinetics reaction order there is no change in the temperature profile. Hence the effective thermal strain in each ply is directly proportional to cure shrinkage strain. In addition, since cure shrinkage depends on degree of cure, lower the degree of cure for a given time step lower is the cure shrinkage strain. Besides the longitudinal (E_{11}) and transverse (E_{22}) moduli are directly proportional to degree of cure. Hence lower the degree of cure lower is the E_{11} and E_{22} . From parametric study we know that lower the E_{11} higher the warpage and lower the E_{22} lower the warpage. Therefore net thermal strain of laminate at any given time step is the function of combined effect of E_{11} and E_{22} , and cure shrinkage strain. Figure 6.1 also shows the cumulative thermal strain in y-direction retrieved from the stress module as a function of process time for the node at the top corner of the arm of angle laminate. From this it is clear that thermal strain is low for high value of A, and high for low value of n_0 .

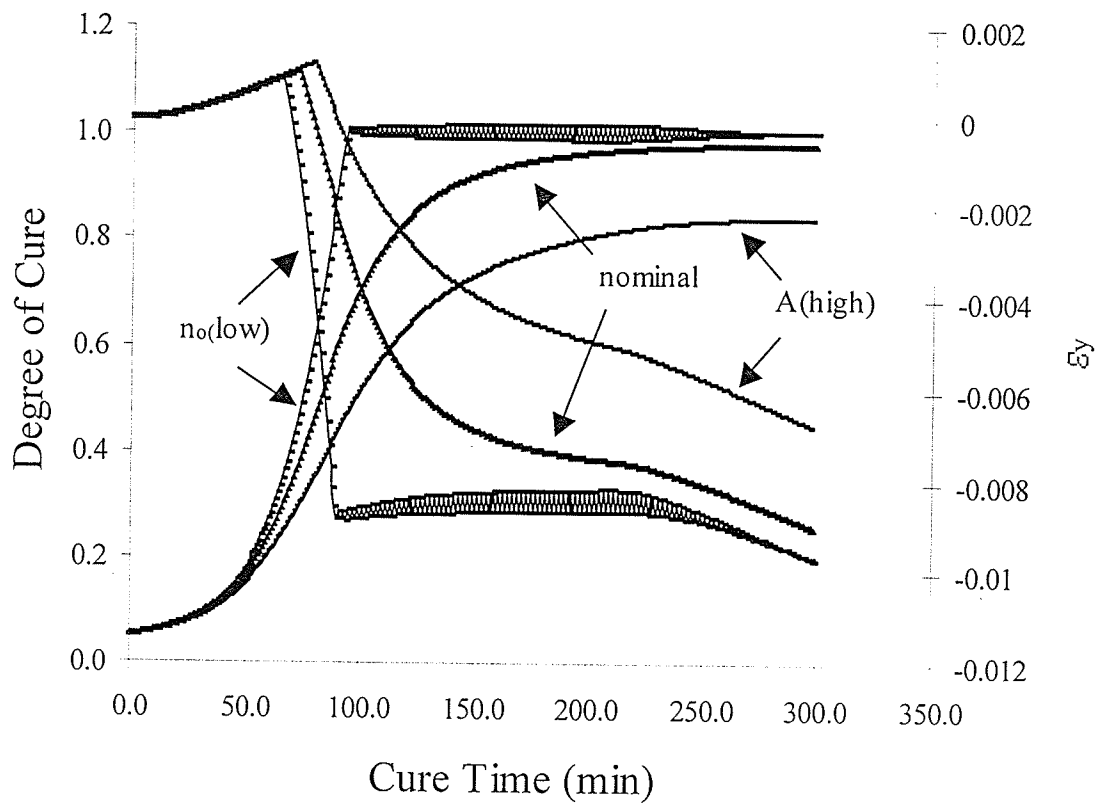


Figure 6.1 Sensitivity of reaction order model constants on degree of cure prediction and predicted thermal strain in through the thickness direction

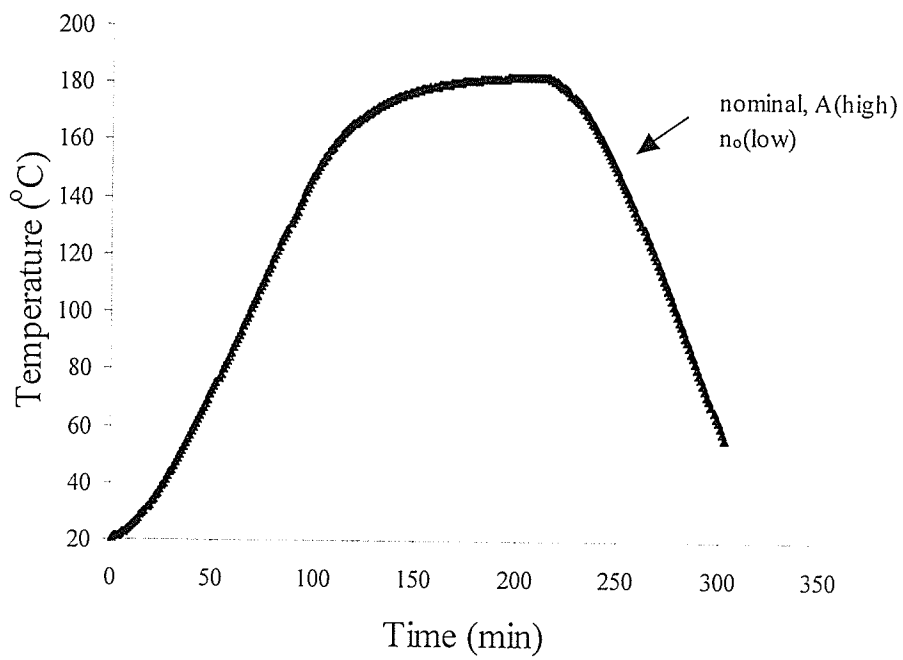


Figure 6.2 Predicted part temperatures for variation in reaction order model constants

From Figure 6.1 we can also observe that the effective thermal strain initially increases due to the type of through-the-thickness cure shrinkage model used. The cure shrinkage starts around 0.37 degree of cure and hence we do not see the effect of cure shrinkage strain on effective thermal strain. However after 0.37 degree of cure effective thermal strain builds up rapidly as the material shrinks. In addition, a scatter in the prediction was observed for n_0 low value. This is due to the numerical error associated with ANSYS program.

6.3 LAMINATE THICKNESS

It has been observed in section 5.2.3.2 that the process-induced spring back decreases with increase in laminate thickness. Figure 6.2 shows the predicted part temperature and degree of cure for the three laminate thicknesses. From this figure it could be observed that the variation in the part temperature profile and cure path for three cases is negligibly small. Hence, in this case, the decrease in the spring back with increase in laminate thickness is not due to the change in the cure path or temperature profile or ply thermal strain. In addition, since all the material parameters are constant, the decrease in laminate thickness should be due to the increase in the bending stiffness of the laminate. This could be illustrated by using equations for in-plane and out-of-plane bending stiffness coefficients that are given by,

$$A_{ij} = \sum_{k=1}^n Q_{ij}^k t_k \quad (6.3)$$

$$D_{ij} = \sum_{k=1}^n Q_{ij}^k t_k^3 \quad (6.4)$$

where,

Q matrix is function of E_{11} and E_{22}

t - thickness of each ply, and

n – number of plies, and

k – ply number

From the above equations it is clear that with the increase in laminate thickness or ply thickness the bending stiffness of the laminate increases. Hence, for a given effective thermal strain load, the process-induced spring back decreases with increase in laminate thickness.

6.4 TOOL THERMAL MASS

It has been observed from section 5.3.2.2 that the spring back due to anisotropy in CTE and cure shrinkage was found to be low for tool with low thermal mass. In addition, it was also observed that the part temperature and the degree of cure lagged considerably for the part manufactured using ALH tool compared to that of ALL and Invar tools. Figures 6.4 and 6.5 shows the predicted degree of cure, part temperature and thermal strain for the parts manufactured using three tools and cycle 1. The slope of the degree of cure and part temperature curves was found to be the least for ALH tool and highest for ALL tool. In other words rate of heating and rate of cure were found to be the least for ALH tool. In addition, in this case spring back was found to be highest for ALH tool with least rate of degree of cure and spring back was found to be least for ALL tool with highest rate of cure. This contradicts the argument in section 6.2. Therefore unlike cure kinetics parameters in this case the predicted spring back cannot be compared only with the degree of cure profile but it also depends on the part temperature profile.

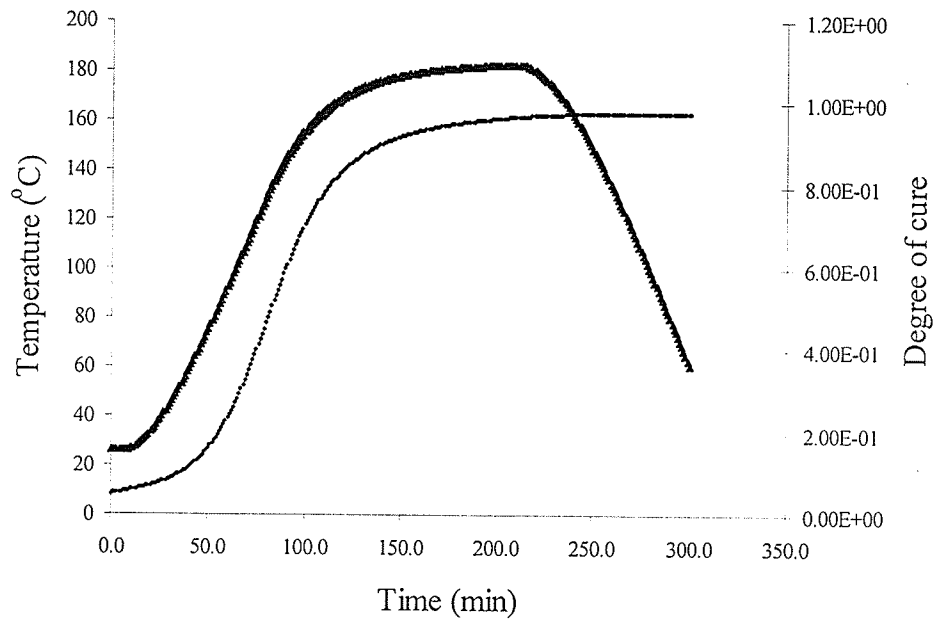


Figure 6.3 Effect of laminate thickness on predicted part temperature and degree of cure for three different laminate thicknesses

From Table 5.4 and Figure 6.5, based on the trend in the predicted spring back angle and predicted part temperature for three tools, it could be inferred that, higher the rate of heating, higher the predicted spring back. From equations 6.1 and 6.2 we know that the predicted effective thermal strain depends on modulus and effective thermal strain for each ply (e_k). The modulus was found to be function of degree of cure only. However, effective thermal strain for each ply is function of degree of cure as well as part temperature profile. Therefore based on the similar trend between predicted spring back and part temperature we can infer that the effect of e_k is much higher than the combined effect of $[a]$ and Q_k on the effective thermal strain. However from equation 6.2 we know that e_k depends on the CTE, cure shrinkage and temperature gradient. In addition, in order to justify the trend in predicted spring back based on tool, it is essential to prove for a given ply,

$$\left[\left(\alpha + \frac{\Delta\varepsilon}{\Delta T}\right)\Delta T\right]_{ALH} > \left[\left(\alpha + \frac{\Delta\varepsilon}{\Delta T}\right)\Delta T\right]_{ALL}$$

Therefore effective CTE for a 0-direction ply was retrieved throughout the cure cycle using material module as shown in Figure 6.6. From this figure it is clear that the effective CTE is highest for ALH tool and least for ALL tool throughout the cure cycle. This confirms the argument that higher the rate of heating, higher the spring back angle, even if the rate of cure is low. From Figure 6.6 a sudden drop in the predicted effective CTE, observed at about degree of cure of 70 % is due to the longitudinal cure shrinkage (ε_{11}) model used in the material module. From material characterization, the measured ε_{11} was found to decrease linearly up to a degree of cure of 0.7 and shrinkage beyond this cure was found to be negligibly small. Therefore the predicted effective CTE in Figure 6.6 shows only the α_{11} of the ply beyond 0.7 degree of cure.

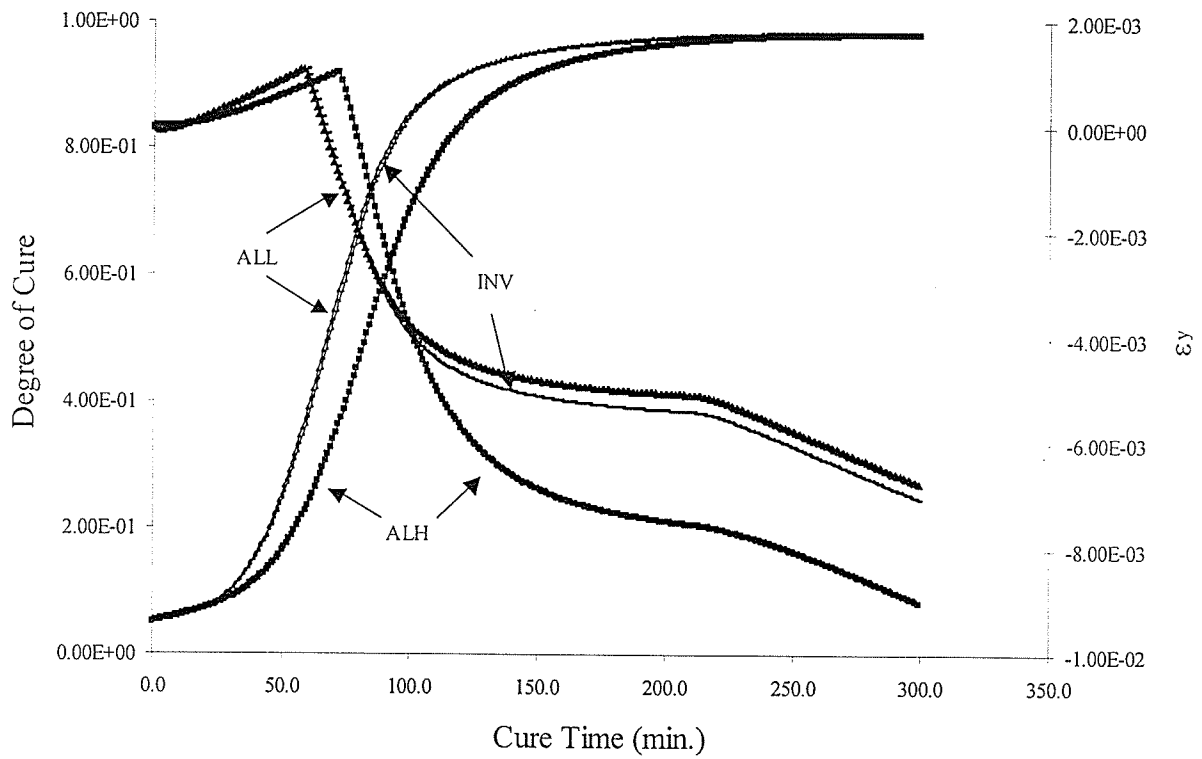


Figure 6.4 Comparison of degree of cure and thermal strain for three tools and cycle 1

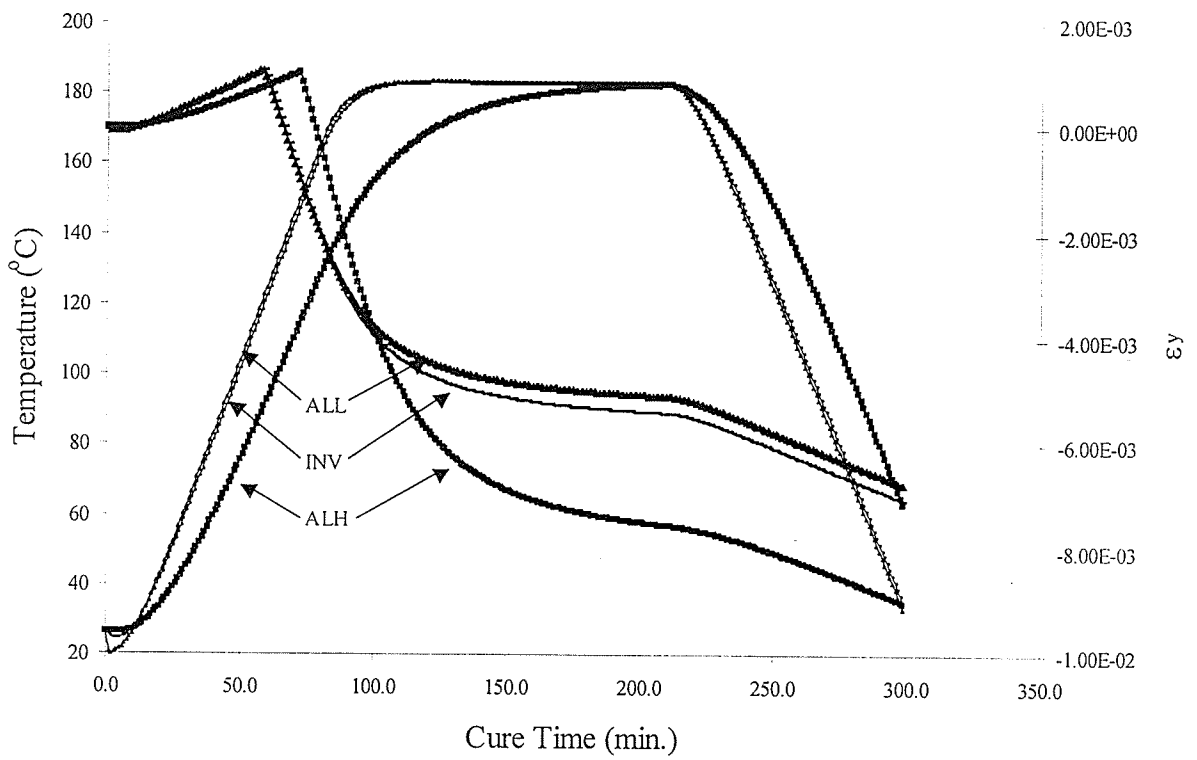


Figure 6.5 Comparison of predicted part temperature and thermal strain for three tools and cycle 1

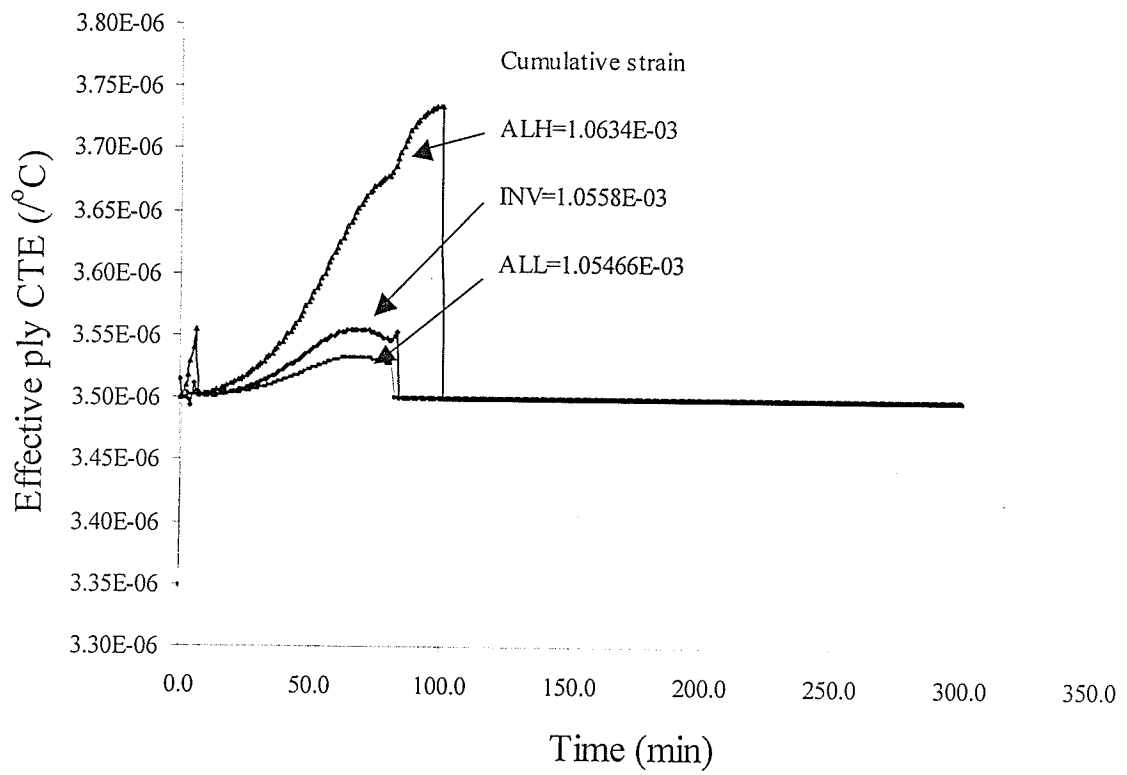


Figure 6.6 Predicted incremental effective CTE for a 0-direction ply

6.5 PROCESS CYCLE PARAMETERS

In the section 5.3.2.1 the spring back was predicted based on measured autoclave air temperature cycles. However a correlation between the predicted part temperature and degree of cure profiles and the predicted spring back angle could not be studied due to the crossing of these profiles. This is thought to be due to the variation in the initial temperature and maximum cure temperature for each cycle. Therefore in order to understand the effect of process parameters on spring back accurately, the previous five cycles were used with same initial temperature and maximum cure temperature. The predicted spring back angle for these five cycles are shown in Table 6.1. From this table by comparing cycles 1 & 2 and 3 & 4 it is clear that the application of dwell increases the process-induced spring back. In addition, by comparing cycles 1 & 3 and 2 & 4, the effect of pressure on spring back was found to be insignificant. Figures 6.7 shows the predicted part temperature for five cycles and ALH tool. From figures 6.7 it can be observed that the heating rate is approximately equal for cycles 1, 3 and MR. Similarly, the heating rate was found to be approximately same for cycles 2 & 4. By comparing the heating rate for two sets of cycles (1,3&MR and 2&4) as explained in previous section it is clear that higher the rate of heating lowers the spring back. As observed in table 5.5 in section 5.3.2.1 the predicted spring angle was found to be the least for cycle with 80°C dwell temperature. Figure 6.8 shows the predicted part temperature and cure for three cycles and ALH tool. From this figure it can be observed that heating rate is approximately same for three cycles but cure rate changes considerably for cycle with 80°C dwell. Similar to the effect of cure kinetics parameters discussed in section 6.2, in this case slower rate of cure decreases the predicted spring back.

Table 6.1 Predicted spring back for five cycles for ALH tool

| Cycle | MR | 1 | 2 | 3 | 4 |
|-----------------------------|-------|-------|------|-------|-------|
| Spring back angle (degrees) | 1.828 | 1.832 | 1.87 | 1.835 | 1.872 |

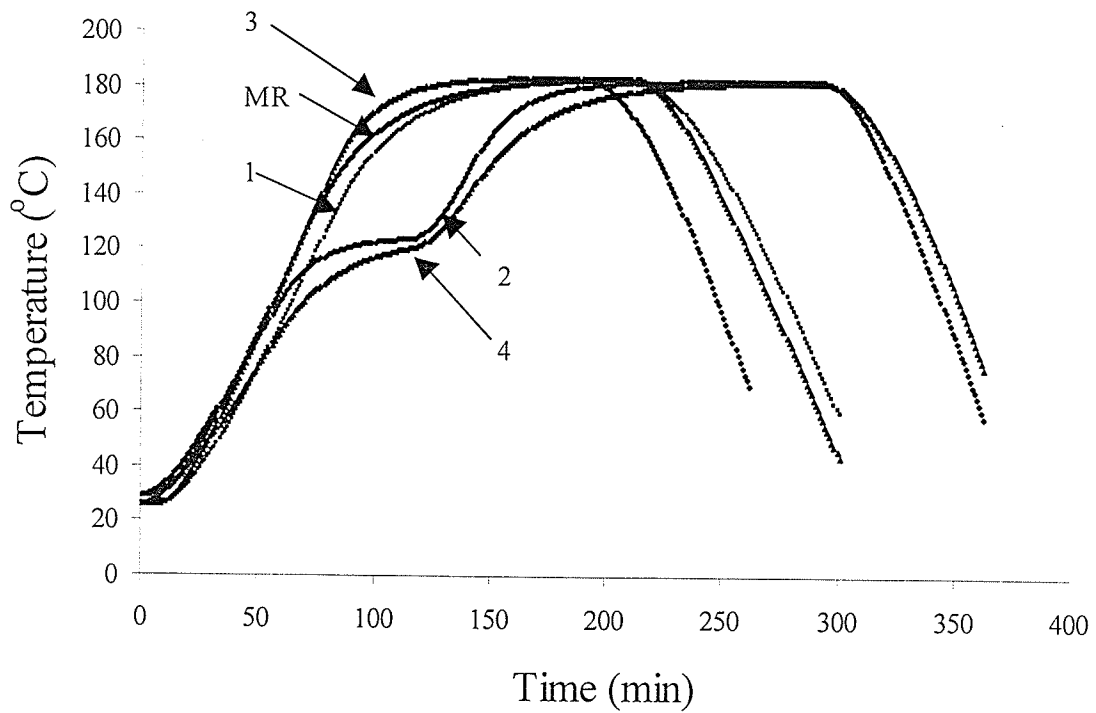


Figure 6.7 Predicted part temperature for five cycles and ALH tool

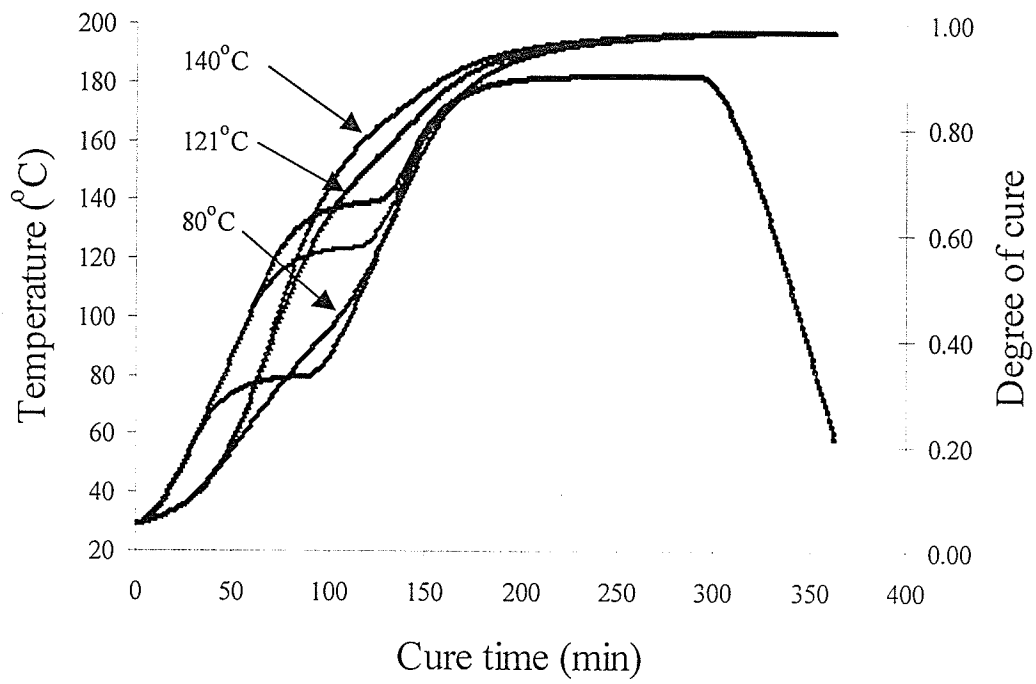


Figure 6.8 Predicted part temperature and degree of cure for different dwell temperature

6.6 DELINEATED WARPAGE DUE TO TOOL-PART INTERACTION

In the current work an effort was made to delineate the process-induced spring back due to the mechanism of tool-part interaction from measured spring back. This was performed by subtracting the predicted spring back due to anisotropy in CTE and cure shrinkage from the measured total spring back in angle laminate. The delineated warpage due to tool-part interaction is shown in Figure 6.9. Similar to the measured spring back in angle laminates, a trend in the dependence of this delineated warpage on process cycle parameters and thermal mass was not observed. In addition, by comparing the delineated warpage (Figure 6.9) with measured warpage due to tool-part interaction (Figure 5.19), the following can be inferred,

- In both the cases the warpage due to tool-part interaction was found to be least for Invar tool for all process cycles.
- The effect of process parameters on warpage due to tool-part interaction was found to follow similar trend in both the cases except for cycle 2. However, in both the cases there was no trend in the warpage between one cycle to other.
- The similar trend in the influence of thermal mass on tool-part interaction warpage was observed except for cycle 2. However, effect of thermal mass on warpage could not be discerned from both cases.

This discrepancy in the observed trend for cycle 2 could be due to,

- The scatter in the measured spring back angle using ROMER instrument, and
- The variation in the autoclave air temperature cycles for a given manufacturer set temperature cycle as shown in Figure 6.10.

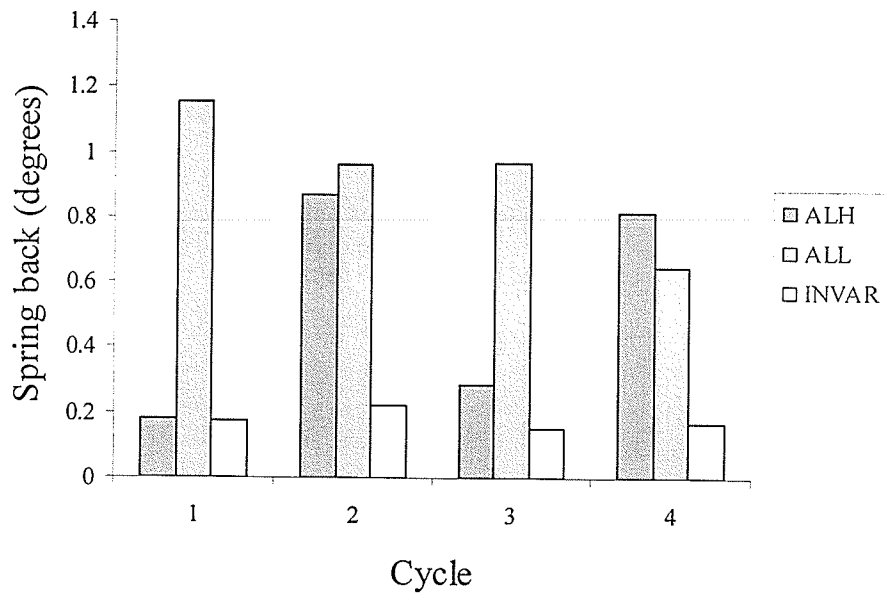


Figure 6.9 Warpage due to tool-part interaction delineated from the measured spring back

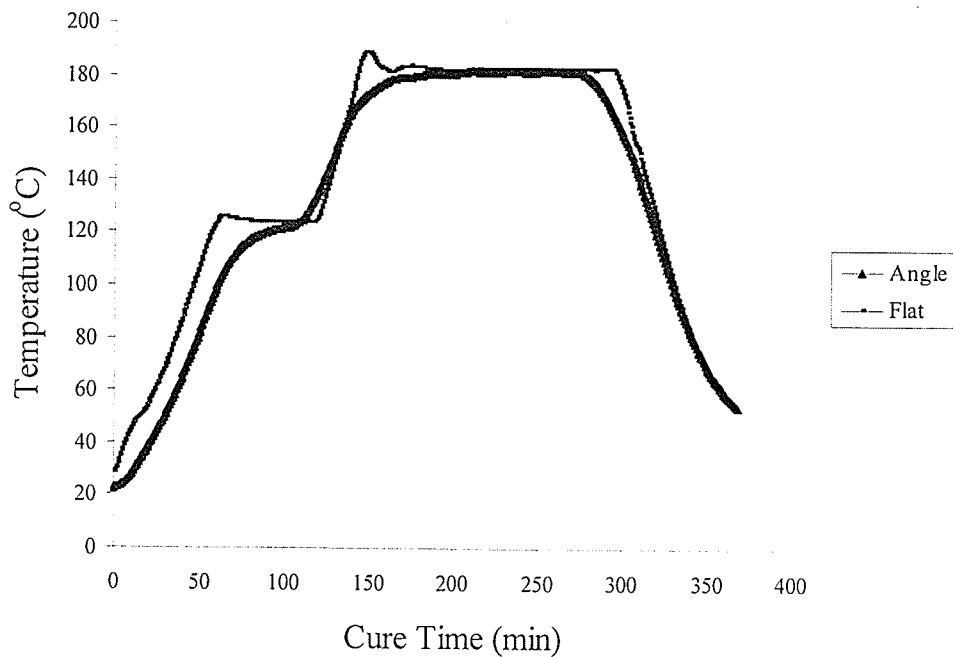


Figure 6.10 Variation in the autoclave air temperature during manufacturing of angle laminates and flat laminates

CHAPTER 7

CONCLUSIONS AND RECOMMENDATIONS

In the current study ANSYS based process model was used for the prediction of spring back angle due to the mechanism of anisotropy in composite CTE and cure shrinkage. The experimental and simulation parametric study was performed in order to understand the effect of various process, geometric and material parameters on spring back. In addition, an effort was made to reason the higher impact of one parameter over the others on the spring back. The summary and conclusions based on the current study are presented here.

7.1 SUMMARY OF THE CURRENT WORK

7.1.1 Process Model:

In the current study an existing ANSYS based process model was improved as follows:

- Improved the existing process model to read geometry, mesh and mechanical boundary conditions directly using GUI of ANSYS
- Developed a material module to predict accurately the continuous evolution of composite thermophysical and mechanical properties throughout the cure cycle.
- Modified the stress module to predict the spring-back due to anisotropy in CTE and cure shrinkage alone and this was used to delineate the contribution from tool-part interaction. Such delineation was not done in previous studies.

7.1.2 Experimental Parametric Study:

- The effect of process parameters and thermal mass on spring back could not be discerned based on experimental measurement.
- The spring back was found to increase with increase in CTE mismatch between tool material and the composite.
- Temperature gradient within the part and thickness variation in the part was not a source of spring back in our case study.
- The delineated contribution of tool-part interaction from measured spring-back was found to be lower than the contribution from anisotropy in CTE and cure shrinkage.
- In addition warping of the arms of the angle laminate was observed. Using experimental results from flat laminates, this warpage was confirmed to be due to tool-part interaction.
- The effect of process parameters and thermal mass on warping of arm could not be discerned based on experimental measurement.
- The warping of arm was found to increase with increase in CTE mismatch between tool material and the composite.
- Higher warping of the arm found to result in low spring back.

7.1.3 Simulation Parametric Study:

This parametric study focused only on the contribution to spring back from anisotropy in CTE and cure shrinkage. From simulation study it could be summarized that,

- The autoclave heat transfer coefficient was found to be relatively significant parameter in the part temperature prediction. However due to negligible temperature gradient within the part in our case study the effect of autoclave heat transfer coefficient on spring back was relatively insignificant.
- The application of dwell in the cycle was found to increase the spring back.
- The effect of compaction pressure on spring back was found to be insignificant.
- Higher tool thermal mass results in higher spring back.
- The spring back decreased with increase in the thickness of the laminate.
- The cure-kinetics reaction order that changes the cure path and cure path dependent composite properties such as, through the thickness composite cure shrinkage coefficient, and composite longitudinal and transverse moduli were found to be the most important parameters influencing the spring back.

7.2 CONCLUSIONS BASED ON CURRENT WORK

Based on the current work it could be concluded that,

- Process-induced spring back is cure-cycle dependent and prediction based on cured composite properties corresponding to the end state of cure cycle will lead to erroneous spring back prediction.
- The spring back will decrease with decrease in rate of cure if the rate of heating is constant.
- If the rate of heating of the part also changes with rate of cure during processing, then the measured spring-back will be a complex function of the influences of

both the rate of cure and rate of heating. In this study, high rate of heating of the part has been found to cause a decrease in spring back.

- Finally, the parts with low spring back could be manufactured, by choosing a tool with low CTE and low thermal mass, and by selecting a process cycle that results in high rate of heating of the part.

7.3 RECOMMENDATIONS

Based on the experimental and simulation results few issues arose which indicate the need for future investigations. Some of the potential areas of future work that might lead to better understanding of autoclave processing of composites and more accurate prediction of spring back are listed below.

- In material characterization, the through-the-thickness cure shrinkage (ϵ_{33}) and shear modulus of the composite (G_{12}) were found to be temperature dependent. However in the current study they were modeled as only cure dependent and effect of temperature was not taken into account. Therefore for more accurate prediction of spring back it is necessary to model these material parameters as function of both degree of cure and temperature.
- The accuracy of ROMER for the measurement of spring back angle of order 1-2° was found to be insufficient. Hence in future experimental spring back measurements there is need for use of equipment that can measure spring back more accurately.
- For better understanding of the process parameters on spring back it is necessary to understand the mechanism of resin flow during curing. Therefore the current

process model requires further improvement in terms of development of a flow module that works with the stress module.

- Finally, to compare the delineated warpage and measured warpage due to the mechanism of tool-part interaction it is advisable to manufacture the set of angle laminates and flat laminates in a single autoclave run.

REFERENCES

1. H.T.Hahn and N.L.Pagano, "Curing Stresses in composite Laminates", Journal of Composite Materials, **9** (1975) pp. 91-108.
2. Alfred C Loos & George S Springer, "Curing of Epoxy Matrix Composites", Journal of Composite Materials, **17** (March 1983), pp.135-169.
3. T.A.Bogetti, "Process-Induced Stress and Deformation in Thick-section Thermosetting Composites", CCM Report 89-32, University of Delaware, 1989.
4. White, S.R. and H.T. Hahn, "Process modeling of composite materials: residual stress development during cure, part I. model formulation", Journal of Composite Materials, **26**(16), (1992), pp. 2402-2422.
5. White, S.R. and H.T. Hahn, "Process modeling of composite materials: residual stress development during cure, part II. Experimental validation", Journal of Composite Materials, **26**(16), (1992), pp. 2423-2453.
6. Andrew Johnston, "An integrated model of the development of process-induced deformation in autoclave processing of composite structures", PhD thesis, University of British Columbia, (1997).
7. Jose Daniel, D.Melo & Donald. W. Radford, "Modeling Manufacturing Distortions In Flat, Symmetric Composite Laminates", 31st International SAMPE Technical Conference, **31**, October 26-30, (1999).
8. M.T.Cann & Daniel. O. Adams, "Effect Of Part-Tool Interaction On Cure Distortion Of Flat Composite Laminates", 46th International SAMPE Conference, Long Beach, CA, **46**,May 6-10, (2001).

9. Pascal Hubert, "Aspects Of Flow And Compaction Of Laminated Composite Shapes During Cure", PhD thesis, University of British Columbia, (July 1996).
10. Michael Hudek, Matt Shewfelt, R. Mark Shead, Andrew Johnston, Nezhir Mrad, Rick Cole, J. Raghavan, and Loren Hendrickson, "Examination of Heat Transfer in Autoclaves", 46th International SAMPE symposium and Exposition, Long Beach, CA, 46, May 6-11, (2001).
11. M.Hojjati and S.V.Hoa, "Curing simulation of thick thermosetting composites", *Composites Manufacturing*, **5**, November 3 (1994), pp. 159-169.
12. J.Bailey, T.Bogetti, X.Haung & W.Gillepse, "Cure behavior of thick-section thermoset composites", ANTEC, (1998), pp. 725-729.
13. Andrew Johnston, Pascal Hubert, Karl Nelson, Goran Fernlund and Anoush Poursartip, "A sensitivity analysis of modeling predictions of the warpage of a composite structure", 43rd International SAMPE Symposium, 43, May 31-June 4, (1998).
14. Lalit K Jain, Yiu-Wing Mai, "Stress and deformation induced during Manufacturing. Part I", *Journal of composite materials*, **31**, No.7 (1997), pp.672-695.
15. Lalit K Jain, Yiu-Wing Mai, "Stress and deformation induced during Manufacturing. Part II, A Study of spring in phenomenon", *Journal of composite materials*, **31**, No.7 (1997), pp.696-719.
16. H.W.Wiersma, L.J.B.Peeters and R.Akkerman, "Prediction of spring forward in continuous-fiber/polymer L-shaped parts", *Composites Part A*, **29A**, (1998), pp. 1333-1342.

17. Sarrazin, H., B. Kim, S.H. Ahn, and G.S. Springer, "Effects of Processing Temperature and Lay-up on Spring back", *Journal of Composite Materials* **29**(10), (1995), pp. 1278-1294.
18. Goran Fernlund & Anoush Poursartip, "The Effect Of Tooling Material, Cure Cycle, And Tool Surface Finish On Spring-In Of Autoclave Processed Cured Composite Parts", *ICCM – 12*, **12**,(1999).
19. Ray Y Kim, Brian P Rice, Allan S Crasto & John D Rusell, "Influence Of Process Cycle On Residual Stress Development In BMI Composites", 45th International SAMPE symposium, Long Beach, CA, **45**,May (2000).
20. Barton J.M, "The Application of Differential Scanning Calorimetry (DSC) to the Study of Epoxy Resin Curing Reactions", *Advances in Polymer Science 72: Epoxy Resin and Composites I*, K. Dusek, Ed., Springer-Verlag, (1985), pp. 111-154.
21. Ryan L.Karkkainen and Madhu S.Madhukar, "Empirical modeling of in-cure volume changes of 3501-6 Epoxy", 44th International SAMPE conference, **44**,May (2000).
22. J Mijovic & H T Wang, "Cure Kinetics Of Neat And Graphite-Fiber-Reinforced Epoxy Formulations", *Journal of Applied Polymer Science*, **37**, (1989), pp. 2661-2673.
23. A Yousefi, P.G. Lafleur & R. Gauvin, "Kinetic Studies Of Thermoset Cure Reactions: A Review", *Polymer Composites*, **18**, No.2, April (1997), pp. 157-168
24. Shengong Fu and Donald W.Radford, "Effects of lamination angle on the 3-D thermal expansion coefficients", 31st International SAMPE Technical Conference, **31**,October (1999).

25. Peter R. Criscioli, Qiuling Wang and George S. Springer, "Autoclave Curing-Comparisons of Model and Test Results", *Journal of Composite Materials*, **26**, No. 1 (1992), pp.90-103.
26. J. Mijovic & J.Wijaya, "Effect Of Graphite Fiber & Epoxy Matrix Physical Properties On The Temperature Profile Inside Their Composite During Cure", *SAMPE Journal*, **25**, No.2, (March/April 1989), pp.35-39.
27. Shi-Chang Tseng & Tim A Osswald, "Prediction Of Shrinkage And Warpage Of Fiber Reinforced Thermoset Composite Parts", *Journal of Reinforced Plastics & Composites*, **13**, (August 1994), pp.698-721.
28. Laszlo P Kollar, "Approximate Analysis Of The Temperature Induced Stress & Deformations Of Composite Shells", *Journal of Composite Materials*, **28**, No.5 (1994), pp.392-415.
29. Ajit K Roy, "Response Of Thick Laminated Composites Rings To Thermal Stresses", *Composite Structures*, **18**, (1991), pp. 125-138.
30. N. Zahlan & J. M. O'Neil, "Design & Fabrication Of Composite Components, The Spring Forward Phenomena", *Composites*, **20**, No.1, (January 1989), pp. 77-81.
31. P.Hubert, R.Vazeri, and A.Poursartip, "A two-dimensional Flow Model for the Process Simulation of Complex Shape Composite Laminates", *International Journal for Numerical Methods in Engineering*, **44** (1999) pp. 1-26.
32. R.Dave, J.L.Kardos & M.P.Dudukovic, "A Model For Resin Flow During Composite Processing: Part 1 - General Mathematical Development", *Polymer Composites*, **8**, No.1, (February 1987),pp. 29-38.

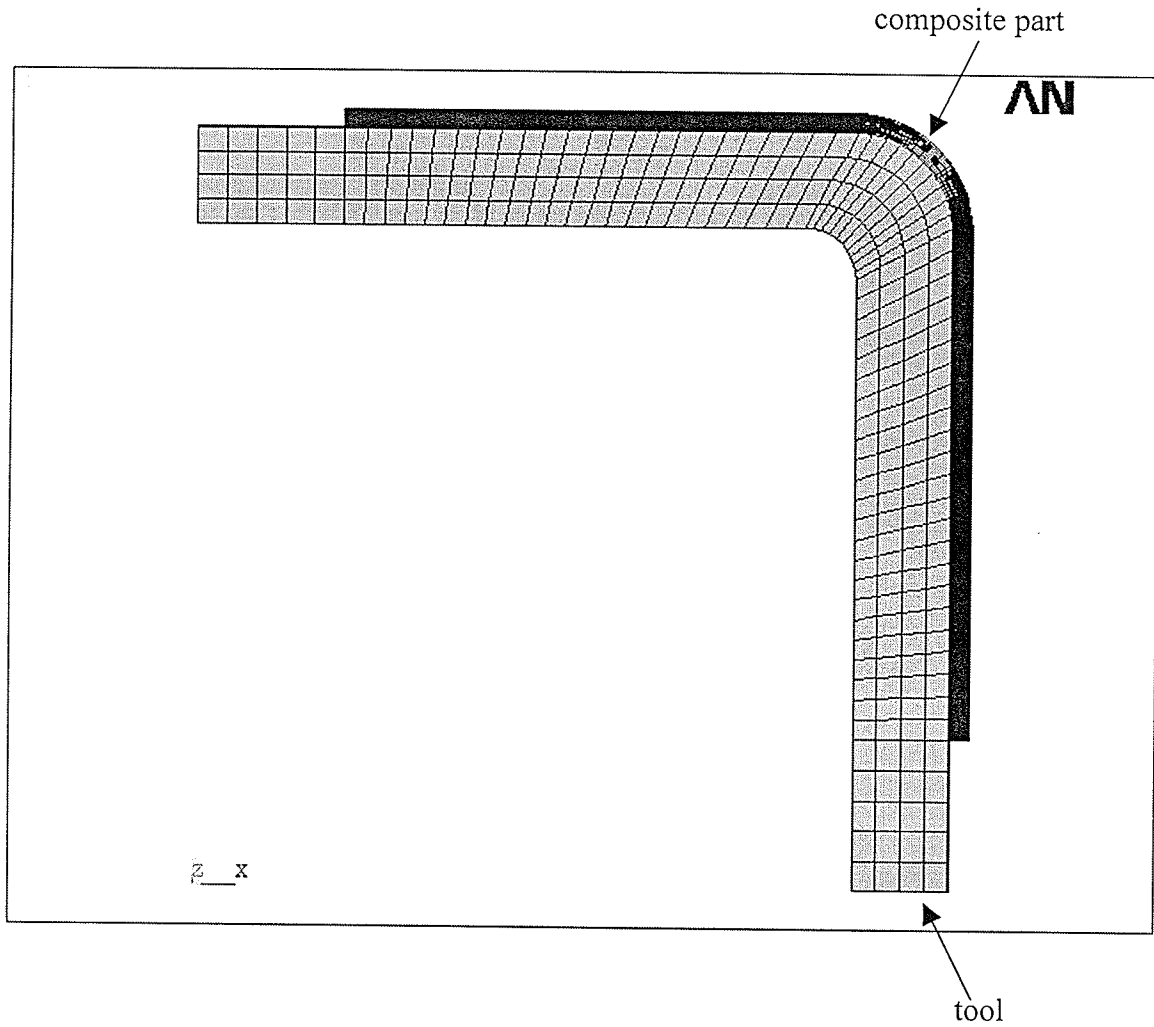
33. R.Dave, J.L.Kardos & M.P.Dudukovic, "A Model For Resin Flow During Composite Processing: Part 2 – Numerical Analysis For Unidirectional Graphite/Epoxy Laminates", *Polymer Composites*, **8**, No.2, (April 1987), pp. 123-132.
34. Wen-Bin Young, "Resin Flow Analysis In The Consolidation Of Multi-Directional Laminated Composites", *Polymer Composites*, **16**, No.3, (June 1995), pp. 250-257.
35. Yeong K Kim & Scott R White, "Stress Relaxation Behavior Of 3501-6 Epoxy Resin During Cure", *Polymer Engineering & Science*, **36**, No.23, (December 1996), pp. 2852-2862.
36. Yeong K Kim & Scott R White, "Process-Induced Stress Relaxation Analysis Of AS4/3501-6 Laminate", *Journal Of Reinforced Plastics & Composites*, **16**, No. 1, (1997), pp. 2-16.
37. T.G.Gutowski, Z.Cai, S.Bauer & D.Boucher, "Consolidation Experiments For Laminate Composites", *Journal Of Composite Materials*, **21**, (July 1987), pp. 650-669.
38. Xianwei Zeng & J.Raghavan, "Finite Element Modeling Of The Processing Of Thermoset Composite Laminates", a report submitted at University of Manitoba, (1998).
39. M.P.Koteshwara & J.Raghavan, "Parametric study of process-induced deformation in composite laminates", 46th International SAMPE symposium and Exposition, Long Beach, CA, 46, May 2001.
40. ANSYS User's manual for Release 5.6.2, ANSYS Inc.
41. A material data sheet from FIBERITE, pp. V.b-5 – V.b-17, (December 15, 1991).

42. Isaac M. Daniel & Ori Ishai, Engineering Mechanics of Composite Materials, Oxford University Press, New York, c1993.
43. A. Brent Strong, Fundamentals of Composites Manufacturing: Materials, Methods, and Applications, Society of Manufacturing Engineers, Michigan, 1989.

APPENDIX

APPENDIX - A

Figure shows a typical finite element mesh for tool/part configuration generated using GUI of ANSYS.



APPENDIX – B

Table B-I gives the properties of tool material used in the prediction of process-induced warpage in composite laminates.

Table B-I. Properties of the tool material

| Properties | Al – 6061 Tool | Invar-36 Tool |
|---|----------------|---------------|
| Density kg/m^3 | 2820 | 8000 |
| Specific heat capacity $\text{J/kg } ^\circ\text{k}$ | 880 | 514 |
| Thermal conductivity $\text{W/m } ^\circ\text{k}$ | 152.2 | 10.5 |
| CTE $/^\circ\text{C}$ | 22.14E-06 | 1.7E-06 |
| E GPa | 68.25 | 148.24 |
| ν | 0.33 | 0.23 |

Figure B-1 shows the geometry of the three tools used in the manufacturing of angle and flat laminates.

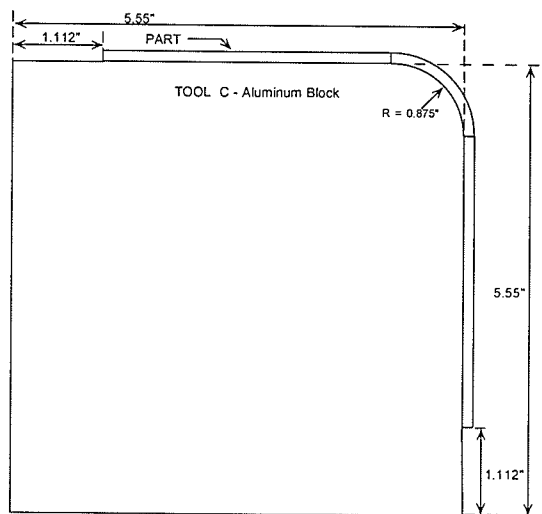
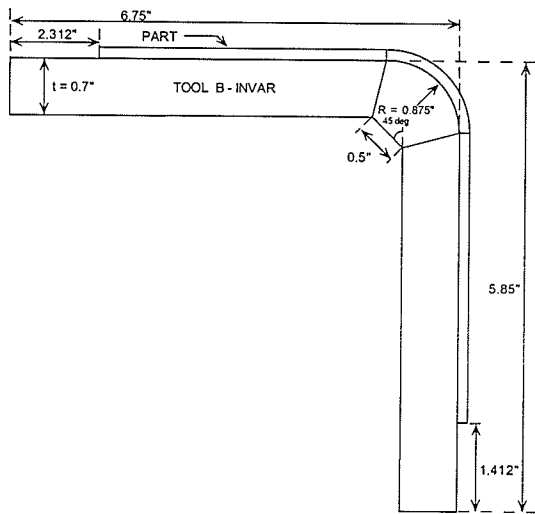
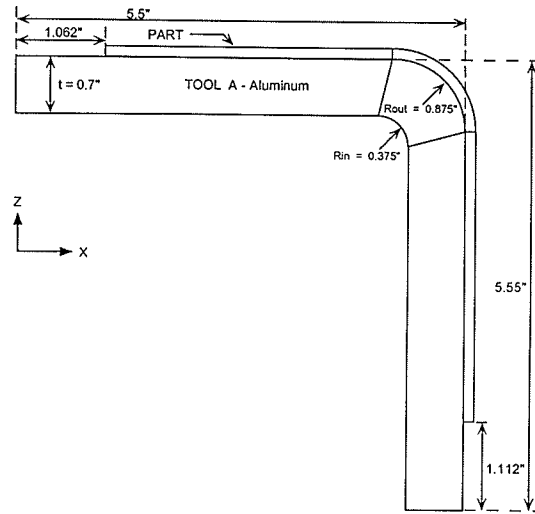


Figure B-1. Geometry and dimension of three tools

APPENDIX - C

Individual trial results for the Cytec-Fiberite material are given below.

C.1 Cure Kinetics Results:

C.1.1 Data for 934-Resin:

Dynamic scan:

| Heating Rate °C/min | Heat of Reaction, kJ/kg °C | | | |
|------------------------|----------------------------|-------|-------|---------|
| | 1 | 2 | 3 | Average |
| 20 | 494.2 | 491.3 | 415.3 | 466.93 |
| 10 | 497.3 | 479.9 | 472.1 | 483.1 |
| 5 | 518.5 | 505.6 | 501.3 | 508.47 |

Isothermal Kinetics:

| Temperature °C | 1 | | 2 | | Average | |
|-------------------|-----------|-------|--------|------|---------|-------|
| | k (1/min) | n | k | n | k | n |
| 100 | 0.0167 | 14.16 | 0.0375 | 12.2 | 0.026 | 13.18 |
| 130 | 0.049 | 10.94 | 0.075 | 8.84 | 0.062 | 9.89 |
| 160 | 0.0537 | 3.17 | 0.091 | 2.64 | 0.072 | 2.9 |
| 190 | 0.208 | 1.79 | 0.209 | 2.08 | 0.2085 | 1.93 |

C.1.2 Data for Prepreg:

Dynamic scan:

| Heating Rate °C/min | Heat of Reaction, kJ/kg °C | | | |
|------------------------|----------------------------|-------|-------|---------|
| | 1 | 2 | 3 | Average |
| 20 | 162.5 | 174.6 | - | 168.55 |
| 10 | 165.8 | 177.1 | 186.4 | 176.4 |
| 5 | 162.0 | - | - | 162.0 |
| 2 | 163.4 | 169.4 | - | 166.4 |

Isothermal Kinetics:

| Temperature °C | k (1/min) | n |
|-------------------|--------------|------|
| 100 | 0.0177 | 8.36 |
| 130 | 0.038 | 9.93 |
| 160 | 0.0698 | 1.76 |
| 177 | 0.178 | 1.84 |
| 190 | 0.166 | 2.63 |

C.2 Specific Heat Capacity of composite:

| Degree of cure | Heat Capacity of the composite kJ/kg C |
|----------------|--|
| 0 | $C_p = 0.003 * T + 1.475$ |
| 75 | $C_p = 0.003 * T + 0.9867$ |
| 80 | $C_p = 0.0029 * T + 0.9641$ |
| 100 | $C_p = 0.0023 * T + 0.9625$ |

The measured Cp of the composite as a function of temperature and degree of cure is given by equation,

$$C_p = 3.0 \cdot T + (1454.8 - 561.19 \cdot \alpha) \text{ J/kg K}$$

C.3 Thermal conductivity of composite:

Heat flux of the hot plate:

| Trial | 1 | 2 | 3 | Average |
|--------------------------------|-------|-------|------|---------|
| Heat flux kW/m ² | 46.79 | 42.34 | 42.5 | 43.87 |

Longitudinal thermal conductivity:

| Temperature | K ₁₁ W/m K |
|-------------|-----------------------|
| 140 | 10.62 |
| 153 | 11.08 |
| 160 | 11.59 |
| 180 | 12.75 |
| 200 | 12.75 |

Transverse thermal conductivity:

| Temperature | K ₂₂ & K ₃₃ W/m K |
|-------------|---|
| 130 | 4.25 |
| 150 | 4.44 |
| 170 | 4.98 |
| 200 | 5.1 |

C.4 Thermal expansion coefficient of the composite:

Transverse CTE:

| | $\alpha_{22} \text{ \& } \alpha_{33} \times E-06 / ^\circ C$ | | | | | | | | | | | |
|----------------|--|------|------|------|------|------|------|------|------|------|------|------|
| Degree of cure | 100 % | | | | 57 % | | | | 32 % | | | |
| Trial | 1 | 2 | 3 | Ave | 1 | 2 | 3 | Ave | 1 | 2 | 3 | Ave |
| TMA | 34.8 | 36.2 | 38.7 | 36.5 | 36.0 | 36.3 | 38.7 | 37.0 | 36.2 | 35.1 | 39.5 | 36.9 |

Longitudinal CTE:

| Degree of Cure % | $\alpha_{11} \times 10E-06 / ^\circ C$ | | | |
|------------------|--|---------|---------|---------|
| | Trial 1 | Trial 2 | Trial 3 | Average |
| 100 | 2.85 | 3.59 | 4.05 | 3.5 |
| 32 | 3.5 | - | - | 3.5 |

C.5 Cure shrinkage of the composite:

Transverse & longitudinal cure shrinkage coefficient:

| Temperature (C) | $\epsilon_{33}^c \text{ \& } \epsilon_{22}^c$ | ϵ_{11}^c |
|-----------------|---|-------------------|
| 177 | -2.49% | -0.048% |
| 160 | -2.3% | - |

C.6 Gel Point:

| System | Gel point Temperature °C ($\alpha \approx 0.4$) | |
|-----------|---|-------|
| Resin | 171.4 | 172.5 |
| Composite | 174.5 | - |

C.7 Viscosity of 934-Resin:

| Heating Rate °C/min | Number of runs performed |
|------------------------|--------------------------|
| 5 | 2 |
| 3 | 2 |
| 2 | 1 |

C.8 Modulus of the composite:

| Temperature °C | E_{11} , E_{22} & G_{12} Number of runs performed |
|-------------------|--|
| 177 | 2 |
| 160 | 2 |
| 130 | 2 |

APPENDIX – D

Predicted part temperature and degree of cure for aluminum low mass and Invar tools are presented here.

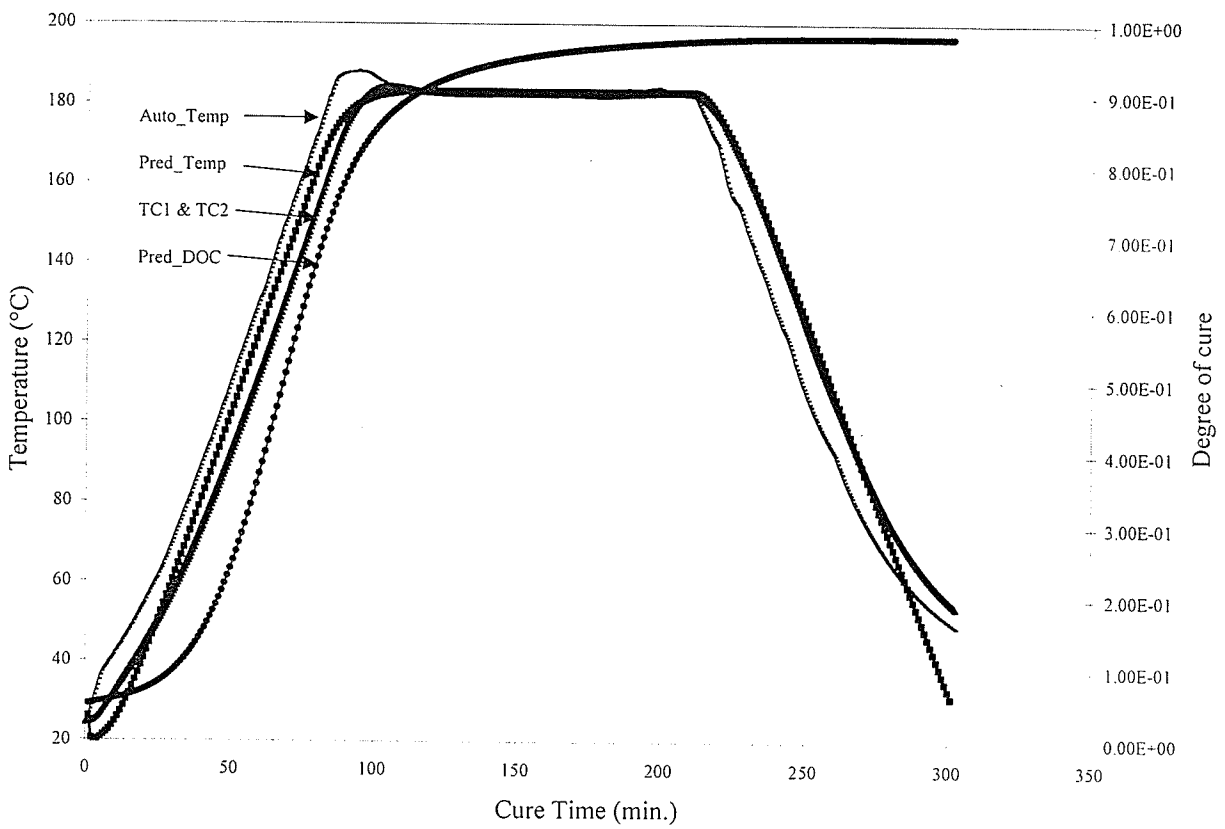


Figure D1. Predicted part temperature and degree of cure for ALL tool and cycle 1

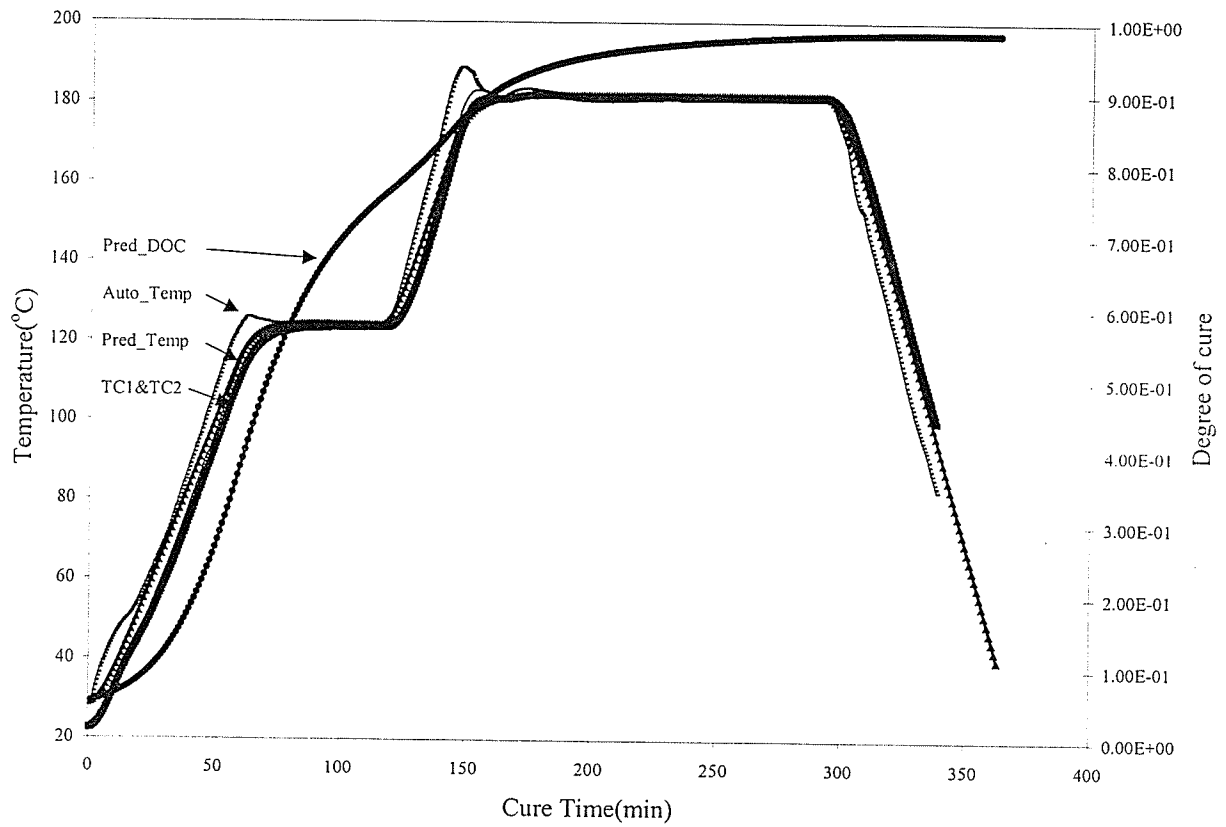


Figure D2. Predicted part temperature and degree of cure for ALL tool and cycle 4

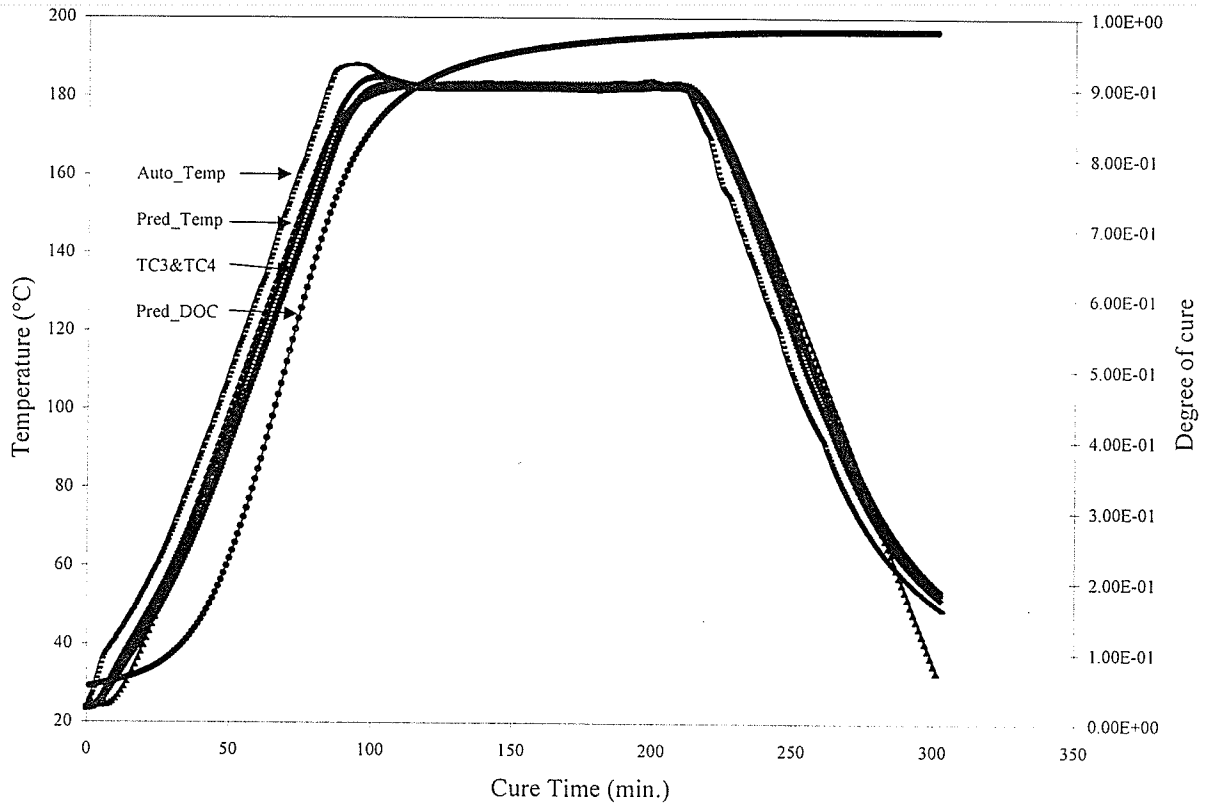


Figure D3. Predicted part temperature and degree of cure for INVAR tool and cycle 1

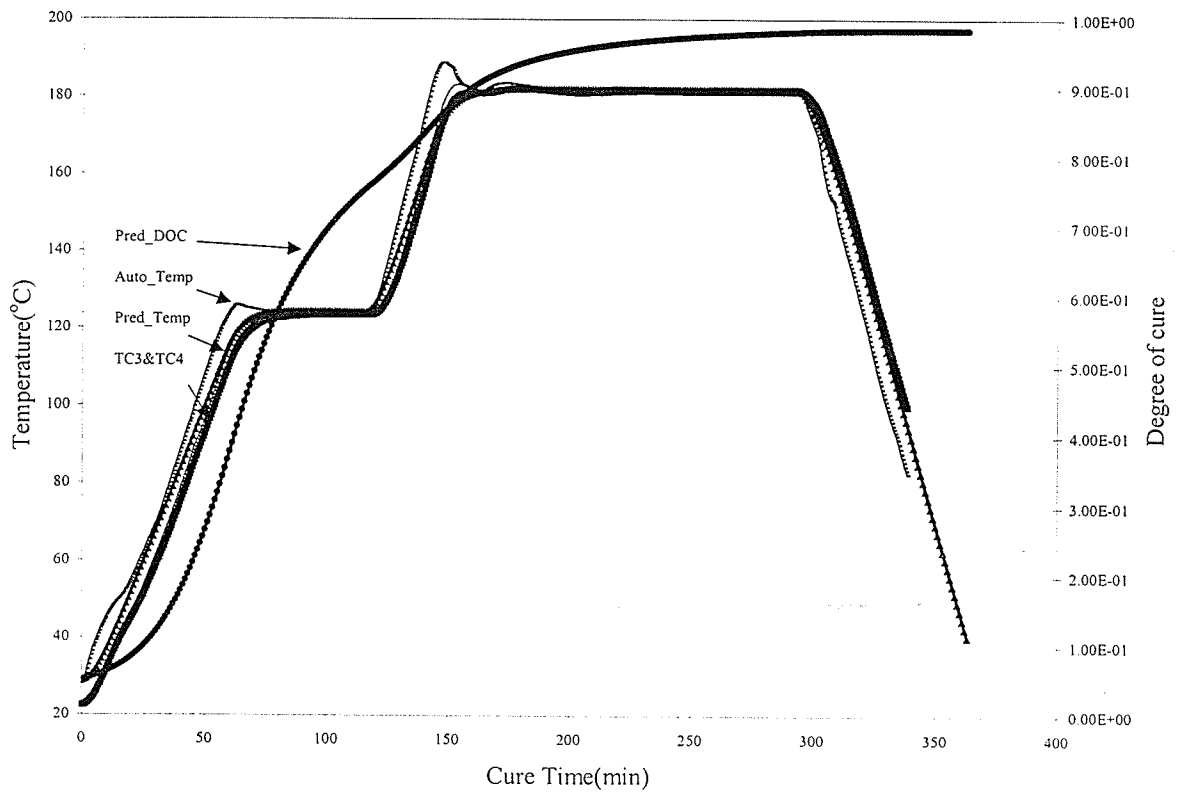


Figure D4. Predicted part temperature and degree of cure for INVAR tool and cycle 4